The University of British Columbia

FACULTY OF GRADUATE STUDIES

PROGRAMME OF THE

FINAL ORAL EXAMINATION

FOR THE DEGREE OF

DOCTOR OF PHILOSOPHY

of

PAULUS ARIE GOUD

B.Sc., The University of Alberta, 1959

M.A.Sc., The University of British Columbia, 1961

TUESDAY, NOVEMBER 24, 1964, at 3:45 P.M.

IN ROOM 208, MacLEOD BUILDING

COMMITTEE IN CHARGE

Chairman: I. McT. Cowan

E. V. Bohn	F. Noakes
R. E. Burgess	A. C. Soudack
M. Kharadly	C. A. Swanson

External Examiner: G. S. Kino

Microwave Laboratory
Stanford University
Stanford, California

A STUDY OF ELECTRON BEAMS AND THEIR FORMATION IN ELECTROSTATIC ELECTRON GUNS

ABSTRACT

A theoretical study is made of the formation of electron beams in electrostatic fields. The electron motion is assumed to be normal, congruent and regular, so that the equations governing the motion can be set up in terms of the action function. By assuming convenient functional forms of the action function, of the potential and of the metrical coefficients, some new solutions are then found by the method of separation of variables. These solutions are studied in detail, and are shown to have some desirable properties.

In order to employ a given space-charge flow solution in electron gun design, a method is developed to take into account the distortion of the field due to the anode aperture. In this method, the gun is considered to be made up of two regions, separated outside the beam by an auxiliary anode. The desired space-charge flow is assumed to exist in the cathode region, while in the anode region the effect of space-charge on the electrostatic field is assumed to be negligible. An estimate is made of the accuracy of these assumptions.

The fields about four idealized anode geometries are obtained by using Schwarz-Christoffel transformations, and a study is made of the relevant properties of these fields. One of these fields, which has been called the "wrap-around field", is shown to have properties that are very desirable for convergent electron guns.

The above design method is illustrated by two examples; namely, a gun producing a beam that is initially parallel and rectilinear, and a gun producing a beam that is initially radial and convergent; the latter incorporates the wrap-around field in the anode region.

Physical considerations involved in the determination of the electrodes to maintain a given beam are briefly discussed, and it is shown that the sensitivity of the field conditions at the beam boundary to errors in the field at other locations decreases at an exponential

rate with distance. A method is suggested for determining beam-forming electrodes that avoids the need for an auxiliary anode to maintain the beam.

GRADUATE STUDIES

Field of Study: Electrical Engineering

Applied Electromagnetic Theory	G.B. Walker
Electronic Instrumentation	F.K. Bowers
Network Theory	A.D. Moore
Servomechanisms	E.V. Bohn
Communication Theory	A.D. Moore
Digital Computers	E.V. Bohn
Electron Dynamics	G.B. Walker

Related Studies:

Noise in Physical Systems	R.E. Burgess
Computational Methods	C. Froese
Computer Programming	C. Froese
Theory and Applications of Differential Equations	C.A. Swanson
Differential Equations	C.A. Swanson

A STUDY OF ELECTRON BEAMS AND THEIR FORMATION IN ELECTROSTATIC ELECTRON GUNS

by

PAULUS ARIE GOUD

B.Sc., University of Alberta, 1959
M.A.Sc., University of British Columbia, 1961

A THESIS SUBMITTED IN PARTIAL FULFILMENT OF
THE REQUIREMENTS FOR THE DEGREE OF
DOCTOR OF PHILOSOPHY

in the Department of
Electrical Engineering

We accept this thesis as conforming to the
required standard

Members of the Department
of Electrical Engineering
THE UNIVERSITY OF BRITISH COLUMBIA
October, 1964

In presenting this thesis in partial fulfilment of the requirements for an advanced degree at the University of British Columbia, I agree that the Library shall make it freely available for reference and study. I further agree that permission for extensive copying of this thesis for scholarly purposes may be granted by the Head of my Department or by his representatives. It is understood that copying or publication of this thesis for financial gain shall not be allowed without my written permission.

Department of Electrical Engineering

The University of British Columbia,
Vancouver 8, Canada

Date 24 November , 1964

ABSTRACT

A theoretical study is made of the formation of electron beams in electrostatic fields. The electron motion is assumed to be normal, congruent and regular, so that the equations governing the motion can be set up in terms of the action function. By assuming convenient functional forms of the action function, of the potential and of the metrical coefficients, some new solutions are then found by the method of separation of variables. These solutions are studied in detail, and are shown to have some desirable properties.

In order to employ a given space-charge flow solution in electron gun design, a method is developed to take into account the distortion of the field due to the anode aperture. In this method, the gun is considered to be made up of two regions, separated outside the beam by an auxiliary anode. The desired space-charge flow is assumed to exist in the cathode region, while in the anode region the effect of space-charge on the electrostatic field is assumed to be negligible. An estimate is made of the accuracy of these assumptions.

The fields about four idealized anode geometries are obtained by using Schwarz-Christoffel transformations, and a study is made of the relevant properties of these fields. One of these fields, which has been called the "wrap-around field", is shown to have properties that are very desirable for convergent electron guns.

The above design method is illustrated by two examples; namely, a gun producing a beam that is initially parallel and

rectilinear, and a gun producing a beam that is initially radial and convergent; the latter incorporates the wrap-around field in the anode region.

Physical considerations involved in the determination of the electrodes to maintain a given beam are briefly discussed, and it is shown that the sensitivity of the field conditions at the beam boundary to errors in the field at other locations decreases at an exponential rate with distance. A method is suggested for determining beam-forming electrodes that avoids the need for an auxiliary anode to maintain the beam.

TABLE OF CONTENTS

LIST OF ILLUSTRATIONS

LIST OF TABLES

ACKNOWLEDGEMENTS

I wish to record my thanks to Dr. G. B. Walker, the supervisor of this project, for his encouragement and guidance throughout the course of the work.

I wish also to express my appreciation to Dr. C. G. Englefield, Dr. C. R. James, Mrs. W. L. Magar, and Mr. D. R. McDiarmid for helpful discussions.

The encouragement and help of my wife, Miriam, is valued greatly.

Acknowledgement is gratefully given to the National Research Council for the award of Studentships in 1961 and '62, and for a Research Assistantship, made available through the National Research Council Block Grant to the Department of Electrical Engineering, U.B.C., during the remainder of this project.

CHAPTER I - INTRODUCTION

1.1 Introduction

Until the invention of the klystron twenty-five years ago, the major devices employing electron beams were cathode-ray tubes and electron microscopes. The current requirements of the latter devices are modest, being of the order of a few μa to several ma. New and difficult electron gun design problems were posed by the advent of beam-type microwave tubes, which require a high-current-density beam at a comparatively low voltage.

Valuable indicators of electron gun performance are provided by the concepts of perveance and area-compression ratio. For an idealized model of space-charge-limited flow, in which physical considerations such as initial thermal velocities and variation of the work function, of the conductivity and of the contact potential at the cathode are ignored, the perveance K is described by

$$K = \frac{I}{V^{\frac{3}{2}}} \qquad (1.1)$$

where V is the potential difference between the cathode and anode — both of which may be of arbitrary shape — and I is the total current*. Equation (1.1) is commonly used to specify the perveance of an electron gun or of an electron beam, even in cases where this relation does not strictly apply. The area-

*For a brief informative history of equation (1.1) and the term "perveance", see reference #1.

compression ratio of an electron beam is defined as the ratio of the cathode area to the ultimate beam cross-sectional area. Electron guns that produce beams with an area-compression ratio greater than one are called convergent guns.

Despite the simplicity of equation (1.1), the theoretical evaluation of K is, in general, very difficult. This can be appreciated if it is considered that the electrostatic field in the cathode-anode region is determined by the space-charge distribution in the beam and by the shape of, and potential difference between, the electrodes. The space-charge distribution is, however, dependent on the dynamic properties of the electron flow, and these properties are, in turn, prescribed by the electrostatic field. A mutual interdependence, known as the self-consistency condition, thus exists between the space-charge distribution and the electrostatic field.

Until 1949, space-charge flow solutions were known for rectilinear flow only. In rectilinear flow, the trajectories coincide with lines of force of the electrostatic field, simplifying the problem greatly. There are three known cases of rectilinear flow; namely, lines of flow (a) parallel[2], (b) radiating normally from (or converging to) an axis[3], and (c) radiating from (or converging to) a point[4]. These three cases correspond to flow between two infinite parallel plates, two concentric cylinders, and two concentric spheres, respectively.

Within a year after the invention of the klystron, Pierce[5] published a method for the design of electron guns that was based on the rectilinear space-charge flow solutions. In this

design method the electron beam in the cathode-anode region of the gun is taken to be a section of a space-charge-limited rectilinear flow. The potential variation along the lines of flow is therefore known, and it is implicitly assumed that the anode is perfectly gridded; i.e., the anode allows the beam to pass through it, but maintains the prescribed potential. Since the flow is assumed to be rectilinear, the potential variation perpendicular to the lines of flow must be zero both inside the beam and at the beam boundary. The electrostatic field outside a rectilinear-flow beam must, therefore, be such that at the beam boundary (a) the potential variation is as prescribed by the rectilinear flow, and (b) the normal potential gradient is zero. The electrodes that produce the desired electrostatic field are called beam-forming electrodes.

The general problem of determining the electrostatic field outside a curvilinear electron beam on the surface of which the potential variation and the normal derivative of potential are prescribed is termed the Pierce-Cauchy problem. It is the first known physical problem involving an elliptic differential equation, Laplace's equation, with Cauchy-type boundary conditions on an open boundary. The solution to this problem is unstable in the sense that an infinitesimal change in the boundary conditions causes a large change in potential some distance from the beam[6]. The physical significance of this instability is that (a) the boundary conditions can be satisfied within finite, but arbitrarily small, limits by beam-forming electrodes that are quite different in shape, and (b) the electrodes do not need to extend an infinite distance away from

the beam, but can be truncated[7].

The Pierce-Cauchy problem can be solved by analytical, numerical, or analogue methods. Analogue methods, such as electrolytic-tank models, are often used in preference to the other two methods because, by their use, beam-forming electrodes of convenient shapes can generally be determined more easily.

In electron guns producing beams with high power densities it often is not possible to place a grid at the anode aperture (for thermal considerations). The grid at the anode of a Pierce gun may be dispensed with, without greatly affecting the beam in the cathode-anode region, if the width of the beam at the anode is small w.r.t. the cathode-anode distance. The defocusing action may then be calculated by means of the well-known Davisson-Calbick equation[8]. It is assumed in this calculation that the electron trajectories remain rectilinear until they reach the anode aperture. The aperture is represented by a thin lens, and at the principal plane of this lens the trajectories are assumed to undergo a discontinuous change in slope. The accuracy of the Davisson-Calbick formula can be improved by applying a space-charge correction[9,10,11].

As the perveance is increased, the field distortion due to the anode aperture becomes progressively more severe, and the thin lens model of the anode aperture rapidly becomes inadequate beyond a perveance of about 0.1×10^{-6} amp/volt$^{3/2}$ [12]. Initially the Pierce theory can be extended by treating the anode as a modified thin lens[13], or by a perturbation analysis of the rectilinear space-charge flow solutions[14].

Danielson *et al.*[15] made a very complete study of the divergent effect of the anode aperture, including the effect of

thermal velocities, valid for perveances up to 0.7×10^{-6}. They determined the field in the anode region by two different methods. In the first method the principle of superposition is used; the actual potential distribution is approximated by the sum of a space-charge-free potential distribution, obtained from the electrolytic tank, and the potential distribution as prescribed by the rectilinear-flow solution. In the second method it is assumed that the effect of space-charge on the potential distribution can be neglected in the anode region. A third electrode, of a shape and at a potential as prescribed by the rectilinear-flow solution, is placed between the cathode and the anode in the electrolytic tank, and the field in the anode region is then probed. The information from either of these methods is then used to modify the Davisson-Calbick formula. The second method for obtaining the potential distribution is essentially the same as one described earlier by Brown and Süsskind[16].

In the extended Pierce theory it is assumed that conditions in the cathode region are relatively unaffected by the anode aperture. This assumption is generally considered to be satisfactory up to a perveance of about 1.0×10^{-6}. For higher-perveance Pierce guns, the field distortion extends to the cathode, reducing the off-cathode gradient, and hence the emission, in a non-uniform manner. For these guns the actual perveance is thus lower than the design value, and the current density is non-uniform across the beam. The latter condition is aggravated by the spherical aberration of the anode field.

Müller[17] found an approximate relation between the actual value and the design value of the perveance of a conical-flow Pierce gun from electrolytic-tank studies. Amboss[18] carried

out a first-order perturbation analysis for guns of this type, and obtained expressions for the change in current density across the cathode and elsewhere, for the loss in perveance, and for several other variables. In his analysis he assumed that the potential distribution in the anode region could be obtained from the space-charge-free potential. Experimental measurements on a Pierce gun with a design perveance of 3.25×10^{-6} gave good agreement with his theory. If a non-optimum gun design is acceptable, a Pierce gun of a desired perveance can thus be designed by applying the perveance correction of Müller[17] or Amboss[18], and the gun performance predicted from Amboss'[18] work.

Müller[17] and Brewer[12] developed quite similar electrolytic-tank methods, by means of which uniformity of cathode emission and initially rectilinear flow can be partially restored. In these methods the off-cathode potential gradient is made more uniform by reshaping the beam-forming electrode (from the Pierce shapes) in such a way that the field along the initial part of the beam edge is weakened. Guns with a perveance of 1.58×10^{-6} and an area-compression ratio up to 30 have been made by Müller's method[17]. Brewer[12] appears to have obtained gun perveances of 2.2×10^{-6} by his method.

To study the electron trajectories in a proposed high-perveance gun, use is often made of analogue equipment such as an electrolytic tank, a resistance network, or a rubber membrane, in which space-charge is simulated. An analogue of the gun structure set up on one of these devices provides electrostatic field data, which are used by an analogue or digital computer

coupled into the system to solve the electron-dynamical equations and to trace out the trajectories*. More recently, numerical methods have been used to obtain, by means of a digital computer, both the electrostatic field data and the trajectories, from a mathematical model of an electron gun[26].

With the aid of the above-mentioned equipment, the influence of the shape of the electrodes on the trajectories of a proposed gun can be investigated empirically prior to the construction and testing of one or more gun prototypes. The testing of the latter is generally carried out in a demountable vacuum system. The variation of current density across the electron beam emerging from a gun prototype may be studied by intercepting the beam with a fluorescent screen, or by moving across it an intercepting anode containing a pin-hole. In the latter case, if the current collector behind the pinhole is a split Faraday cage, information about the variation across the beam of the transverse electron velocities can be obtained simultaneously[27]. This information can also be obtained by repeating the measurement of current density across the beam at various distances from the gun.

Mathias and King[28] obtained a gun with a perveance of 2×10^{-6} from an experimental investigation of gun prototypes based on a Müller design[17]. A knowledge of the variation of emission across the cathode, and of the aberration of the anode, was ingeniously obtained by leaving various sections of the cathode uncoated in some of the prototypes, and by noting the resultant changes in the current density patterns of the emerging

*A comprehensive article discussing these methods was written by Süsskind[19] in 1956. Papers representative of more recent work are listed in references (20 - 26).

beams.

Frost et al.[27] developed an elaborate design method that resulted in the successful construction of a gun with a perveance of 2.2×10^{-6} and a compression ratio of 300, and also a gun with perveance 5×10^{-6} and compression ratio 6. Starting with a design based on Müller's[17] or Brewer's[12] methods, a gun was then built using the cathode and anode as designed, but with the beam-forming electrode replaced by about five annular disc electrodes. The potentials of these discs were adjusted experimentally until the desired beam was obtained. By the use of an electrolytic tank a beam-forming electrode shape was then obtained which gave approximately the same field conditions in the region of the beam.

In empirical design methods, cathode shapes other than those required by the known space-charge flow solutions can be used. A very successful gun resulting from empirical design is the Heil gun[29,30]. The cathode of this gun is part of an ellipsoid of rotation. Heil[29] obtained a design with a perveance of 4.4×10^{-6} and a compression ratio of 230, while Reed[30] built a Heil gun for a 5 mm klystron with a perveance of 3×10^{-6} and a compression ratio of 75. Kawamura[31] has designed high perveance guns with oblate spheroidal cathodes. The success of these cathode shapes is due to the fact that they tend to correct for the spherical aberration of the anode by starting the electrons off on trajectories that have a different centre of curvature, depending on the starting point. Lucken[32] corrected for the spherical aberration by distorting the shape of a spherical-cap cathode in such a manner that its centre

of rotation lay on a circle.

It is clear that the designing of high perveance electron guns is still to a large extent a trial and error process. There have been many significant advances in the analysis of proposed gun designs, but, when proceeding to improve the design on the basis of these analyses, the gun designer still needs to rely on his intuition to decide how the proposed design should be changed.

1.2 Objectives and Procedure

This study of the formation of electron beams in electrostatic fields has been divided into four sub-problems; namely, (1) electron flow in electrostatic fields, (2) space-charge-free electrostatic fields in idealized anode geometries, (3) design of electron beams based on (1) and (2), and (4) the Pierce-Cauchy problem.

In Chapter II, the theory of electron flow in electrostatic fields is derived, and the underlying physical assumptions are discussed. Past methods of solution are noted. New solutions are then found by the method of separation of variables. These solutions are studied in detail, and are shown to have desirable characteristics.

To adapt a given space-charge-flow solution for use in the design of high-perveance electron guns with anode apertures, a knowledge of the form of the electrostatic fields of various apertured anodes is highly desirable. In Chapter III, use is made of the Schwarz-Christoffel transformation to compute and plot the space-charge-free fields of three different idealized anode

geometries. In Chapter IV, the characteristics of these fields relevant to electron-beam design are analysed. The information obtained from this analysis is used to design an anode field with improved characteristics. This design involves a lengthy Schwarz-Christoffel transformation, so that for the sake of continuity the mathematical derivation is included in Chapter III, although its real importance does not become clear until Chapter IV. In Chapter IV, a new gun design method is also formulated, showing how known space-charge-flow solutions can be matched to the above-mentioned space-charge-free fields. The procedure is illustrated by two examples, and it is shown how the electron trajectories may be computed in the anode region, taking space-charge into account.

A further adaptation of the present space-charge-flow solutions for electron beam applications is necessitated by the fact that these solutions involve unbounded flows; i.e., space-charge occupies the entire space between two equipotential surfaces. This adaptation, the Pierce-Cauchy problem, is the subject of Chapter V. The error growth in potential is evaluated for a cylindrical beam.

The results of this investigation are summarized in Chapter VI.

CHAPTER II - ELECTRON FLOW IN ELECTROSTATIC FIELDS

2:1 Introduction

In discussing the self-consistent flow of electrons, it is convenient to disregard the discrete nature of the electron. Instead, the flow is treated as a continuous compressible fluid. This approach will be used here to formulate the theory of space-charge flow in the absence of externally applied magnetic fields. It will be assumed that the flow is congruent, normal, regular and laminar. Relativistic effects and the effects of self-magnetic forces are neglected. This places an upper limit of about 20 keV on the electron energy, as is discussed in Appendix A.

The term "congruent flow"[39] means that the velocity is in general a single-valued function of position, so that only a single flow line passes through any point*. The mathematical significance of congruence is that the flow is differentiable.

By normal flow two slightly different concepts are implied. Meltzer[33] defined normal flow (as opposed to abnormal flow) as flow in which the sum of the kinetic and potential energy is constant for any point in the flow. Meltzer showed that this requires a unipotential cathode. A necessary and sufficient condition for this normal flow is that $\vec{v} \times (\nabla \times \vec{v}) = 0$. The second interpretation of normal flow is a geometric one. For normal congruent flow in this sense to occur, it is necessary and sufficient that $\vec{v} \cdot \nabla \times \vec{v} = 0$. When this is the case, then there exists a one-parameter family of surfaces $W(q_1, q_2, q_3) = c_1$ ortho-

*This is called "single streaming" by some workers.

gonal to the flow lines[34].

The assumption of laminar or irrotational flow requires that $\nabla \times \vec{v} = 0$ throughout the flow. If flow is laminar, both normality criteria are therefore satisfied, and the flow originates from a unipotential cathode. Conversely, if $\nabla \times \vec{v} = 0$ at the cathode, it will be zero throughout the flow. This is true by Lagrange's Invariant theorem, which states that $\nabla \times \vec{v} =$ constant throughout a flow.

The term "regular flow" is due to Gabor[35], and refers to the assumption that the electrons are emitted from the cathode with zero velocity.

The theory of space-charge flow can also be derived under more general conditions. Gabor[35] showed that skew congruent flow is possible in the presence of an externally applied magnetic field, provided that at the cathode the magnetic field has no normal component. Kirstein[36] derived the theory for this case, and found some new solutions, which were basically simple extensions of electrostatic ones. Pease[37] extended the theory to include time-dependent flow. These more general formulations are not needed for our purposes, since it is our ultimate aim to study the applications of the theory to electrostatic electron guns.

2:2 Fundamental Theory

For an electrostatic field Maxwell's equations are

$$\nabla \times \vec{E} = 0 \qquad (2.1)$$

$$\nabla \cdot \vec{D} = \rho \qquad (2.2)$$

and

$$\vec{D} = \varepsilon \vec{E} \quad . \qquad (2.3)$$

These equations are solved by

$$\vec{E} = -\nabla\Phi \tag{2.4}$$

where Φ is the electric potential. Substituting expressions (2.3 and 4) into (2.2), Poisson's equation is obtained, namely

$$\nabla^2\Phi = -\rho/\varepsilon \quad . \tag{2.5}$$

The current density $\vec{J}$ is given by

$$\vec{J} = \rho\vec{v} \tag{2.6}$$

and the time independent form of the continuity equation is

$$\nabla.\vec{J} = 0 \quad . \tag{2.7}$$

By considering the Newton force on each electron, it follows that

$$\frac{d\vec{v}}{dt} = -\eta\vec{E} \tag{2.8}$$

where $\eta = \frac{e}{m}$, the charge-to-mass ratio of an electron, a positive quantity.

Equation (2.8) has time as a parameter, and this will be eliminated next. The complete time differential d/dt applied to a dynamical variable X is

$$\frac{dX}{dt} = (\vec{v}.\nabla)X + \frac{\partial X}{\partial t} \quad . \tag{2.9}$$

Since the electron motion is taken to be steady-state congruent flow, X in equation (2.9) can represent the velocity of an electron, and

$$\frac{\partial\vec{v}}{\partial t} = 0$$

and hence

$$\frac{d\vec{v}}{dt} = (\vec{v}.\nabla)\vec{v} \quad . \tag{2.10}$$

But

$$(\vec{v}\cdot\nabla)\vec{v} = \frac{1}{2}\nabla(\vec{v}\cdot\vec{v}) - \vec{v}\times(\nabla\times\vec{v}) \quad . \tag{2.11}$$

From (2.10 and 11) therefore

$$\frac{d\vec{v}}{dt} = \frac{1}{2}(\nabla v^2) - \vec{v}\times(\nabla\times\vec{v}) \quad .$$

Combining this result with (2.4 and 8),

$$\frac{1}{2}(\nabla v^2) - \vec{v}\times(\nabla\times\vec{v}) = \eta\nabla\Phi$$

or

$$\nabla\left[\frac{1}{2}v^2 - \eta\Phi\right] = \vec{v}\times(\nabla\times\vec{v}) \quad . \tag{2.12}$$

If the electrons start with equal energy from a uni-potential cathode, then $\nabla\times\vec{v} \equiv 0$ and equation (2.12) can be integrated to give

$$\frac{1}{2}v^2 - \eta\Phi = \text{a constant} \tag{2.13}$$

which is independent of the trajectory chosen. If the electrons start from rest at a zero-potential cathode, this constant is zero.

A step of fundamental importance was taken in going from equation (2.12) to (2.13). Equation (2.12) was still concerned with the trajectory traced out by a single electron, whereas equation (2.13) applies throughout the flow, because the constant of equation (2.13) is independent of the trajectory chosen. If we do not choose $\nabla\times\vec{v} \equiv 0$, it is found that

$$\frac{1}{2}v^2 - \eta\Phi = C \quad , \tag{2.14}$$

where C is a constant for the motion of the particular electron considered*. This result is readily obtained by taking the dot product of $\vec{v}$ and equation (2.8), and substituting (2.4)

$$\vec{v} \cdot \frac{d\vec{v}}{dt} = +\eta (\vec{v} \cdot \nabla) \Phi \quad . \tag{2.15}$$

In a frame of reference moving with the electron, the potential variation is found from equation (2.9) to be

$$\frac{d\Phi}{dt} = (\vec{v} \cdot \nabla) \Phi \quad . \tag{2.16}$$

If, finally, equations (2.15 and 16) are combined, and the result is integrated, the relation (2.14) is obtained for the electron considered.

For the case $\nabla \times \vec{v} \equiv 0$, it is possible to express the velocity as the gradient of a scalar potential function

$$\vec{v} = \nabla W \tag{2.17}$$

where W is called the action function. It is apparent that surfaces of constant action are orthogonal to the lines of flow.

The equations to be satisfied by the flow are thus

Poisson's equation in free space	$\nabla^2 \Phi = -\rho/\varepsilon_0$	(2.5)
Definition of current density	$\vec{J} = \rho \vec{v}$	(2.6)
Continuity equation	$\nabla \cdot \vec{J} = 0$	(2.7)
Conservation of energy	$\frac{1}{2} v^2 - \eta \Phi = 0$	(2.13)
Action function relation	$\vec{v} = \nabla W$.	(2.17)

These equations will be referred to as the space-charge-flow

*In fact C is the Hamiltonian, the total energy of a particle, which would be different for particles released from rest at different equipotentials.

equations. Equations (2.13 and 17) may be combined to give the Hamilton-Jacobi equation

$$\frac{1}{2}(\nabla W \cdot \nabla W) - \eta\Phi = 0 \quad . \tag{2.18}$$

In beams in which the space-charge causes a negligible perturbation of the electrostatic field, ρ can be set equal to zero. The potential now is determined only by the boundary conditions, and to obtain an electron flow solution it is necessary to satisfy equations (2.5 and 18) only.

When $\rho \neq 0$, it is possible to combine the required equations so that an equation in W or $\vec{v}$ alone results. From (2.5 and 18)

$$\rho = -\varepsilon_0 \nabla^2 \left[\frac{1}{2\eta} \nabla W \cdot \nabla W\right] \quad .$$

If this is combined with (2.6, 7 and 17), then

$$\nabla \cdot \left[(\nabla W) \nabla^2 (\nabla W \cdot \nabla W)\right] = 0 \quad . \tag{2.19}$$

The space-charge flow must satisfy this fourth-order, third-degree equation in W. Once a solution for W obeying (2.19) has been found, the other variables of the flow are also defined and can be obtained from the space-charge-flow equations.

By combining the first four of the space-charge-flow equations, there results

$$\nabla \cdot \left[\vec{v} \nabla^2 (\vec{v} \cdot \vec{v})\right] = 0$$

which can be rewritten as

$$(\nabla^2 v^2) \nabla \cdot \vec{v} + \vec{v} \cdot \nabla (\nabla^2 v^2) = 0$$

or

$$\nabla \cdot \vec{v} = - \frac{1}{\nabla^2 v^2} \vec{v} \cdot \nabla (\nabla^2 v^2) \quad . \tag{2.20}$$

Equation (2.20) can be expressed as

$$\nabla \cdot \vec{v} = - \vec{v} \cdot \nabla (\ln \nabla^2 v^2) \quad . \tag{2.21}$$

Since equation (2.17) is equivalent to the condition $\nabla \times \vec{v} = 0$, the vector identity

$$\nabla \times (\nabla \times \vec{v}) = \nabla (\nabla \cdot \vec{v}) - \nabla^2 \vec{v}$$

becomes

$$\nabla (\nabla \cdot \vec{v}) = \nabla^2 \vec{v} \quad . \tag{2.22}$$

Substitution of (2.21) into (2.22) gives the desired result,

$$\nabla^2 \vec{v} = - \nabla \left[\vec{v} \cdot \nabla (\ln \nabla^2 v^2) \right] \quad . \tag{2.23}$$

This equation does not apply in the absence of space-charge.

To obtain realizable space-charge-limited flows, equations (2.19 or 23) must be solved under boundary conditions

$$\Phi = 0, \frac{\partial \Phi}{\partial n} = 0, \text{ and } \frac{\partial^2 \Phi}{\partial n^2} \longrightarrow - \infty \tag{2.24}$$

at the cathode, where " $\frac{\partial}{\partial n}$ " indicates differentiation normal to the cathode surface.

2:3 Methods of Solution

The complexity of equations (2.19 and 23) has so far precluded their being solved directly except for the simplest of cases. For instance, Spangenberg[38] solved equation (2.19) for parallel rectilinear flow. Trial and error approaches are not

likely to produce useful solutions on account of the self-consistency requirement and the boundary conditions. Thus, if a particular form of $\vec{v}$ or W is assumed, the potential is immediately defined by the equation for conservation of energy (2.13). However, the potential has to satisfy Poisson's equation also, and with trial and error procedures it is difficult to satisfy both requirements at once.

Realizable space-charge-limited flow solutions have previously been obtained by using coordinate systems that made one of the variables of the flow a function of only one coordinate. Walker[39], Meltzer[40], and Rosenblatt[41] set up the equations so that the lines of flow lay along one coordinate. Walker[39] also found solutions for space-charge-limited flow between two inclined planes and between two cones with coinciding vertices. In these latter solutions the potential is a function of only one variable. Meltzer[40] found a realizable solution in which the lines of flow are concentric circles.

Kirstein *et al.*[36, 42, 43] assumed an action function of the form

$$W = \prod_{i=1}^{3} W_i(q_i) ,$$

where the q_i represent curvilinear coordinates. It then became possible to use the method of separation of variables to solve the space-charge flow equations in Cartesian, cylindrical polar, spherical polar, and equiangular spiral coordinates. These solutions correspond to axially symmetric curvilinear flows originating from cylindrical and conical cathodes, and also

to planar curvilinear flows from an equiangular spiral cathode, from two inclined planes, and from a circular-section cathode.

Harker and Colburn[44] devised a stable numerical method to obtain flows with axial symmetry; this method is also applicable to planar flows. In this method, an analytic form of cathode shape and cathode current density are assumed. This then makes it possible to set up the space-charge-flow equations in hyperbolic form, by making an analytic continuation into the complex domain. Since hyperbolic differential equations are mathematically stable when solved by finite-difference methods, the space-charge-flow equations can thus be numerically integrated away from the cathode in discrete steps.

The problem of electron motion in electrostatic fields and with negligible space-charge effects has been studied extensively. Goursat[45] showed that if the potential Φ has the functional form

$$\Phi = \sum_{i=1}^{3} \varphi^{1i} \Phi_i(q_i) \qquad (2.25)$$

the Hamilton-Jacobi equation is integrable by separation of variables. The term φ^{1i} is the first row of a matrix $\|\varphi^{ij}\|$ called a Staeckel matrix. The elements of a Staeckel matrix are functions of the coordinates q_i alone. Iwata[46], assuming the functional form (2.25), found electrostatic fields satisfying the Laplace equation for the eleven coordinate systems of Staeckel.

In this chapter the approach to the problem of determining solutions of the space-charge-flow equations is to assume an action function or a potential function that is the

sum of terms. Two cases are considered:

Case I: Action function assumed to be of the form

$$W = W_1(q_1) + W_2(q_2)$$

and the potential of the form

$$\Phi = \frac{1}{f^2(q_1,q_2)} \left[A_{11}(q_1)A_{12}(q_2) + A_{21}(q_1)A_{22}(q_2)\right] . \quad (2.26)$$

Case II: Potential assumed to be of the form

$$\Phi = \Phi_1(q_1) + \Phi_2(q_2)$$

and the action function of the form

$$W = B_1(q_1)\, B_2(q_2) \quad (2.27)$$

where (q_1, q_2) are orthogonal curvilinear coordinates.

Motion with negligible space-charge effects is treated first. With W and Φ of the form assumed in either Case I or II, coordinate systems are then found for which the Hamilton-Jacobi and Laplace equations are separable. The solution of the motion is then extended to the space-charge domain by assuming that one term of the action function and the potential function remain as determined previously in the absence of space-charge. When this is possible, the second term of Φ and W is then determined by a complete differential equation.

In Section 2:4 the theory is first formulated in Cartesian coordinates. In this coordinate system the functional forms of W and Φ are assumed to be those of equations (2.26a and 27a)*.

*In Cartesian coordinates, equation (2.26b) reduces to the simpler form (2.27a).

In Section 2:5 the separability conditions are obtained for two-dimensional flow with negligible space-charge effects. These conditions are in terms of assumed functional forms of the metrical coefficients "h_i" of general orthogonal curvilinear coordinates. Case I is treated first and is illustrated by two examples, formulations in logarithmic spiral, and in polar coordinates. It was not found possible to extend these two examples to include space-charge effects by the methods mentioned. The functional forms of Case II are studied next. Two more examples follow, in which logarithmic spiral, and polar coordinates are again used. These latter solutions are extended to the space-charge domain.

Certain of the solutions obtained by the Case I and II formulations have been obtained by other investigators by independent means, and these will be indicated.

2:4 Solutions in Cartesian Coordinates by the Method of Separation of Variables

2:4:1 Electron Motion with Negligible Space-Charge Effects

It was shown in Section 2:2 that in the absence of space-charge effects, electron motion in electrostatic fields is described by the Hamilton-Jacobi equation

$$(\nabla W)^2 - 2\eta\Phi = 0 \qquad (2.18)$$

where the potential Φ has to satisfy the Laplace equation

$$\nabla^2\Phi = 0 \quad . \qquad (2.5)$$

We shall assume a solution of these equations of the functional

forms

$$W = W_1(x') + W_2(y') + W_3(z') \qquad (2.28)$$

and

$$\Phi = \Phi_1(x') + \Phi_2(y') + \Phi_3(z') \quad . \qquad (2.29)$$

With Φ of the form (2.29), the Laplace equation (2.5) separates into three ordinary differential equations. When these are solved, Φ is found to be

$$\Phi = \frac{1}{2}\left[C_1 x'^2 + C_2 y'^2 - (C_1 + C_2) z'^2\right] + d_1 x' + d_2 y' + d_3 z' + d_4 \quad . \qquad (2.30)$$

In general, equipotential surfaces are thus hyperboloids. It is convenient to change the origin of coordinates to the centre of symmetry of the field. Equation (2.30) then becomes

$$\Phi = \frac{1}{2}\left[C_1 x^2 + C_2 y^2 - (C_1 + C_2) z^2\right] + \Phi_o \quad . \qquad (2.31)$$

The Cartesian coordinate system is one of the eleven coordinate systems of Staeckel, and the separable form of the potential function Φ described by equation (2.31) was noted by Iwata[46].

The motion of an electron released from rest at an arbitrary point (x_o, y_o, z_o) on the surface $\Phi = 0$ will next be obtained. If equations (2.28 and 31) are substituted into the Hamilton-Jacobi equation (2.18), we obtain

$$\left[\left(\frac{dW_1(x)}{dx}\right)^2 - \eta C_1 x^2\right] + \left[\left(\frac{dW_2(y)}{dy}\right)^2 - \eta C_2 y^2\right] + \left[\left(\frac{dW_3(z)}{dz}\right)^2 + \eta(C_1 + C_2) z^2\right]$$

$$+ 2\eta\Phi_o = 0 \quad .$$

This equation can be separated into the three equations

$$\left.\begin{aligned}\left[\frac{dW_1(x)}{dx}\right]^2 - \eta(\Phi_1 + K_1 + C_1x^2) &= 0 \\ \left[\frac{dW_2(y)}{dy}\right]^2 - \eta(\Phi_2 + K_2 + C_2y^2) &= 0 \\ \left[\frac{dW_3(z)}{dz}\right]^2 - \eta\left[\Phi_3 - (K_1 + K_2) - (C_1 + C_2)z^2\right] &= 0\end{aligned}\right\} \quad (2.32)$$

where

$$\Phi_o = \frac{1}{2} \sum_{i=1}^{3} \Phi_i$$

and K_1 and K_2 are separation constants. Each of the three separate equations (2.32) constitutes a conservation theorem of the motion.

Equations (2.32) can be immediately integrated between the limits x_o and x, y_o and y, and z_o and z respectively, where (x_o, y_o, z_o) is an arbitrary starting point on the zero equipotential, and (x, y, z) is any point on the trajectory of an electron released from (x_o, y_o, z_o). However, as we are interested in obtaining the trajectories as well as the action function, it is more convenient first to eliminate the separation constants in (2.32). The result will in any case be the same.

It will be recalled that the condition for writing the Hamilton-Jacobi equation (2.18) was that $\nabla x \vec{v} = 0$, and that this condition is realized for a regular beam; that is, when the electrons are emitted by the cathode at zero velocity. From equation (2.31) we see that the cathode surface, $\Phi = 0$, is described by

$$\frac{1}{2}\left[C_1x_o^2 + C_2y_o^2 - (C_1 + C_2)z_o^2\right] + \Phi_o = 0 \quad . \quad (2.33)$$

The condition of zero initial velocity is

$$\left.\frac{dW_1(x)}{dx}\right|_{x_o} = \left.\frac{dW_2(y)}{dy}\right|_{y_o} = \left.\frac{dW_3(z)}{dz}\right|_{z_o} = 0 \quad .$$

When these initial conditions are applied to (2.32), we obtain

$$\left.\begin{aligned} \Phi_1 + K_1 + C_1 x_o^2 &= 0 \\ \Phi_2 + K_2 + C_2 y_o^2 &= 0 \\ \Phi_3 - (K_1 + K_2) - (C_1 + C_2) z_o^2 &= 0 \quad , \end{aligned}\right\}$$

and when these equations are substituted back into (2.32), there results

$$\left.\begin{aligned} \left(\frac{dW_1(x)}{dx}\right)^2 - \eta C_1 (x^2 - x_o^2) &= 0 \\ \left(\frac{dW_2(y)}{dy}\right)^2 - \eta C_2 (y^2 - y_o^2) &= 0 \\ \left(\frac{dW_3(z)}{dz}\right)^2 - \eta (C_1 + C_2)(z_o^2 - z^2) &= 0 \quad . \end{aligned}\right\} \qquad (2.34)$$

Equations (2.34) describe the action W at an arbitrary point (x, y, z) on the trajectory originating from a point (x_o, y_o, z_o) on the cathode. The electron velocity is, from equations (2.17 and 34),

$$\vec{v} = \left[\pm\sqrt{\eta C_1 (x^2 - x_o^2)},\ \pm\sqrt{\eta C_2 (y^2 - y_o^2)},\ \pm\sqrt{\eta (C_1 + C_2)(z_o^2 - z^2)}\right] . \qquad (2.35)$$

The signs of the velocity components depend on the field constants C_1 and C_2, and on the instantaneous position of the electron on its trajectory. The trajectory equations can be obtained directly from equation (2.35):

$$\int_o^t dt = \int_{x_o}^{x} \frac{dx}{\sqrt{\eta c_1 (x^2 - x_o^2)}} = \int_{y_o}^{y} \frac{dy}{\sqrt{\eta c_2 (y^2 - y_o^2)}} = \int_{z_o}^{z} \frac{dz}{\sqrt{\eta (c_1 + c_2)(z_o^2 - z^2)}} \,. \tag{2.36}$$

Equations (2.36) have the solutions

$$\left.\begin{aligned} x &= x_o \cosh\left(\sqrt{\eta c_1}\, t\right) \\ y &= y_o \cosh\left(\sqrt{\eta c_2}\, t\right) \\ z &= z_o \cos\left(\sqrt{\eta (c_1 + c_2)}\, t\right) \end{aligned}\right\} \tag{2.37}$$

with time t as a parameter. This may be eliminated to give

$$z = z_o \cos\left\{\left[\cosh^{-1}\left(\frac{x}{x_o}\right)\right]^2 + \left[\cosh^{-1}\left(\frac{y}{y_o}\right)\right]^2\right\}^{\frac{1}{2}} \,. \tag{2.38}$$

The motion is seen to be oscillatory, with an amplitude equal to the initial coordinate. A sketch of the cathode surface and a trajectory for two characteristic cases is shown in Figures (2-1a and b).

The action W along the trajectories described by equations (2.37 or 38) can be obtained directly upon integration of equations (2.34) between the limits x_o and x, y_o and y, and z_o and z respectively, and taking their sum:

$$\begin{aligned} W = {} & \tfrac{1}{2}\sqrt{\eta c_1}\left[x\sqrt{x^2 - x_o^2} - x_o^2 \cosh^{-1}\left(\frac{x}{x_o}\right)\right] \\ & + \tfrac{1}{2}\sqrt{\eta c_2}\left[y\sqrt{y^2 - y_o^2} - y_o^2 \cosh^{-1}\left(\frac{y}{y_o}\right)\right] \\ & + \tfrac{1}{2}\sqrt{\eta (c_1 + c_2)}\left[z\sqrt{z_o^2 - z^2} - z_o^2 \cos^{-1}\left(\frac{z}{z_o}\right)\right] \,. \end{aligned} \tag{2.39}$$

Because of the oscillatory nature of the electron motion, trajectory cross-over occurs. The function W is therefore multivalued. It might be supposed that on account of the cross-over of trajectories it is not possible to construct a one-parameter family of surfaces of constant action perpendicular to the flow lines. This, however, is not so; because the electron motion satisfies the condition $\nabla \times \vec{v} = 0$, it is in principle still possible to construct this orthogonal family of surfaces (see Appendix B). Care must be taken, however, to associate the correct branch of W with the appropriate trajectories (or sections of trajectories). This point is illustrated in

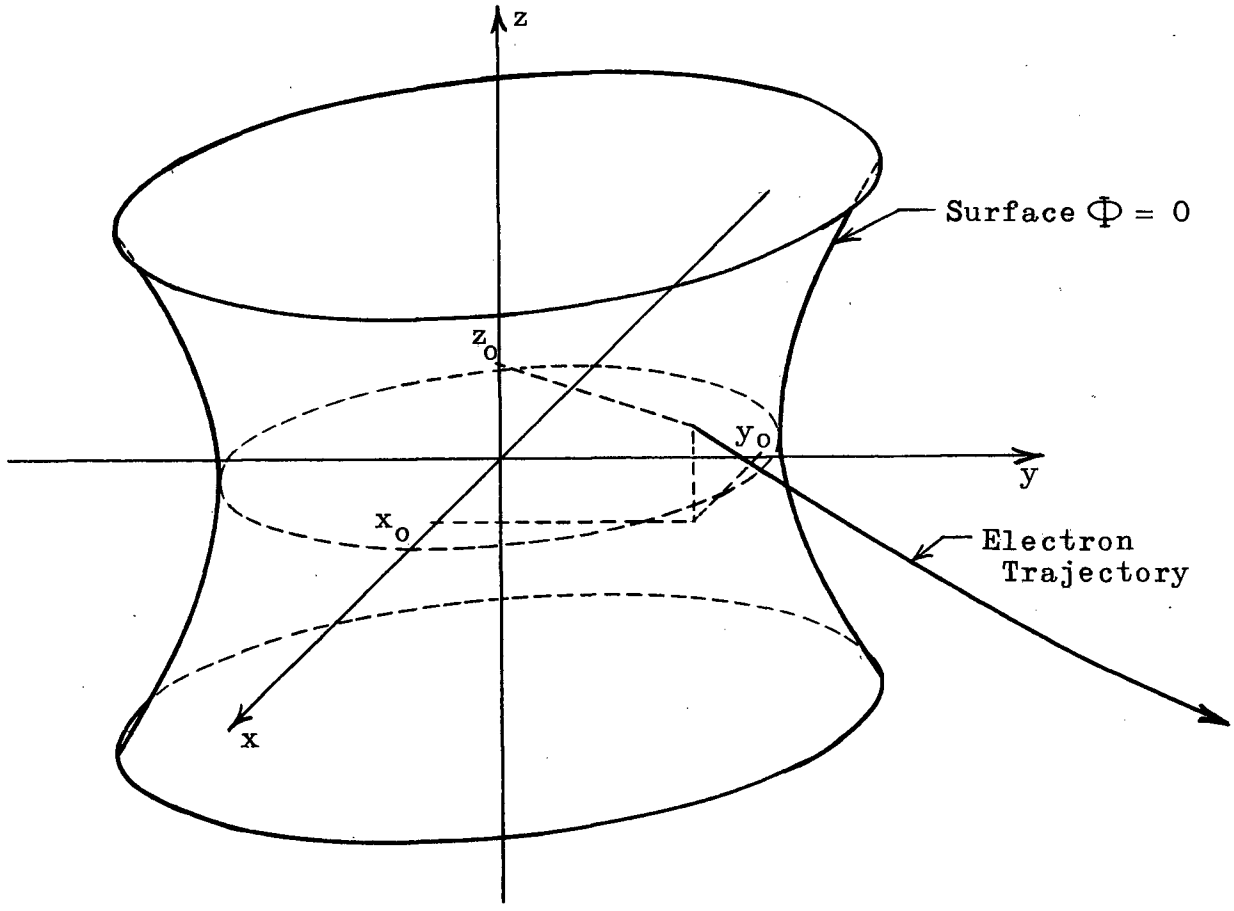

Figure (2-1a). Sketch of a trajectory and of the surface $\Phi = 0$ when the latter is a hyperboloid of one sheet. For this case $C_1 > 0$, $C_2 > 0$, $\Phi_0 < 0$

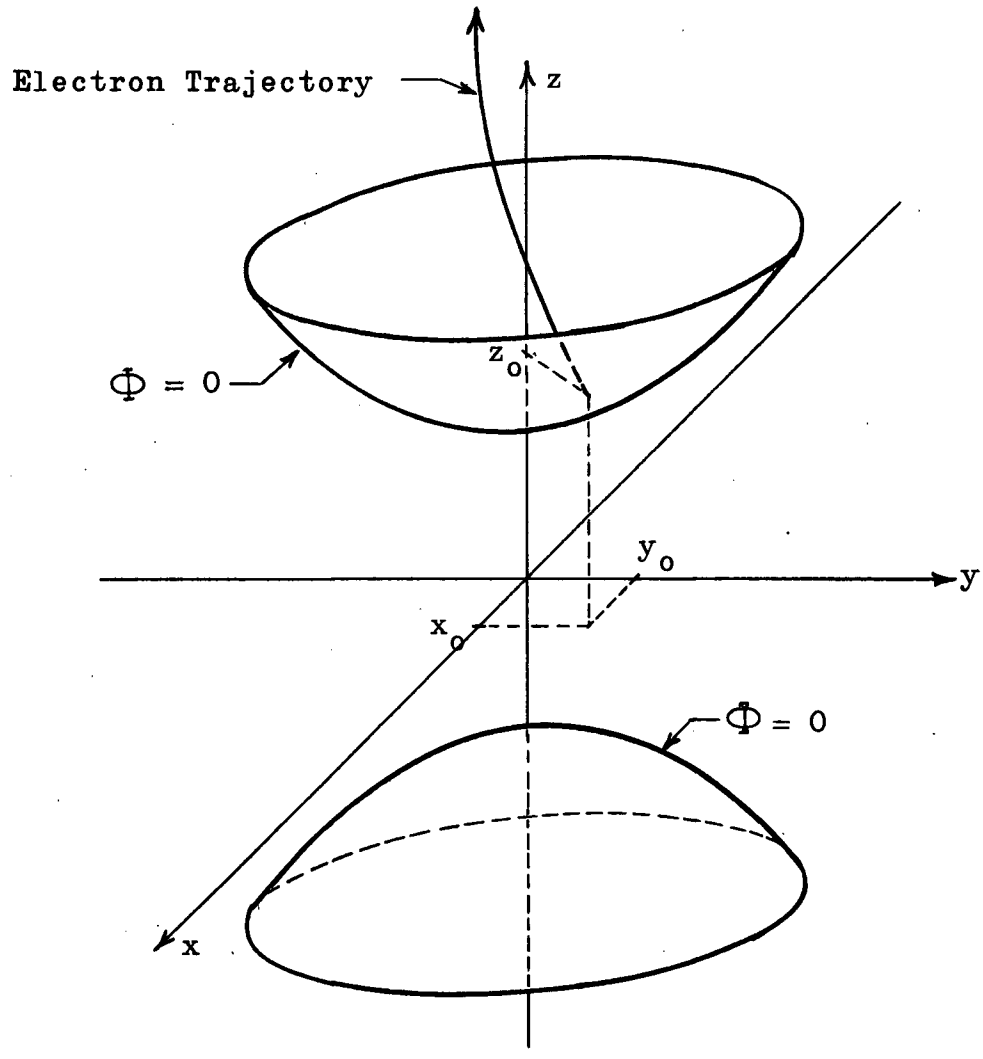

Figure (2-1b). Sketch of a trajectory and of the surface $\Phi = 0$ when the latter is a hyperboloid of two sheets. For this case $C_1 < 0$, $C_2 < 0$, $\Phi_o < 0$

Figures (2-2a and b) for a two-dimensional case, electron motion from a right-angled cathode. This motion results for the special case when the field constants Φ_o, and C_1 or C_2 are set equal to zero in the solution just obtained. From equations (2.37), the trajectory equations for this case are

$$\left.\begin{aligned} x &= x_o \cosh\left(\sqrt{\eta C_1}\, t\right) \\ z &= z_o \cos\left(\sqrt{\eta C_1}\, t\right) \end{aligned}\right\}$$

and the slope along the trajectories is

$$\frac{dz}{dx} = - \left(\frac{z_o}{x_o}\right) \frac{\sin(\sqrt{\eta c_1}\ t)}{\sinh(\sqrt{\eta c_1}\ t)} \quad .$$

In Figure (2-2a) are sketched several trajectories originating from the lower half of the cathode. An envelope which is tangential to these trajectories prior to their first downward deflection is also shown. Similar envelopes occur for the second, third and subsequent reflections, and the second and third envelopes are indicated. These envelopes are straight lines, as may be readily observed from the trajectory equations. It is further apparent, from symmetry considerations, that conditions which are a mirror image of those just discussed will prevail for electron trajectories originating from the upper half of the cathode.

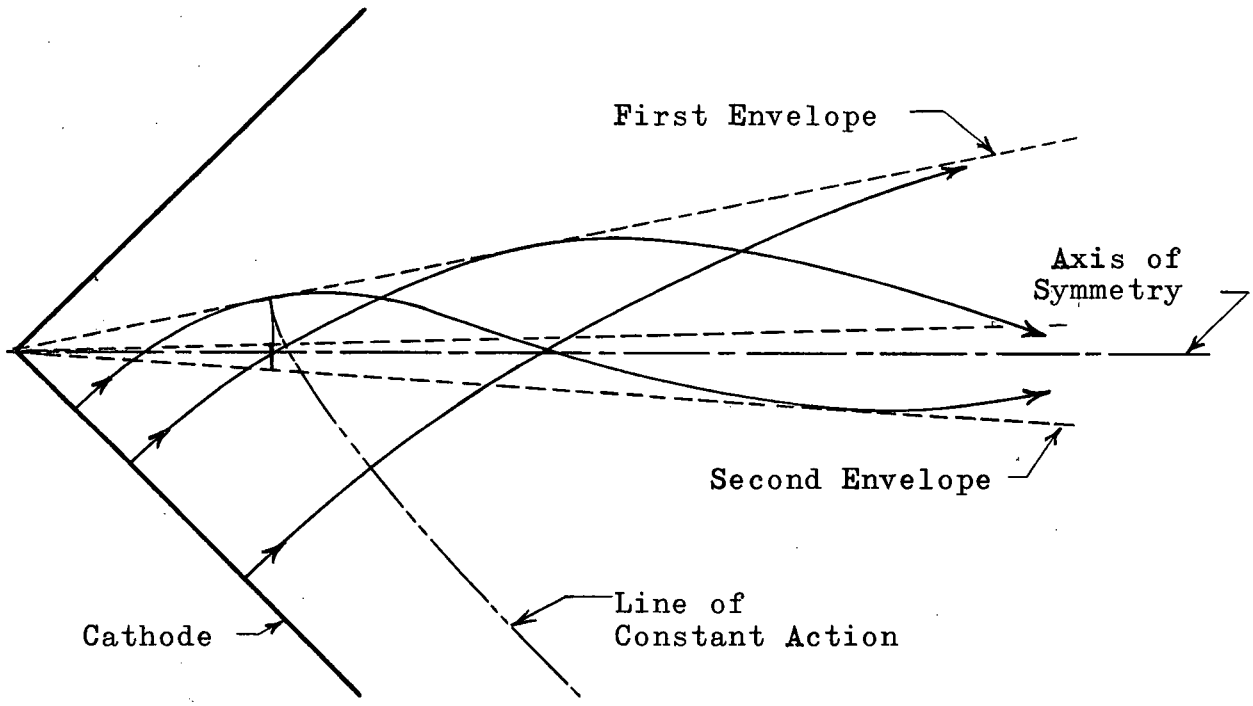

Figure (2-2a). Sketch of electron motion from a right-angled cathode

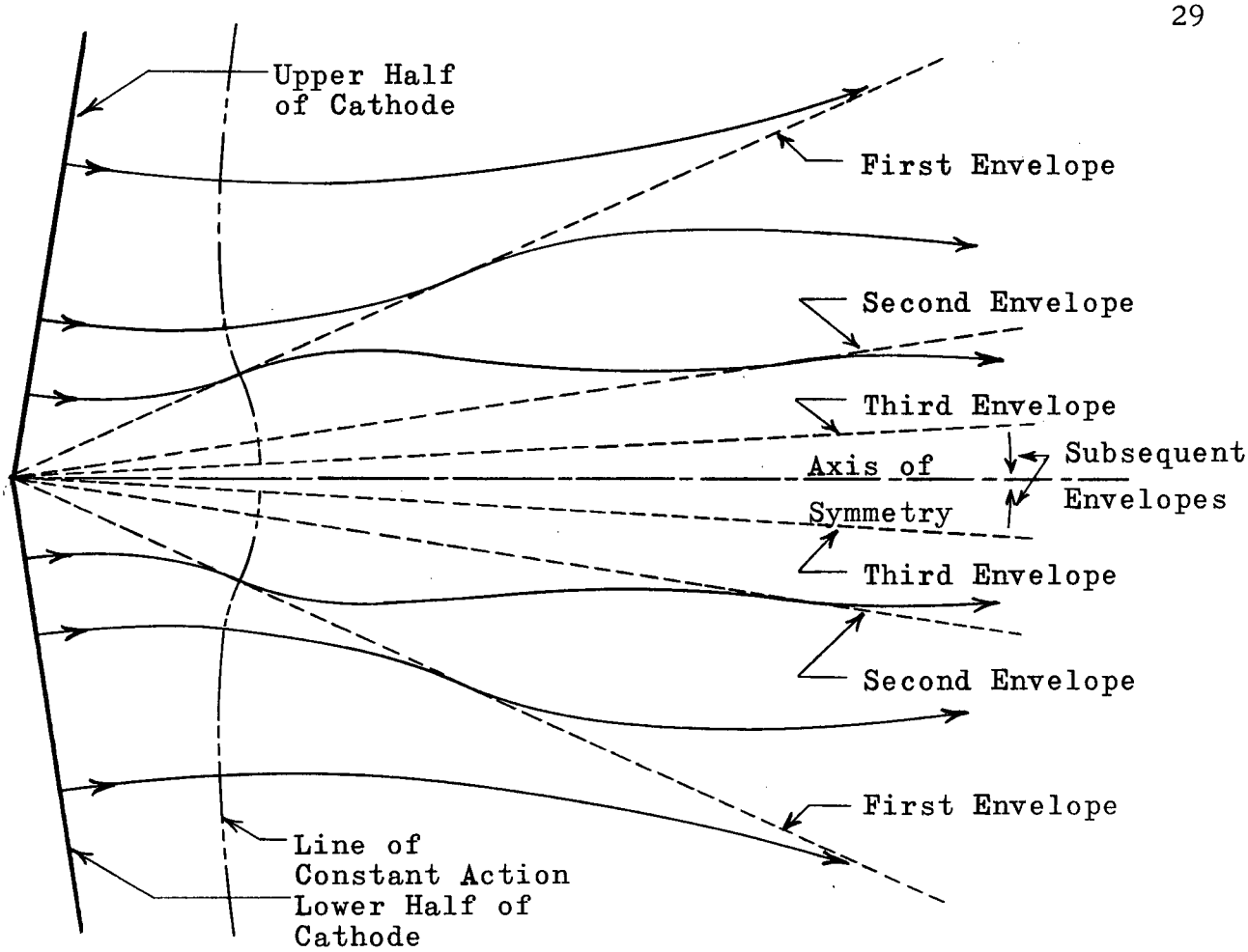

Figure (2-2b). Sketch of the electron motion of Figure (2-2a) when the sheets are unfolded

Since the trajectories are tangential to the trajectory envelopes, action surfaces must be perpendicular to the latter. A line of constant action is sketched in Figure (2-2a), illustrating the multivalued nature of W. Although lines of flow and lines of constant action are orthogonal families of curves, they cannot be represented in this example by the level lines of conjugate harmonic functions[39]. The "complex velocity potential" $W(x,z) + i\Psi(x,z)$, where $\Psi(x,z)$ is the stream function, is therefore not analytic. Nevertheless, the Riemann-surface concept of generalizing the (x,z) plane to a surface of more than one sheet, so that the multivalued "complex velocity potential" has only one value corresponding to each point on that surface, may profitably

be used here. This is illustrated in Figure (2-2b). Consider the trajectories that originate from the lower half of the cathode. The first sheet contains the section of these trajectories between the cathode and their point of tangency to the first trajectory envelope, and it also contains the first branch of W. The second sheet contains the section of the trajectories between the first and second envelopes and the second branch of W, etc., resulting in a surface on which the flow is single-valued. The surface similarly obtained for electron motion originating from the upper half of the cathode can be conjoined to the first surface as shown in Figure (2-2b).

2:4:2 Electron Motion under Space-Charge Conditions

The approach of Sub-section 2:4:1 will now be extended to the space-charge domain. Solutions of the action function W and the potential Φ will once again be sought of the form

$$\left.\begin{aligned} W &= W_1(x) + W_2(y) + W_3(z) \\ \Phi &= \Phi_1(x) + \Phi_2(y) + \Phi_3(z) \quad . \end{aligned}\right\} \tag{2.40}$$

It will be assumed that $W_1(x)$ and $W_2(y)$ are unaltered by the presence of space-charge, so that from equation (2.39)

$$\left.\begin{aligned} W_1(x) &= \tfrac{1}{2}\sqrt{\eta C_1}\left[x\sqrt{x^2 - x_o^2} - x_o^2 \cosh^{-1}\left(\frac{x}{x_o}\right)\right] \\ W_2(y) &= \tfrac{1}{2}\sqrt{\eta C_2}\left[y\sqrt{y^2 - y_o^2} - y_o^2 \cosh^{-1}\left(\frac{y}{y_o}\right)\right] . \end{aligned}\right\} \tag{2.41}$$

The charge density ρ is therefore allowed to be only z-dependent.

From equations (2.41) the velocity is

$$\vec{v} = \nabla W = \left[\pm\sqrt{\eta C_1(x^2 - x_o^2)},\ \pm\sqrt{\eta C_2(y^2 - y_o^2)},\ \frac{dW_3(z)}{dz}\right] . \tag{2.42}$$

When this is substituted into the Hamilton-Jacobi equation, we obtain for the potential

$$\Phi = \frac{1}{2\eta}(\nabla W)^2 = \frac{1}{2}C_1(x^2 - x_o^2) + \frac{1}{2}C_2(y^2 - y_o^2) + \frac{1}{2\eta}\left(\frac{dW_3(z)}{dz}\right)^2 \tag{2.43}$$

which is seen to be of the desired form (2.40b). Substituting this result in turn into the Poisson equation produces

$$\rho = -\varepsilon_o \nabla^2\Phi = -\varepsilon_o\left[C_1 + C_2 + \frac{1}{2\eta}\frac{d^2}{dz^2}\left(\frac{dW_3(z)}{dz}\right)^2\right].$$

Using the above equations for ρ and $\vec{v}$, the remaining space-charge-flow equation to be satisfied, the continuity equation, becomes

$$\nabla\cdot(\rho\vec{v}) = -\varepsilon_o \nabla\cdot\left\{\left[C_1 + C_2 + \frac{1}{2\eta}\frac{d^2}{dz^2}\left(\frac{dW_3(z)}{dz}\right)^2\right]\left[\pm\sqrt{\eta C_1(x^2 - x_o^2)}\,,\ \pm\sqrt{\eta C_2(y^2 - y_o^2)}\,,\ \frac{dW_3(z)}{dz}\right]\right\} = 0$$

which can be rewritten in the form

$$\left[C_1 + C_2 + \frac{1}{2\eta}\frac{d^2}{dz^2}\left(\frac{dW_3(z)}{dz}\right)^2\right]\left[\sqrt{\eta C_1}\,\frac{x}{(x^2 - x_o^2)^{\frac{1}{2}}} + \sqrt{\eta C_2}\,\frac{y}{(y^2 - y_o^2)^{\frac{1}{2}}}\right]$$

$$+ \frac{d}{dz}\left\{\left(\frac{dW_3(z)}{dz}\right)\left[C_1 + C_2 + \frac{1}{2\eta}\frac{d^2}{dz^2}\left(\frac{dW_3(z)}{dz}\right)^2\right]\right\} = 0\ . \tag{2.44}$$

For this equation to be an equation in z only, it is necessary that

$$x_o = y_o = 0\ . \tag{2.45}$$

The equation that must be satisfied by $W_3(z)$ is therefore, from (2.44 and 45),

$$\left[\eta(C_1+C_2)+\left(\frac{d^2W_3(z)}{dz^2}\right)^2+\left(\frac{dW_3(z)}{dz}\right)\left(\frac{d^3W_3(z)}{dz^3}\right)\right](\sqrt{\eta C_1}+\sqrt{\eta C_2}$$

$$+\eta(C_1+C_2)\frac{d^2W_3(z)}{dz^2}+\left[4\left(\frac{dW_3(z)}{dz}\right)\left(\frac{d^2W_3(z)}{dW(z)^2}\right)\left(\frac{d^3W_3(z)}{dz^3}\right)\right.$$

$$\left.+\left(\frac{d^2W_3(z)}{dz^2}\right)^3+\left(\frac{dW_3(z)}{dz}\right)^2\left(\frac{d^4W_3(z)}{dz^4}\right)\right]=0\ . \qquad (2.46)$$

The dependent variable is missing in (2.46); if we set

$$\mathcal{V}_z(z)=\frac{dW_3(z)}{dz}$$

the order of (2.46) can be reduced by one, resulting in

$$\left[\eta(C_1+C_2)+\left(\frac{d\,\mathcal{V}_z(z)}{dz}\right)^2+\mathcal{V}_z(z)\left(\frac{d^2\mathcal{V}_z(z)}{dz^2}\right)\right](\sqrt{\eta C_1}+\sqrt{\eta C_2})$$

$$+\eta(C_1+C_2)\frac{d\,\mathcal{V}_z(z)}{dz}$$

$$+\left[4\mathcal{V}_z(z)\left(\frac{d\mathcal{V}_z(z)}{dz}\right)\left(\frac{d^2\mathcal{V}_z(z)}{dz^2}\right)+\left(\frac{d\,\mathcal{V}_z(z)}{dz}\right)^3+\mathcal{V}_z(z)^2\left(\frac{d^3\mathcal{V}_z(z)}{dz^3}\right)\right]=0\ . \qquad (2.47)$$

For space-charge flow to be possible according to our assumptions, equation (2.47) must be satisfied. Let us try a solution of the form

$$\mathcal{V}_z(z)=Dz^m\ . \qquad (2.48)$$

Then (2.47) becomes

$$(\eta C_1+\eta C_2)(\sqrt{\eta C_1}+\sqrt{\eta C_2})+(\eta C_1+\eta C_2)mDz^{m-1}$$

$$+(\sqrt{\eta C_1}+\sqrt{\eta C_2})m(2m-1)D^2z^{2(m-1)}+D^3m(2m-1)(3m-2)z^{3(m-1)}=0\ . \qquad (2.49)$$

Equation (2.49) is satisfied under the following conditions:

$$m = 1,\ C_1 = \frac{A^2}{\eta}\ ,\ C_2 = \frac{B^2}{\eta}\ ,\ \text{and}\ D = -(A + B)\ . \qquad (2.50)$$

The z-component of velocity is therefore, from (2.48 and 50)

$$v_z(z) = -(A + B)z\ . \qquad (2.51)$$

Combining this result with equations (2.42, 45 and 49), the velocity of the flow is

$$\vec{v} = \left[Ax,\ By,\ -(A + B)z \right]\ . \qquad (2.52)$$

The electrostatic potential of the flow is obtained from equations (2.43, 45, 50 and 51), and is

$$\Phi = \frac{1}{2\eta}\left[A^2x^2 + B^2y^2 + (A^2 + B^2)z^2\right]\ . \qquad (2.53)$$

Equipotential surfaces are seen to be concentric ellipsoids. The charge density of the flow is, from Poisson's equation and (2.53),

$$\rho = -\frac{2\varepsilon_o}{\eta}(A^2 + B^2 + AB)\ . \qquad (2.54)$$

The charge density is thus constant throughout the motion. The action function W is readily found to be

$$W = \frac{1}{2}\left[Ax^2 + By^2 - (A + B)z^2\right]$$

which is harmonic. The equations of the trajectories are easily obtained from equation (2.52):

$$\int_{t_o}^{t} dt = \frac{1}{A}\int_{x_o}^{x}\frac{dx}{x} = \frac{1}{B}\int_{y_o}^{y}\frac{dy}{y} = -\frac{1}{(A + B)}\int_{z_o}^{z}\frac{dz}{z}$$

and hence the trajectories are at the intersections of the two families of surfaces

$$\left.\begin{aligned} \frac{x^{\frac{1}{A}}}{y^{\frac{1}{B}}} &= K_1 \\ \frac{x^{\frac{1}{A}}}{z^{\frac{-1}{A+B}}} &= K_2 \end{aligned}\right\} .$$

The trajectories lie in the surface of the rectangular hyperboloidal family

$$xyz = x_o y_o z_o = \text{constant} .$$

When either A or B is set equal to zero, or B = -A, the motion becomes planar. The equipotential surfaces become concentric cylinders, and the trajectories become plane rectangular hyperbolae. A sketch of this flow is shown in Figure (2-3).

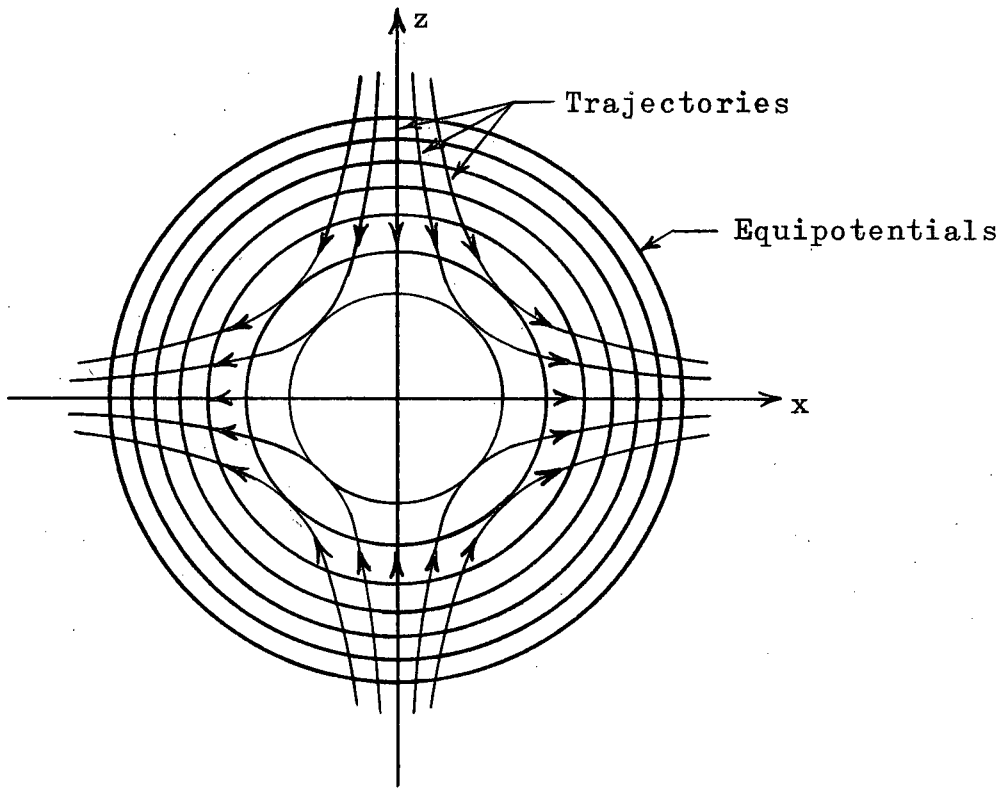

Figure (2-3). Hyperbolic space-charge flow

The space-charge flow according to equations (2.52-54) has also been discovered by Meltzer[33], by a different method.

Another solution of the differential equation (2.47) can be obtained for the special case $C_1 = C_2 = 0$. If equation (2.48) again be substituted into (2.47), there results

$$m(2m - 1)(3m - 2)z^{3(m-1)} = 0,$$

which is satisfied for $m = 0$, $1/2$ and $2/3$. It is readily verified that these three values correspond to parallel rectilinear electron motion (a) in the absence of an electrostatic field, (b) with negligible space-charge effects from the plane $z = 0$, and (c) that is space-charge-limited and originates from a cathode at $z = 0$, respectively, all known cases. No further solutions of equation (2.47) have been obtained.

The hyperbolic flow solution of equations (2.52-54) brings out an important point about the initial conditions that are required for space-charge-limited flow from a zero-potential cathode. Kirstein[36] states:

> "If we require that the motion be physically realizable under space-charge-limited conditions from a zero-potential cathode K, then it is required that, on K, Φ and $\frac{\partial \Phi}{\partial n}$ be zero, where $\vec{n}$ is the unit vector normal to K."

From equation (2.53) we see that for hyperbolic flow the conditions mentioned by Kirstein are satisfied at the origin. Yet the flow is not due to a cathode at the origin. The reason for this disparity is that the charge density ρ for this solution is constant throughout the motion, whereas for space-charge-limited electron flow originating from a zero potential cathode $\rho \rightarrow -\infty$

at the cathode. From Poisson's equation the equivalent condition for Φ is

$$\frac{\partial^2 \Phi}{\partial n^2} \longrightarrow -\infty \text{ at the cathode.}$$

This initial condition thus needs to be applied at the cathode in addition to the conditions

$$\Phi = \frac{\partial \Phi}{\partial n} = 0 \quad .$$

In this section electron-flow solutions were found by formulating the theory in Cartesian coordinates under the assumption that W and Φ could be represented as the sum of terms, each term being a function of only one coordinate. In the next section we will adapt this approach to a formulation of the theory in orthogonal curvilinear coordinates, and determine the conditions for separation of variables to occur.

2:5 Solutions in Plane Curvilinear Coordinates by the Method of Separation of Variables

2:5:1 Action Function of the Form "$W_1(q_1) + W_2(q_2)$"

(a) Conditions for separation of variables

Let (q_1, q_2) be an orthogonal curvilinear coordinate system in which an infinitesimal line element "$d\ell$" is described by

$$d\ell^2 = \sum_{i=1}^{2} h_i^2 dq_i^2 \quad ,$$

where the h_i are the metrical coefficients, defined by

$$h_i^2 = \left(\frac{\partial x}{\partial q_i}\right)^2 + \left(\frac{\partial y}{\partial q_i}\right)^2 \quad .$$

The gradient of the action function W can then be written as

$$\nabla W = \sum_{i=1}^{2} \vec{k}_i \frac{1}{h_i} \frac{\partial W}{\partial q_i} \quad ,$$

and the Hamilton-Jacobi equation is therefore

$$\sum_{i=1}^{2} \frac{1}{h_i^2} \left(\frac{\partial W}{\partial q_i}\right)^2 - 2\eta\Phi = 0 \quad . \tag{2.55}$$

The Laplace equation becomes

$$\nabla^2\Phi = \frac{1}{h_1 h_2}\left[\frac{\partial}{\partial q_1}\left(\frac{h_2}{h_1}\frac{\partial\Phi}{\partial q_1}\right) + \frac{\partial}{\partial q_2}\left(\frac{h_1}{h_2}\frac{\partial\Phi}{\partial q_2}\right)\right] = 0 \quad . \tag{2.56}$$

Let it be assumed that W is of the form

$$W = W_1(q_1) + W_2(q_2) \quad . \tag{2.26a}$$

Equation (2.55) can therefore be rewritten as

$$\frac{1}{h_1^2}\left(\frac{dW_1}{dq_1}\right)^2 + \frac{1}{h_2^2}\left(\frac{dW_2}{dq_2}\right)^2 = 2\eta\Phi \, . \tag{2.57}$$

We must next determine the form of the potential Φ for which equations (2.56 and 57) will separate. If we assume that the h_i are of the functional form

$$h_i = f(q_1, q_2) f_{i1}(q_1) f_{i2}(q_2) \tag{2.58}$$

then it is clear that the left-hand side of equation (2.57) can be separated by multiplying it by $\left(f(q_1, q_2) f_{12}(q_2) f_{21}(q_1)\right)^2$. If this is done, there results

$$\left(\frac{f_{21}(q_1)}{f_{11}(q_1)}\right)^2\left(\frac{dW_1}{dq_1}\right)^2 + \left(\frac{f_{12}(q_2)}{f_{22}(q_2)}\right)^2\left(\frac{dW_2}{dq_2}\right)^2 = 2\eta\left[f(q_1,q_2) f_{12}(q_2) f_{21}(q_1)\right]^2\Phi \, . \tag{2.59}$$

To complete the separation of the Hamilton-Jacobi equation, it is required that the right-hand side of equation (2.59) be of the form

$$g_1(q_1) + g_2(q_2) = 2\eta\left[f(q_1,q_2)f_{12}(q_2)f_{21}(q_1)\right]^2\Phi \,. \tag{2.60}$$

The potential Φ must satisfy (2.56); let the solution be of the form

$$\Phi = \frac{A_{11}(q_1)A_{12}(q_2)}{f^2(q_1, q_2)} + \frac{A_{21}(q_1)A_{22}(q_2)}{f^2(q_1, q_2)} \,. \tag{2.26b}$$

From equations (2.26b and 60) the conditions for separating the variables such that the left side of equation (2.60) is satisfied are therefore

$$\left.\begin{aligned} &1\text{:}\quad (a)\quad f_{12}{}^2(q_2) = \frac{1}{A_{12}(q_2)} \text{ or/and } (b)\quad f_{21}{}^2(q_1) = \frac{1}{A_{11}(q_1)} \\ &2\text{:}\quad (a)\quad f_{21}{}^2(q_1) = \frac{1}{A_{21}(q_1)} \text{ or/and } (b)\quad f_{12}{}^2(q_2) = \frac{1}{A_{22}(q_2)} \end{aligned}\right\} \tag{2.61}$$

where the $f_{i,j}$ and the $A_{i,j}$ are as defined by equations (2.58 and 26b) respectively. At least one part of each of these two conditions must be satisfied for the Hamilton-Jacobi equation to be separable when W is of the form (2.26a) and h_i of the form (2.58). If, for example, the solution of the Laplace equation in a particular coordinate system is of the form of equation (2.26b) and satisfies conditions 1(a) and 2(a), then the potential is of the form

$$\Phi = \frac{A_{11}(q_1)}{f_{12}^2(q_2)f^2(q_1, q_2)} + \frac{A_{22}(q_2)}{f_{21}^2(q_1)f^2(q_1, q_2)}$$

and the Hamilton-Jacobi equation is reduced to quadratures.

(b) Examples

Example #1: Solution in Plane Polar Coordinates

For plane polar coordinates the metrical coefficients are

$$h_1 = 1, \quad h_2 = r \quad .$$

Referring to equation (2.58), it follows that

$$\left.\begin{aligned} f(r,\theta) = f_{11}(r) = f_{12}(\theta) = f_{22}(\theta) = 1 \\ \text{and} \\ f_{21}(r) = r \quad . \end{aligned}\right\}$$

The separability conditions for the Hamilton-Jacobi equation are thus seen to be, from equation (2.61),

$$1: \quad (a) \quad A_{12}(\theta) = 1 \text{ or/and } (b) \quad A_{11}(r) = \frac{1}{r^2}$$

$$2: \quad (a) \quad A_{21}(r) = \frac{1}{r^2} \text{ or/and } (b) \quad A_{22}(\theta) = 1 \quad .$$

With Φ of the assumed functional form of equation (2.26b) the Laplace equation becomes, in plane polar coordinates,

$$A_{12}(\theta)\left[\frac{dA_{11}(r)}{dr} + r\,\frac{d^2A_{11}(r)}{dr^2}\right] + A_{22}(\theta)\left[\frac{dA_{21}(r)}{dr} + r\,\frac{d^2A_{21}(r)}{dr^2}\right]$$

$$+ \frac{A_{11}(r)}{r}\,\frac{d^2A_{12}(\theta)}{d\theta^2} + \frac{A_{21}(r)}{r}\,\frac{d^2A_{22}(\theta)}{d\theta^2} = 0 \quad .$$

When conditions 1(a) and 2(a) are tried in this equation, separation

of variables is achieved, and there results

$$\left.\begin{aligned} r^3\left(\frac{dA_{11}(r)}{dr} + r\,\frac{d^2A_{11}(r)}{dr^2}\right) &= a \\ \text{and} \qquad \frac{d^2A_{22}(\theta)}{d\theta^2} + 4A_{22}(\theta) &= -a \ . \end{aligned}\right\} \qquad (2.62)$$

where "a" is a constant. Φ is of the form

$$\Phi = A_{11}(r) + \frac{1}{r^2}\,A_{22}(\theta) \ .$$

The solutions of the separated differential equations (2.62) are

$$\left.\begin{aligned} A_{11}(r) &= \tfrac{1}{4}\,ar^{-2} + b_1 \ln r + c_1 \\ A_{22}(\theta) &= -\tfrac{1}{4}\,a + b_2 \sin(2\theta) + c_2 \cos(2\theta) \ , \end{aligned}\right\}$$

where a, b_i and c_i are constants. The potential Φ is therefore

$$\Phi = c_1 + b_1 \ln r + r^{-2}\left[b_2 \sin(2\theta) + c_2 \cos(2\theta)\right] \ . \qquad (2.63)$$

The electrostatic field described by this equation is due to a line charge and a double doublet at the origin. The orientation of the double doublet is determined by the relative magnitudes of b_2 and c_2; this is apparent if it is considered that the last two terms of equation (2.63) can be rewritten in the form

$$r^{-2}\sqrt{b_2^{\,2} + c_2^{\,2}}\,\cos\left[2\theta - \tan^{-1}\left(\frac{b_2}{c_2}\right)\right] \ .$$

The constant c_1 in equation (2.63) allows us to assign a reference potential ($\Phi = 0$ in our case) to any equipotential of the field. The electron motion may thus be initiated at any of the equipotentials of the field determined by the values of b_1, b_2 and c_2 by suitably adjusting the constant c_1. Equation (2.63) was also

derived by Iwata[46], by the method of Goursat[45].

The electrostatic field for the case when

$$\Phi = \ln r + \frac{1}{r^2}\sin(2\theta)$$

is illustrated in Figure (2-4). A saddle point of potential is seen to occur at the points $r = \sqrt{2}$, $\theta = \frac{\pi}{4}, \frac{5\pi}{4}$. The saddle point of potential would not have occurred if the field had been due to either the line charge or the double doublet alone. The motion of electrons in this field has some very interesting properties, and these will now be studied.

If we let

$$W = W_r(r) + W_\theta(\theta) \quad ,$$

then the Hamilton-Jacobi equation (2.59) separates into two ordinary differential equations when (2.63) is substituted:

$$\left.\begin{aligned} r^2\left(\frac{dW_r}{dr}\right)^2 - 2\eta r^2(c_1 + b_1 \ln r) &= 2\eta K \\ \text{and} \\ \left(\frac{dW_\theta}{d\theta}\right)^2 - 2\eta\left[b_2\sin(2\theta) + c_2\cos(2\theta)\right] &= -2\eta K \end{aligned}\right\} \quad (2.64)$$

where K is the separation constant. Each of these two equations constitutes a conservation theorem of the motion, and they are in this respect analogous to equations (2.32).

From equation (2.63) it is seen that the coordinates (r_o, θ_o) of an arbitrary point on the zero equipotential are related by

$$r_o^2(c_1 + b_1 \ln r_o) + \left(b_2\sin(2\theta_o) + c_2\cos(2\theta_o)\right) = 0 \quad .$$

At (r_o, θ_o) the velocity is zero; therefore

$$\left.\frac{dW_r}{dr}\right|_{(r_o,\theta_o)} = \frac{1}{r}\left.\frac{dW_\theta}{d\theta}\right|_{(r_o,\theta_o)} = 0 \quad .$$

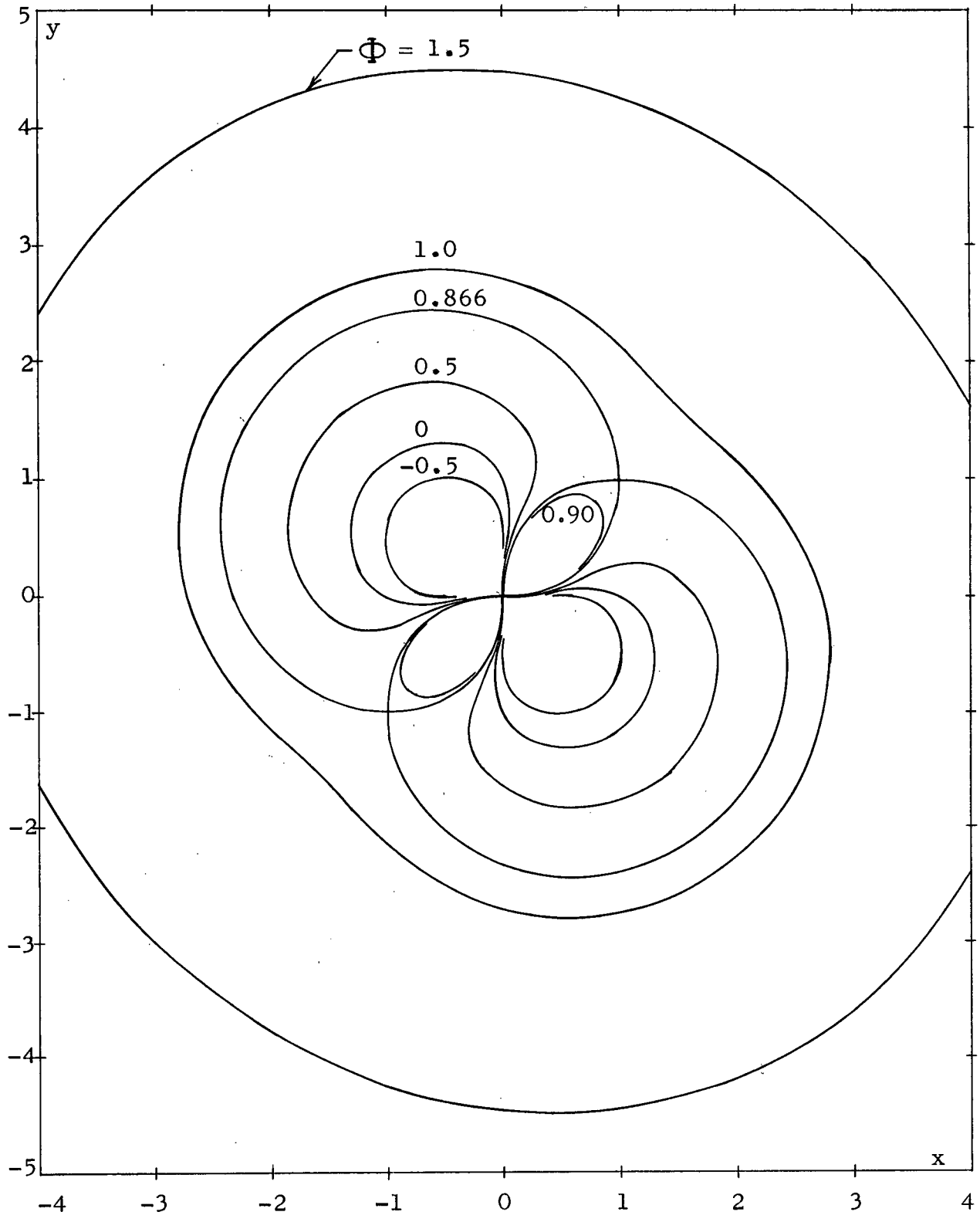

Figure (2-4). Equipotentials of $\Phi = \ln r + \frac{1}{r^2} \sin(2\theta)$

If these initial conditions are substituted into equations (2.64), we obtain

$$\left.\begin{aligned} K + r_o^2(c_1 + b_1 \ln r_o) &= 0 \\ K - \left(b_2 \sin(2\theta_o) + c_2 \cos(2\theta_o)\right) &= 0 \end{aligned}\right\} .$$

The differential equations (2.64) therefore become

$$\left.\begin{aligned} r^2\left(\frac{dW_r}{dr}\right)^2 - 2\eta\left[c_1(r^2 - r_o^2) + b_1(r^2 \ln r - r_o^2 \ln r_o)\right] &= 0 \\ \left(\frac{dW_\theta}{d\theta}\right)^2 - 2\eta\left[b_2\left(\sin(2\theta) - \sin(2\theta_o)\right) + c_2\left(\cos(2\theta) - \cos(2\theta_o)\right)\right] &= 0 \end{aligned}\right\} . \quad (2.65)$$

For an electron starting from rest at a point (r_o, θ_o) on the cathode, the velocity at the point (r, θ) on its trajectory is, from equations (2.17 and 65),

$$\vec{v} = \left[\pm\left\{\frac{2\eta}{r^2}\left(c_1(r^2 - r_o^2) + b_1(r^2 \ln r - r_o^2 \ln r_o)\right)\right\}^{\frac{1}{2}} , \pm\left\{\frac{2\eta}{r^2}\left(b_2(\sin 2\theta - \sin 2\theta_o) + c_2(\cos 2\theta - \cos 2\theta_o)\right)\right\}^{\frac{1}{2}} \right] . \quad (2.66)$$

If we let

$$\left.\begin{aligned} R &= e^{\left(\frac{c_1}{b_1}\right)} r \\ \text{and} \qquad \Theta &= \theta - \tfrac{1}{2} \tan^{-1}\left(\frac{b_2}{c_2}\right) \end{aligned}\right\} \quad (2.67)$$

then equation (2.66) can be rewritten in the form

$$\vec{v} = \left[\pm \sqrt{2\eta b_1} \sqrt{\ln R - \frac{R_o^2}{R^2} \ln R_o}, \pm \frac{\sqrt{4\eta(b_2^2 + c_2^2)^{\frac{1}{2}}}}{r} \sqrt{\sin^2 \Theta_o - \sin^2 \Theta} \right],$$

$$(b_1 > 0)^* .$$

To permit the electron motion in four-dimensional phase-space to be represented in two dimensions independently of the magnitude of the constants b_1, b_2, c_1 and c_2, it is convenient to write the velocity components (v_r, v_Θ) in the form

$$\left.\begin{aligned} \frac{v_r}{\sqrt{2\eta b_1}} &= \pm \sqrt{\ln R - \frac{R_o^2}{R^2} \ln R_o} \\ \frac{v_\Theta r}{\sqrt{4\eta (b_2^2 + c_2^2)^{\frac{1}{2}}}} &= \pm \sqrt{\sin^2 \Theta_o - \sin^2 \Theta} \, . \end{aligned}\right\} \quad (2.68)$$

Equations (2.68) are illustrated in Figures (2-5a and b). It is seen that an electron released from rest at a point (R_o, Θ_o) on the cathode oscillates about the line $\Theta = n\pi$ as the radial velocity component increases in magnitude. If the initial radial coordinate $R_o > 0.60653$, the electron will move away from the coordinate centre, while for R_o less than this value the electron will move towards the centre. This division of the trajectories

* For $b_1 < 0$ the radial velocity component can be written as

$$v_r = \pm \sqrt{-2\eta b_1} \sqrt{\frac{R_o^2}{R^2} \ln R_o - \ln R} \, .$$

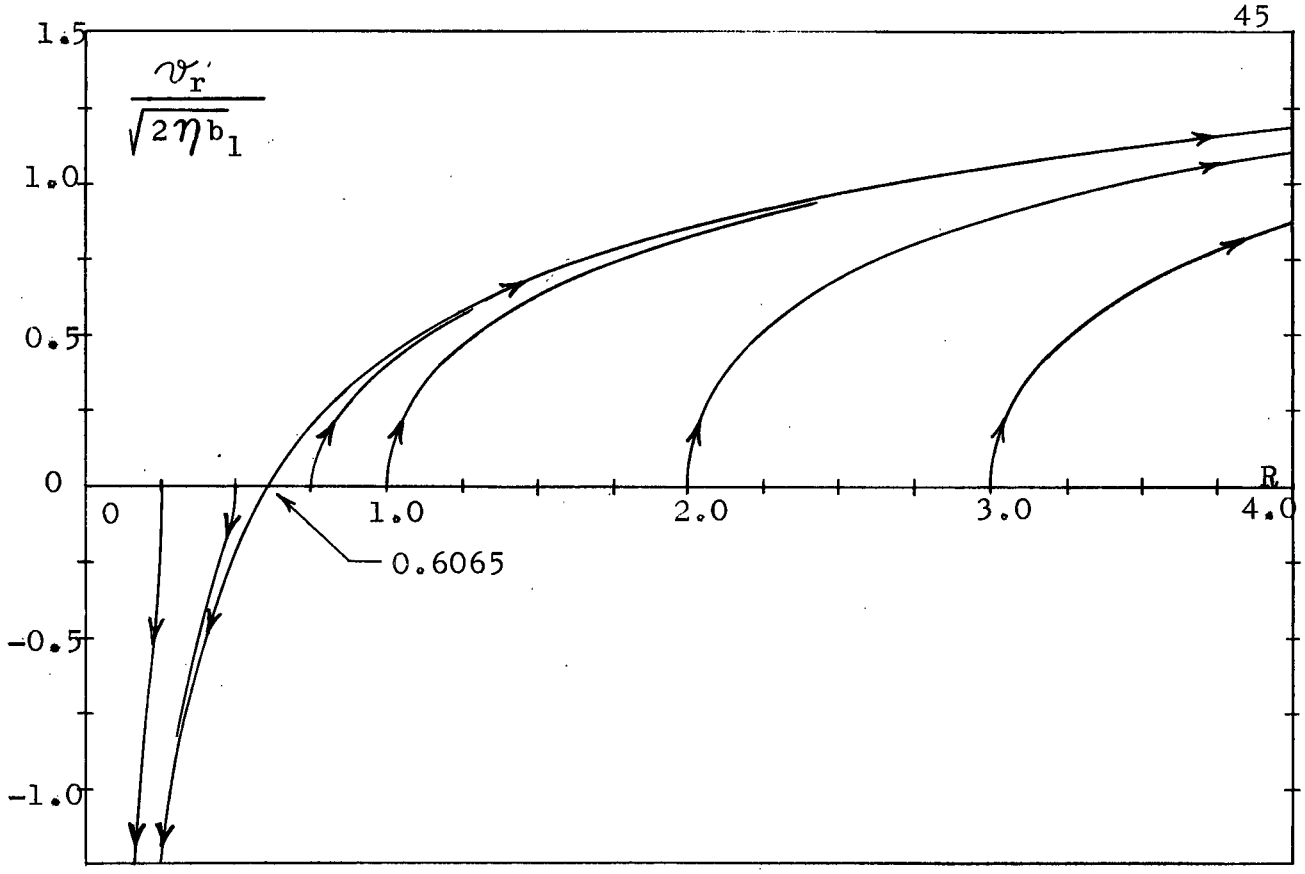

Figure (2-5a). Phase plot of the radial velocity component of equation (2.68)

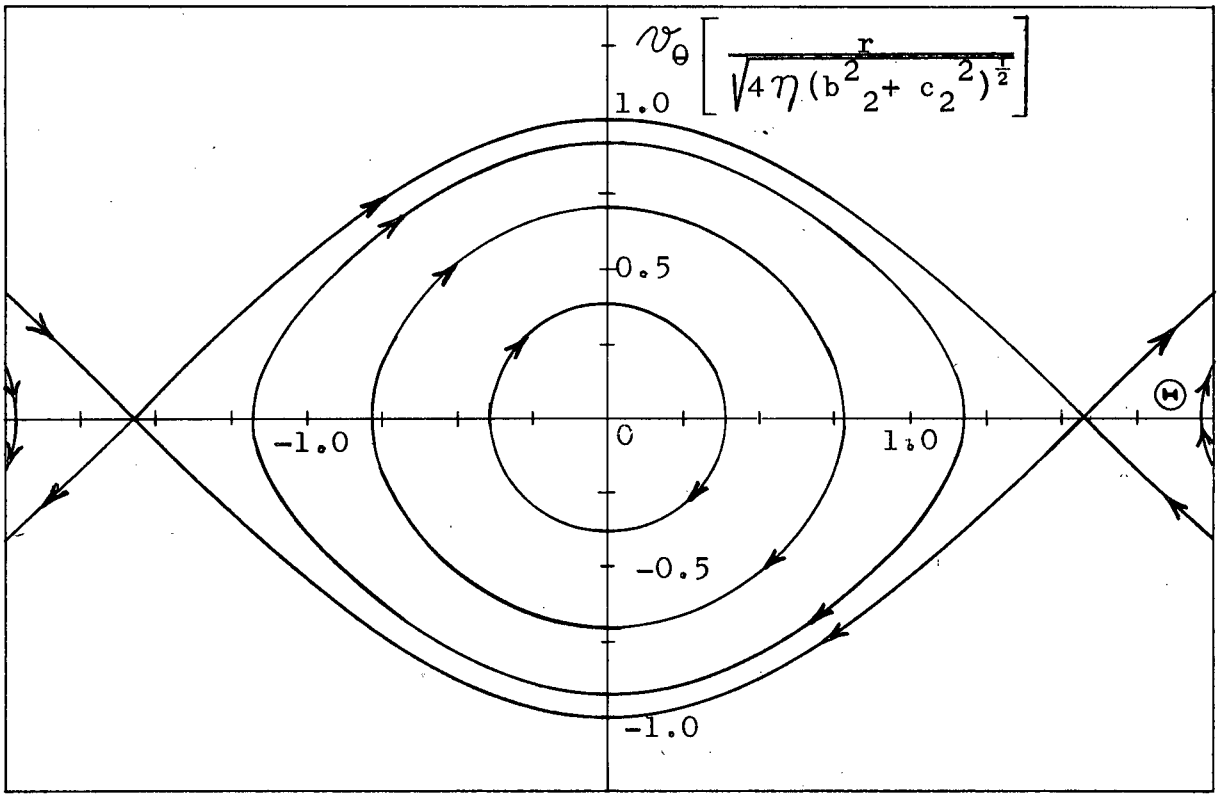

Figure (2-5b). Phase plot of the θ-component of velocity of equation (2.68)

is due to the saddle-shaped nature of the electrostatic field.

For the electrostatic field illustrated in Figure (2-4) the normalized coordinates are

$$\left.\begin{aligned} R &= r \\ \Theta &= \theta - \frac{\pi}{4} \end{aligned}\right\} .$$

For this case the limiting cathode radius dividing inward and outward motion is $r_o = 0.60653$, and the electron oscillation occurs about the line $y = x$.

When the field is due only to a line charge, so that $b_2 = c_2 = 0$, the equipotentials will be concentric circles, and the trajectories lie along radial lines. For this case, it is seen from the initial conditions that the constant $K = 0$, so the radial velocity is simply

$$v_r = \sqrt{2\eta b_1 \ln R} \quad .$$

For the special case when the electrostatic field is due only to a double doublet, so that $b_1 = 0$, the radial velocity component of the motion is, from (2.66),

$$v_r = \pm \sqrt{2\eta\, c_1 \left(1 - \frac{r^2}{r_o^2}\right)} \quad .$$

Thus when the field constant c_1 is greater than or less than zero, the radial velocity will be outward or inward respectively, independent of the starting point on the cathode. When c_1 is zero, however, the radial velocity is zero along the trajectory; an electron released from rest from any point on the zero equipotential thus has the remarkable property of travelling along an arc of a circle. From equation (2.63) the zero equipotentials

of this field can be deduced to be the straight lines

$$\theta = \frac{1}{2}\left(\frac{\pi}{2} + n\pi + \tan^{-1}\left(\frac{b_2}{c_2}\right)\right) \quad .$$

Again for this special case the separation constant K is zero, and the electron velocity is therefore

$$v_\theta = \pm \sqrt{2\,\eta\,(b_2^{\,2} + c_2^{\,2})^{\frac{1}{2}}\; r_o^{\,-2} \cos\,(2\Theta)} \quad .$$

For the general case, the trajectories are described by

$$\frac{v_r}{v_\theta} = \frac{dr}{r d\theta} = \left[\frac{c_1(r^2 - r_o^{\,2}) + b_1(r^2 \ln r - r_o^{\,2} \ln r_o)}{b_2(\sin 2\theta - \sin 2\theta_o) + c_2(\cos 2\theta - \cos 2\theta_o)}\right]^{\frac{1}{2}}$$

which in integral form is

$$\int_{r_o}^{r} \frac{dr}{r\left[c_1(r^2 - r_o^{\,2}) + b_1(r^2 \ln r - r_o^{\,2} \ln r_o)\right]^{\frac{1}{2}}} =$$

$$= \int_{\theta_o}^{\theta} \frac{d\theta}{\left[b_2(\sin 2\theta - \sin 2\theta_o) + c_2(\cos 2\theta - \cos 2\theta_o)\right]^{\frac{1}{2}}} \quad .$$

If use is again made of the normalized variables of equations (2.67), these integrals can be rewritten as

$$\frac{e^{\frac{c_1}{b_1}}}{\sqrt{b_1}} \int_{e^{\frac{c_1}{b_1}} r_o}^{e^{\frac{c_1}{b_1}} r} \frac{dR}{R\sqrt{R^2 \ln R - R_o^{\,2} \ln R_o}} = \frac{|k|}{\sqrt{2}(b_2^{\,2} + c_2^{\,2})^{\frac{1}{4}}} \int_{\theta_o - \frac{1}{2}\tan^{-1}\left(\frac{b_2}{c_2}\right)}^{\theta - \frac{1}{2}\tan^{-1}\left(\frac{b_2}{c_2}\right)} \frac{d\Theta}{\sqrt{1 - k^2 \sin^2 \Theta}}$$

where

$$k = \frac{1}{\sin \Theta_o} \quad , \; b_1 > 0 \quad .*$$

If $R_o = 1$, the substitution

$$R = e^{x^2}$$

changes the integral in r to:

$$I_r\Big|_{R_o = 1} = \frac{2e^{\frac{c_1}{b_1}}}{\sqrt{b_1}} \int_0^{\sqrt{\frac{c_1}{b_1} + \ln r}} e^{-x^2} dx = \left[\frac{\pi e^{\frac{c_1}{b_1}}}{b_1}\right]^{\frac{1}{2}} \operatorname{erf}\left(\sqrt{\frac{c_1}{b_1} + \ln r}\right),$$

where erf (ξ) is the well-known error function, defined by

$$\operatorname{erf}(\xi) \triangleq \frac{2}{\sqrt{\pi}} \int_0^{\xi} e^{-x^2} dx \quad .$$

In the integral in Θ, $|k| \geq 1$. The physical significance of the amplitude of k being greater than unity is that it restricts the motions in the θ-direction to the libration type discussed earlier. The behaviour of the the θ-component of the electron velocity is quite similar to the well-known motion of a

---

* When $b_1 = 0$ the integral in r, I_r, integrates directly to give

$$I_r\Big|_{b_1 = 0} = \frac{1}{r_o \sqrt{c_1}} \cos^{-1}\left(\frac{r_o}{r}\right) \quad .$$

For $b_1 < 0$ the substitution $R = e^{-\frac{c_1}{b_1} r}$ can again be used.

simple pendulum, discussed, for example, by Goldstein[47].

Example #2: Solution in Equiangular Spiral Coordinates

The metrical coefficient of an equiangular spiral (or logarithmic spiral) coordinate system is

$$h = h_1 = h_2 = e^{b_1 u + b_2 v} \quad , \tag{2.69}$$

where b_1 and b_2 are arbitrary constants. If

$$z = x + iy \text{ and } w = u + iv \quad ,$$

then z and w are related by the transformation

$$z = \frac{e^{(b_1 - ib_2)w}}{(b_1^2 + b_2^2)^{\frac{1}{2}}} \quad .$$

This equation is readily expressed in polar coordinates:

$$r = \frac{e^{b_1 u + b_2 v}}{\sqrt{b_1^2 + b_2^2}} \quad , \quad \theta = b_1 v - b_2 u \quad . \tag{2.70}$$

From the polar coordinates the multivalued nature of the (u,v) coordinate system is readily apparent. Thus the coordinates

$$\left.\begin{aligned} u &= u_o - \left(\frac{b_2}{b_1^2 + b_2^2}\right) 2n\pi \\ \text{and} \qquad v &= v_o + \left(\frac{b_1}{b_1^2 + b_2^2}\right) 2n\pi \quad , \end{aligned}\right\} \tag{2.71}$$

where (u_o, v_o) are any initial coordinates and n is any integer, refer to the same point in space. The range of (u,v) therefore needs to be restricted so that the mapping of (u,v) in the z-plane

is single-valued. This will insure that the potential Φ expressed in (u,v) coordinates will be single-valued in space. In Figure (2-6) is shown a sheet of the equiangular spiral coordinate system for which $b_1 = b_2 = 1$.

From equations (2.58 and 69) it is found that

$$\left.\begin{aligned} f(u,v) &= 1 \\ f_{11}(u) = f_{21}(u) &= e^{b_1 u} \\ \text{and} \\ f_{12}(v) = f_{22}(v) &= e^{b_2 v} \quad . \end{aligned}\right\}$$

From equations (2.26b and 61), a possible form of Φ therefore is

$$\Phi = A_{11}(u)e^{-2b_2 v} + e^{-2b_1 u}A_{22}(v) \quad . \qquad (2.72)$$

When this functional form of Φ is substituted into the Laplace equation (2.56), there results

$$\frac{\partial^2\Phi}{\partial u^2} + \frac{\partial^2\Phi}{\partial v^2} = e^{-2b_2 v}\left[\frac{d^2A_{11}(u)}{du^2} + 4b_2{}^2A_{11}(u)\right] + e^{-2b_1 u}\left[\frac{d^2A_{22}(v)}{dv^2} + 4b_1{}^2A_{22}(v)\right] = 0 \quad .$$

This differential equation is of separable form, and separates into the equations

$$\left.\begin{aligned} \frac{d^2A_{11}(u)}{du^2} + 4b_2{}^2A_{11}(u) - ae^{-2b_1 u} &= 0 \\ \frac{d^2A_{22}(v)}{dv^2} + 4b_1{}^2A_{22}(v) + ae^{-2b_2 v} &= 0 \quad , \end{aligned}\right\}$$

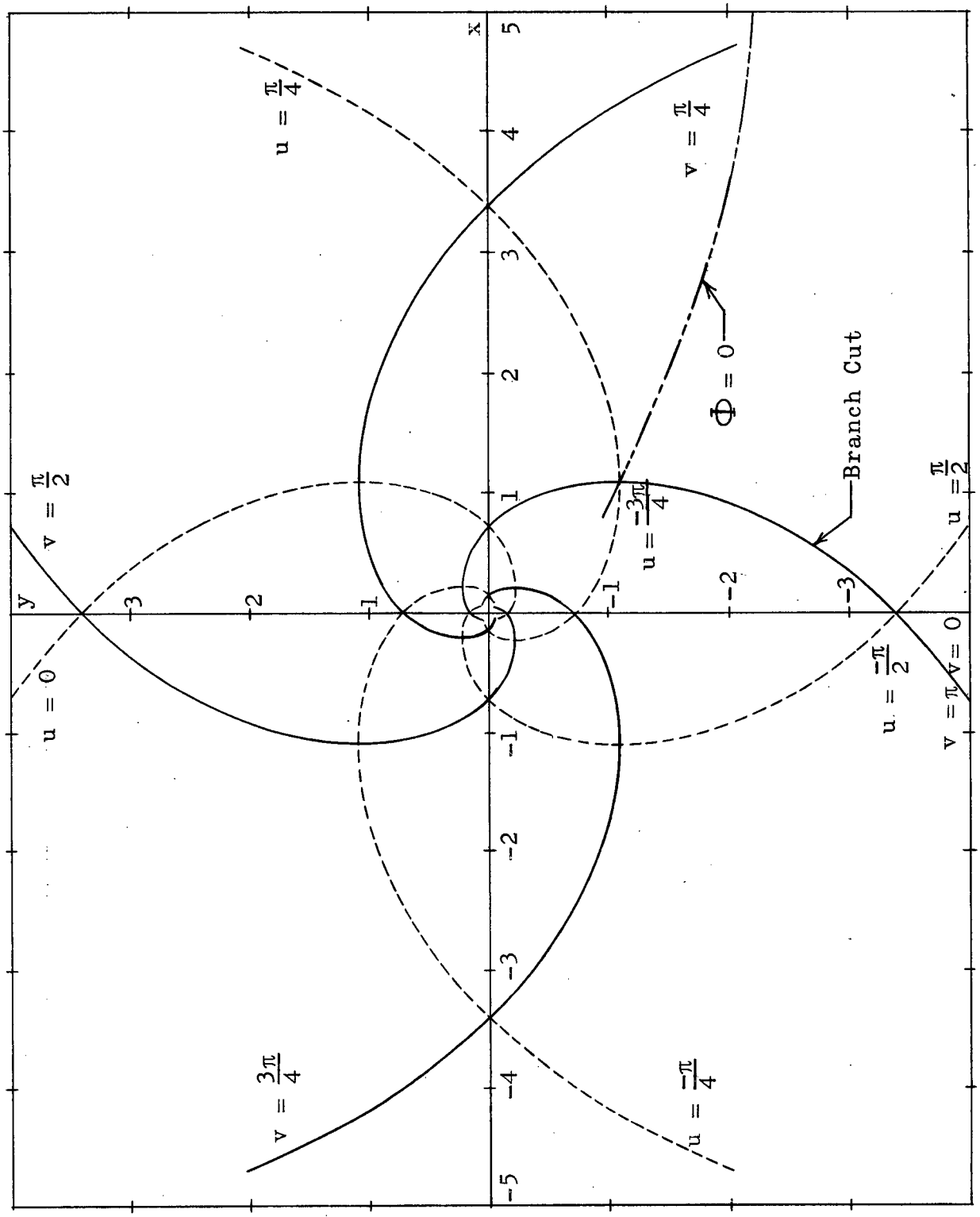

Figure (2-6). Logarithmic spiral coordinates:

$$r = \frac{e^{u + v}}{\sqrt{2}} \quad , \quad \theta = v - u$$

where "a" is a constant. The solutions of these equations are

$$\left.\begin{aligned} A_{11}(u) &= c_1 \sin(2b_2u) + d_1 \cos(2b_2u) + \frac{ae^{-2b_1u}}{4(b_1^2 + b_2^2)} \\ A_{22}(v) &= c_2 \sin(2b_1v) + d_2 \cos(2b_1v) - \frac{ae^{-2b_2v}}{4(b_1^2 + b_2^2)} \end{aligned}\right\} .$$

Substituting these results into equation (2.72), the electrostatic field is

$$\Phi = e^{-2b_2v}\left[c_1 \sin(2b_2u) + d_1 \cos(2b_2u)\right] + e^{-2b_1u}\left[c_2 \sin(2b_1v) + d_2 \cos(2b_1v)\right] ,$$

where c_1, c_2, d_1 and d_2 are constants determined by the boundary conditions. It is convenient to rewrite this equation in the form

$$\Phi = \sqrt{c_1^2 + d_1^2}\; e^{-2b_2v} \cos\left((2b_2u) - \tan^{-1}\left(\frac{c_1}{d_1}\right)\right) + \sqrt{c_2^2 + d_2^2}\; e^{-2b_1u} \cos\left((2b_1v) - \tan^{-1}\left(\frac{c_2}{d_2}\right)\right) . \quad (2.73)$$

To understand the physical behaviour of this electrostatic field, consider first the field Φ_1 due to the first term of (2.73) alone.

That is,

$$\Phi_1 = \sqrt{c_1^2 + d_1^2}\; e^{-2b_2v} \cos\left(2b_2u - \tan^{-1}\left(\frac{c_1}{d_1}\right)\right) .$$

The zero equipotentials of Φ_1 are the logarithmic spirals

$$b_2u = \frac{1}{2}\left[\frac{\pi}{2} + n\pi + \tan^{-1}\left(\frac{c_1}{d_1}\right)\right] ,$$

where n is any integer. Thus, in the coordinate system illustrated in Figure (2-6) for which $b_1 = b_2 = 1$, if we set $c_1 = 0$, the zero equipotentials of Φ_1 are the spirals

$$u = \frac{\pi}{4} + \frac{n\pi}{2} \quad .$$

For a given v, when

$$b_2 u = \frac{1}{2}\left[2n\pi + \tan^{-1}\left(\frac{c_1}{d_1}\right)\right] \quad , \qquad (2.74)$$

Φ_1 is a maximum. It can also be observed from equations (2.70) that when $b_2 v \longrightarrow -\infty$, while u is kept constant, $r \longrightarrow 0$. If we let $b_2 v \longrightarrow -\infty$ along a u-spiral described by equation (2.74), then $\Phi_1 \longrightarrow +\infty$.

For a given v, when

$$b_2 u = \frac{1}{2}\left[\pi + 2n\pi + \tan^{-1}\left(\frac{c_1}{d_1}\right)\right] \quad ,$$

Φ_1 is a minimum, and further when $b_2 v \longrightarrow -\infty$ along a u-spiral described by this equation, then $\Phi_1 \longrightarrow -\infty$. The behaviour of Φ_1 as $b_2 v \longrightarrow -\infty$ is seen to be similar to the behaviour of the potential in the vicinity of a double doublet. We note from equations (2.71), however, that as $b_2 u$ varies over an interval 2π, the coordinates (u,v) encircle the z-plane N times, where

$$N = \frac{b_1^{\,2} + b_2^{\,2}}{b_2^{\,2}} \quad .$$

Thus, for the coordinate system of Figure (2-6), for which $b_1 = b_2 = 1$, the Riemann surface covers two sheets.

The electrostatic field described by the second term of equation (2.73) is

$$\Phi_2 = \sqrt{c_2^2 + d_2^2}\, e^{-2b_1 u} \cos\left(2b_1 v - \tan^{-1}\left(\frac{c_2}{d_2}\right)\right) .$$

The functional form of Φ_2 is seen to be the same as that of Φ_1 when the variables u and v are interchanged. Thus, analogously to Φ_1, zero equipotentials of Φ_2 are the constant v-spirals

$$b_1 v = \frac{1}{2}\left(\frac{\pi}{2} + n\pi + \tan^{-1}\left(\frac{c_2}{d_2}\right)\right)$$

and $\Phi_2 \longrightarrow +\infty$ when $b_1 u \longrightarrow -\infty$ along the spiral

$$b_1 v = \frac{1}{2}\left(2n\pi + \tan^{-1}\left(\frac{c_2}{d_2}\right)\right) ,$$

while $\Phi_2 \longrightarrow -\infty$ when $b_1 u \longrightarrow -\infty$ along the spiral

$$b_1 v = \frac{1}{2}\left(\pi + 2n\pi + \tan^{-1}\left(\frac{c_2}{d_2}\right)\right) .$$

As $b_1 v$ varies over an interval 2π, the coordinates (u,v) encircle the z-plane M times, where

$$M = \frac{b_1^2 + b_2^2}{b_1^2} .$$

Since u and v are orthogonal coordinates, the spirals of constant u and of constant v rotate about the origin of the z-plane in opposite directions. The potential Φ described by equation (2.73) is thus the sum of two potential functions Φ_1 and Φ_2, whose general properties are the same but are oppositely directed. A section of the equipotential $\Phi = 0$ is shown in Figure (2-6) for

the case in which the constants of the electrostatic field are

$$d_1 = c_2 = 1 \text{ and } c_1 = d_2 = 0 \quad .$$

The electron motion in this electrostatic field will be studied next. If an action function of the form

$$W = W_u(u) + W_v(v)$$

is assumed, the Hamilton-Jacobi equation (2.57) can be written as

$$\left.\begin{aligned} &\left(\frac{dW_u}{du}\right)^2 - 2\eta\left[e^{2b_1u}\left(c_1\sin(2b_2u) + d_1\cos(2b_2u)\right) + K\right] = 0 \\ \text{and} \\ &\left(\frac{dW_v}{dv}\right)^2 - 2\eta\left[e^{2b_2v}\left(c_2\sin(2b_1v) + d_2\cos(2b_1v)\right) - K\right] = 0 \end{aligned}\right\} , \tag{2.75}$$

where K is the separation constant.

The coordinates (u_o, v_o) of an arbitrary point on the zero equipotential are found from equation (2.73) to be related by

$$e^{2b_1u_o}\left(c_1\sin(2b_2u_o)+d_1\cos(2b_2u_o)\right) + e^{2b_2v_o}\left(c_2\sin(2b_1v_o)+d_2\cos(2b_1v_o)\right) = 0 \quad .$$

Since by hypothesis the electron velocity is zero at (u_o, v_o), we have

$$e^{-(b_1u+b_2v)}\left.\frac{dW_u}{du}\right|_{(u_o,v_o)} = e^{-(b_1u+b_2v)}\left.\frac{dW_v}{dv}\right|_{(u_o,v_o)} = 0 \quad .$$

If these initial conditions are substituted into equations (2.75), we obtain the following relations for the separation constant:

$$e^{2b_1u_o}\left(c_1\sin(2b_2u_o) + d_1\cos(2b_2u_o)\right) + K = 0$$

and

$$e^{2b_2v_o}\left(c_2\sin(2b_1v_o) + d_2\cos(2b_1v_o)\right) - K = 0 \qquad (2.76)$$

The velocity of an electron starting from an arbitrary point (u_o, v_o) on the cathode is

$$\vec{v} = \left[\pm \frac{\sqrt{2\eta}}{e^{b_2v}}\left(c_1\sin(2b_2u) + d_1\cos(2b_2u) + Ke^{-2b_1u}\right)^{\frac{1}{2}}, \right.$$

$$\left. \pm \frac{\sqrt{2\eta}}{e^{b_1u}}\left(c_2\sin(2b_1v) + d_2\cos(2b_1v) - Ke^{-2b_2v}\right)^{\frac{1}{2}} \right].$$

If the substitutions

$$\left.\begin{aligned} \alpha &= 2b_2u - \tan^{-1}\left(\frac{c_1}{d_1}\right) \\ \beta &= 2b_1v - \tan^{-1}\left(\frac{c_2}{d_2}\right) \end{aligned}\right\}$$

are made, the velocity equation becomes

$$\vec{v} = \left[\pm \frac{\sqrt{2\eta(c_1^2 + d_1^2)^{\frac{1}{2}}}}{e^{b_2v}}\left(\cos\alpha - e^{\frac{b_1}{b_2}(\alpha_o-\alpha)}\cos\alpha_o\right)^{\frac{1}{2}}, \right.$$

$$\left. \pm \frac{\sqrt{2\eta(c_2^2 + d_2^2)^{\frac{1}{2}}}}{e^{b_1u}}\left(\cos\beta - e^{\frac{b_2}{b_1}(\beta_o-\beta)}\cos\beta_o\right)^{\frac{1}{2}} \right].$$

In order to permit the motion in four-dimensional phase-space to be represented in two dimensions for a particular coordinate system (i.e., b_1 and b_2 given), it is convenient to

write the velocity components $(\dot{u},\dot{v})$ in the form

$$\left.\begin{aligned} \dot{u}\left[\frac{e^{b_2 v}}{\sqrt{2\eta(c_1^2+d_1^2)^{\frac{1}{2}}}}\right] &= \pm\left(\cos\alpha - e^{\frac{b_1}{b_2}(\alpha_o-\alpha)}\cos\alpha_o\right)^{\frac{1}{2}} \\ \text{and} \\ \dot{v}\left[\frac{e^{b_1 u}}{\sqrt{2\eta(c_2^2+d_2^2)^{\frac{1}{2}}}}\right] &= \pm\left(\cos\beta - e^{\frac{b_2}{b_1}(\beta_o-\beta)}\cos\beta_o\right)^{\frac{1}{2}}. \end{aligned}\right\} \quad (2.77)$$

Because the functional forms of equations (2.77) are identical, only one phase portrait is required. The phase portrait of equations (2.77) is shown in Figure (2-7).

It is apparent from the phase portrait that the electron motion can be either oscillatory or rotational in either coordinate. Also, if the cathode passes through the points $(\alpha_o,\beta_o) = (-\frac{3\pi}{4}, \frac{\pi}{4})$ or $(\frac{\pi}{4}, -\frac{3\pi}{4})$, a division of trajectories is seen to occur; this is due to a saddle point of potential.

In Example #1 it was found that, as special cases of the general solution, electron motion along either of the coordinates could be obtained. This will now be shown to be true also for the present formulation. If the electrostatic field is due only to Φ_1, so that $c_2 = d_2 = 0$, then it follows from equation (2.76b) that $K = 0$. If an electron is now released from rest at a surface $\Phi_1 = 0$, that is, a spiral

$$u_o = \frac{1}{2b_2}\left[\frac{\pi}{2} + n\pi + \tan^{-1}\left(\frac{c_1}{d_1}\right)\right],$$

then it can be seen from equation (2.77) that the v-component of

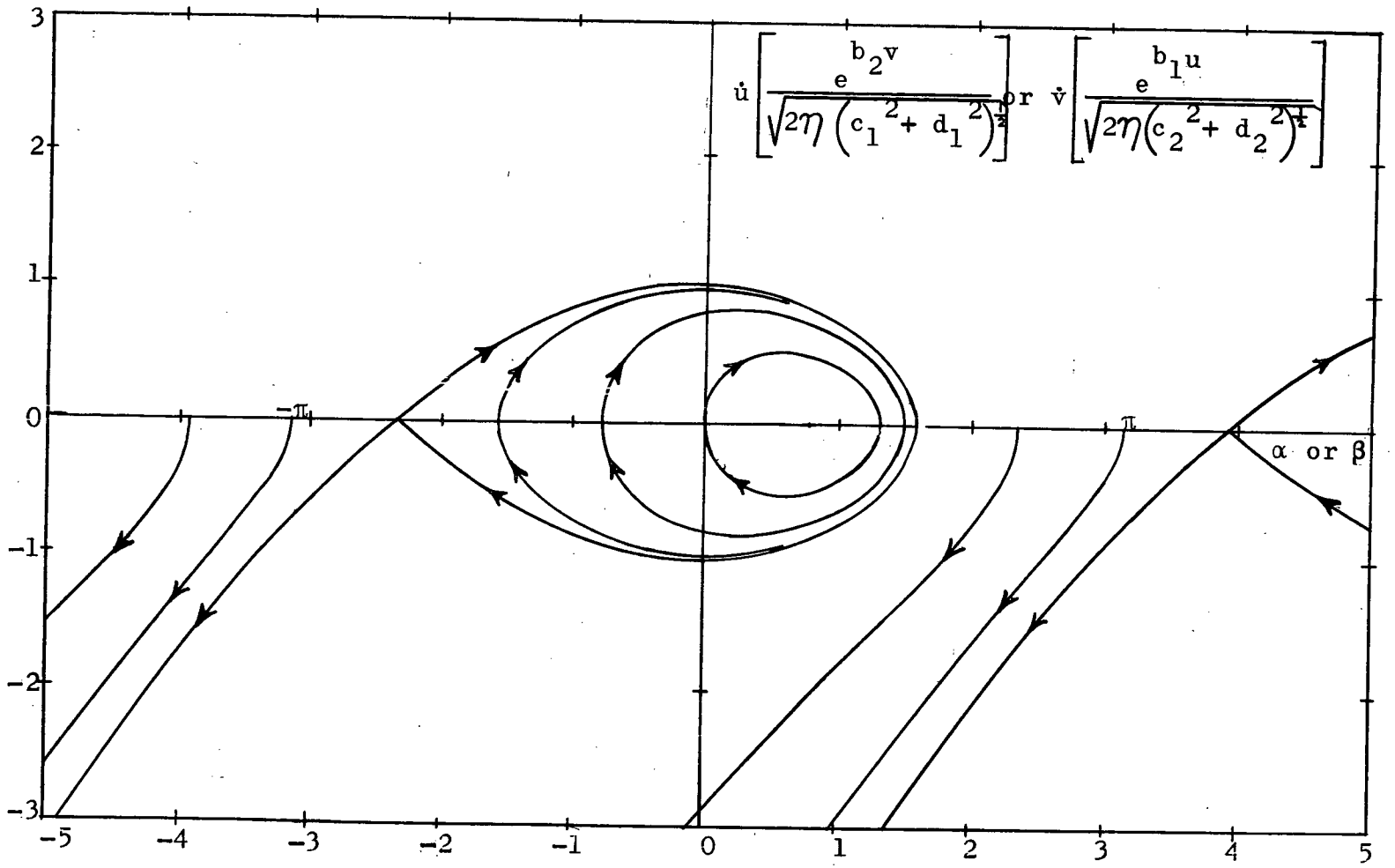

Figure (2-7). Phase plot of electron motion according to equations (2.77)

velocity remains zero. The trajectory is therefore a spiral $v = v_o$, and the velocity along the spiral is

$$\dot{u} = \pm e^{b_2 v_o}\left\{2\eta(c_1^2 + d_1^2)^{\frac{1}{2}} \cos\left[2b_2 u + \tan^{-1}\left(\frac{c_1}{d_1}\right)\right]\right\}^{\frac{1}{2}} .$$

Conversely, if the electrostatic field is due only to Φ_2, so that $c_1 = d_1 = 0$, then the u-component of velocity of an electron released from rest from the cathode will remain zero. The cathode surfaces in this case are the spirals

$$v_o = \frac{1}{2b_1}\left[\frac{\pi}{2} + n\pi + \tan^{-1}\left(\frac{c_2}{d_2}\right)\right],$$

and the electron trajectories are the spirals $u = u_o$, the velocity along these spirals being

$$\dot{v} = \pm e^{-b_1 u_o}\left\{2\eta(c_2^2 + d_2^2)^{\frac{1}{2}} \cos\left[2b_1 v - \tan^{-1}\left(\frac{c_2}{d_2}\right)\right]\right\}^{\frac{1}{2}} .$$

2:5:2 Potential Function of the Form "$\Phi_1(q_1) + \Phi_2(q_2)$"

(a) Conditions for separation of variables

A different class of solutions is obtained if it is assumed that the potential is the sum of a function of one coordinate alone and a function of the second coordinate alone. Let us assume that the metrical coefficients h_i are of the functional form

$$h_i = f_{i1}(q_1) f_{i2}(q_2) \qquad (2.78)$$

and the action function W is of the form

$$W = B_1(q_1) B_2(q_2) \quad . \qquad (2.79)$$

We must next determine under what conditions separation of variables of the Laplace and Hamilton-Jacobi equations is possible. To be able to write the potential Φ in the separated form

$$\Phi = \Phi_1(q_1) + \Phi_2(q_2)$$

it is necessary that $h_1 = h_2$ within the possibility of a scale change. Since $h_1 \equiv h_2$ for all conformal transformations from Cartesian coordinates, it is possible to write Φ in separated form for any member of the class of orthogonal coordinate systems obtained by conformal transform methods[48].

With h, W and Φ of the above assumed functional forms, the Hamilton-Jacobi equation (2.18) becomes

$$\frac{B_2^2(q_2)}{f_{11}^2(q_1)f_{12}^2(q_2)}\left(\frac{dB_1(q_1)}{dq_1}\right)^2 + \frac{B_1^2(q_1)}{f_{21}^2(q_1)f_{22}^2(q_2)}\left(\frac{dB_2(q_2)}{dq_2}\right)^2 = 2\eta\left(\Phi_1(q_1) + \Phi_2(q_2)\right) \quad . \tag{2.80}$$

The first term of this equation is a function of one variable if

$$1: \quad (a) \quad B_2(q_2) = c_1 f_{12}(q_2), \text{ or } \quad (b) \quad \frac{dB_1(q_1)}{dq_1} = c_2 f_{11}(q_1) \quad .$$

The condition for the second term is

$$2: \quad (a) \quad B_1(q_1) = c_3 f_{21}(q_1), \text{ or } \quad (b) \quad \frac{dB_2(q_2)}{dq_2} = c_4 f_{22}(q_2) \quad .$$

If conditions 1(a) and 2(b) are chosen, the requirement for separation of variables is thus

$$\frac{df_{12}(q_2)}{dq_2} = \frac{c_4}{c_1} f_{22}(q_2) \quad . \tag{2.81a}$$

If conditions 1(b) and 2(a) are chosen, the requirement is

$$\frac{df_{21}(q_1)}{dq_1} = \frac{c_2}{c_3} f_{11}(q_1) \qquad (2.81b)$$

where the c_i are arbitrary constants.

An action function of the form

$$W = B_{11}(q_1)B_{12}(q_2) + B_{21}(q_1)B_{22}(q_2)$$

could also have been assumed for this formulation. It is readily shown, however, that when separation of variables is possible with W of this latter form, the second term becomes redundant, so that W reduces to the form of equation (2.79).

(b) Examples

Example #3: Solution in Plane Polar Coordinates

In plane polar coordinates the function $f_{i,j}$ of the metrical coefficients are, from equation (2.78),

$$\left.\begin{aligned} f_{11}(r) = f_{12}(\theta) = f_{22}(\theta) = 1 \\ \text{and} \\ f_{21}(r) = r \quad . \end{aligned}\right\}$$

These functions satisfy equation (2.81b), so it is possible to separate the Hamilton-Jacobi equation when W is of the form (from condition (2a) and equation (2.79)):

$$W = rB_2(\theta) \quad . \qquad (2.82)$$

The potential Φ is of the assumed form

$$\Phi = \Phi_r(r) + \Phi_\theta(\theta) \ ,$$

which, when substituted into the Laplace equation, results in

$$\Phi_r(r) = \Phi_{ro} + a \ln r + b(\ln r)^2$$

and

$$\Phi_\theta(\theta) = \Phi_{\theta o} + c\theta - b\theta^2$$

where Φ_{ro}, $\Phi_{\theta o}$, a, b, and c are constants.
The Hamilton-Jacobi equation (2.80) becomes under these conditions

$$B_2^2(\theta) + \left(\frac{dB_2(\theta)}{d\theta}\right)^2 = 2\eta\left(\Phi_o + a \ln r + b(\ln r)^2 + c\theta - b\theta^2\right) \quad .$$

The left side of this equation is a function of θ only; the right side also must therefore be a function of θ only, requiring that $a = b = 0$. The potential Φ is therefore simply

$$\Phi = \Phi_o + c\theta \qquad (2.83)$$

and the equation to be satisfied by the motion is

$$B_2^2(\theta) + \left(\frac{dB_2(\theta)}{d\theta}\right)^2 = 2\eta\,(\Phi_o + c\theta) \quad . \qquad (2.84)$$

By a rotation of coordinates Φ_o can be eliminated, so that $\Phi = 0$ at $\theta = 0$. Equations (2.83 and 84) describe electron motion between two inclined-plane electrodes. This motion has been discovered previously by Walker[39]. The solution of equation (2.84), when $\Phi_o = 0$, that was obtained by Walker is

$$B_2(\theta) = \sum_{n=1}^{\infty} a_n \theta^{\frac{(4n-1)}{2}}$$

where $a_1 = \frac{2}{3}\sqrt{2\eta c}$, $a_2 = -\frac{2}{21}a_1$, $a_3 = \frac{10}{2079}a_1$, etc. The

electron motion is sketched in Figure (2-8).

Walker found that, with W of the functional form of equation (2.82), it is also possible to take space-charge into account. The extended solution he thus obtained, namely

$$W = r \sum_{n=1}^{\infty} \alpha_n \theta^{\frac{(6n-1)}{3}}$$

and

$$\Phi = \sum_{n=1}^{\infty} \beta_n \theta^{\frac{(6n-2)}{3}}$$

where α_n and β_n are constants determined by the space-charge-flow equations, represents space-charge-limited flow between two inclined planes.

Example #4: Solution in Equiangular Spiral Coordinates

For equiangular spiral coordinates the functions $f_{i,j}$ of the metrical coefficients are, from equations (2.69 and 78),

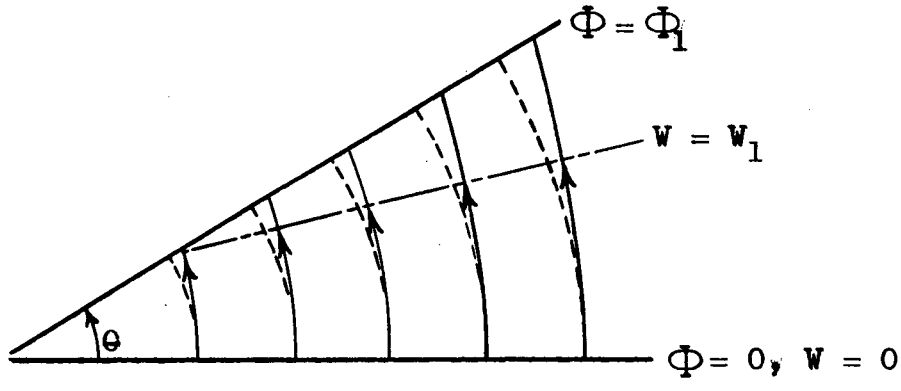

Figure (2-8). Electron motion between two inclined plane electrodes. The field lines, which are arcs of circles, are shown as dashed lines.

$$\left.\begin{aligned} f_{11}(u) &= f_{12}(u) = e^{b_1 u} \\ f_{12}(v) &= f_{22}(v) = e^{b_2 v} \end{aligned}\right\} .$$

Both conditional equations (2.81a and b) are observed to be satisfied by the $f_{i,j}$, and it is thus possible to obtain separation of variables when W is either of the two functional forms

$$W = e^{b_1 u} B_2(v)$$

or

$$W = e^{b_2 v} B_1(u) .$$

If we choose the first of these, and assume that the potential Φ is of the form

$$\Phi = \Phi_u(u) + \Phi_v(v) ,$$

the Hamilton–Jacobi equation (2.80) becomes

$$e^{-2b_2 v}\left[b_1^2 B_2^2(v) + \left(\frac{dB_2(v)}{dv}\right)^2\right] = 2\eta\Phi \qquad (2.85)$$

where Φ is found from the Laplace equation to be

$$\Phi = a(u^2 - v^2) + bu + cv + \Phi_o$$

and a, b, c, and Φ_o are constants. The left side of equation (2.85) is a function of v only; the right side must therefore be a function of v only, as well. It is thus necessary that a = b = 0. For convenience we will also set $\Phi_o = 0$, so that the potential is

$$\Phi = cv$$

and equation (2.85) becomes

$$b_1^2 B_2^2(v) + \left(\frac{dB_2(v)}{dv}\right)^2 = (2\eta c)e^{2b_2 v} \quad .$$

These two equations describe electron motion between two equiangular spiral electrodes. The Hamilton-Jacobi equation is solved by

$$B_2(v) = \sum_{n=1}^{\infty} a_n v^{\frac{(2n+1)}{2}}$$

where $a_1 = \frac{2}{3}\sqrt{2\eta c}$, $a_2 = \frac{3}{5} b_2 a_1$, $a_3 = \frac{2}{21}\left(\frac{9}{4} b_2^2 - b_1^2\right) a_1$, $a_4 = \frac{2}{27} b_2\left(\frac{3}{4} b_2^2 - \frac{1}{3} b_1^2\right) a_1$, etc. The electron motion is sketched in Figure (2-9).

The velocity of the electrons is

$$\vec{v} = \left[e^{b_1 u + b_2 v} \frac{du}{dt}, e^{b_1 u + b_2 v} \frac{dv}{dt}\right]$$

which can be rewritten in terms of the action function as

$$\vec{v} = \left[b_1 e^{-b_2 v} B_2(v), e^{-b_2 v} \frac{dB_2(v)}{dv}\right] .$$

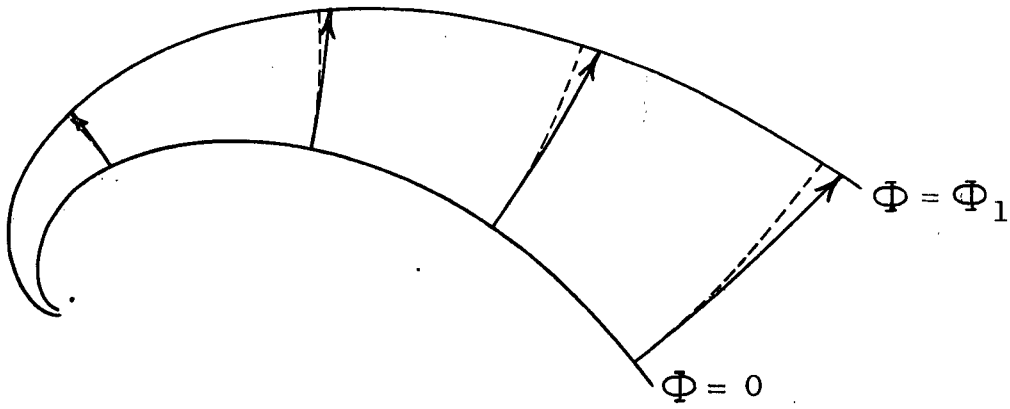

Figure (2-9). Electron trajectories between two equiangular spiral electrodes. The field lines, which are equiangular spirals, are shown as dashed lines

The trajectories are therefore described by the differential equation

$$\frac{du}{dv} = b_1 \frac{B_2(v)}{\left(\frac{dB_2(v)}{dv}\right)}$$

which has the solution

$$u = u_o + b_1 \sum_{n=1}^{\infty} c_n v^{n+1}$$

where $c_1 = \frac{1}{3}$, $c_2 = -\frac{4}{45} b_2$, $c_3 = \frac{2}{21}\left(\frac{1}{5} b_1^2 - \frac{2}{9} b_2^2\right)$, etc.

It will be recalled that there were two possible functional forms for W, and that the first one was chosen for the present solution. To obtain the solution for the second functional form, it is merely necessary to replace u by v, b_1 by b_2, and vice versa, in the above solution.

It is also possible to extend these solutions to include the effects of space-charge, with the same functional forms of W. Again it is only necessary to show the derivation for one case. Let W be of the form

$$W = e^{b_1 u} B(v) \quad . \tag{2.86}$$

The Hamilton-Jacobi equation is therefore

$$b_1^2 B^2(v) + \left(\frac{dB(v)}{dv}\right)^2 = 2\eta\Phi e^{2b_2 v} \quad . \tag{2.87}$$

The potential Φ is thus a function of v only, and Poisson's equation can be written as

$$\rho = -\varepsilon_o \nabla^2\Phi = -\varepsilon_o e^{-2(b_1 u + b_2 v)} \frac{d^2\Phi}{dv^2} \quad . \tag{2.88}$$

From equations (2.17 and 86) the velocity is

$$\vec{v} = \left[b_1 e^{-b_2 v} B(v),\ e^{-b_2 v} \frac{dB(v)}{dv} \right] . \qquad (2.89)$$

Equations (2.88 and 89) can be combined with (2.6) to give the current density

$$\vec{J} = \rho \vec{v} = -\left(\varepsilon_o e^{-2(b_1 u + b_2 v)} \frac{d^2\Phi}{dv^2} \right) \left[b_1 e^{-b_2 v} B(v),\ e^{-b_2 v} \frac{dB(v)}{dv} \right] .$$

If this equation be substituted into the continuity equation (2.7), there results

$$\frac{d^2\Phi}{dv^2} \left(b_1^2 B(v) + 2 b_2 \frac{dB(v)}{dv} + \frac{d^2 B(v)}{dv^2} \right) + \left(\frac{dB(v)}{dv} \right) \left(\frac{d^3\Phi}{dv^3} \right) = 0 . \qquad (2.90)$$

All the space-charge-flow equations have now been used, and are involved in equations (2.87 and 90). If equation (2.87) is differentiated three times with respect to v, the second and third derivatives of Φ may be substituted into equation (2.90). An ordinary differential equation in B(v) only will then result. This differential equation is very lengthy, so it will not be given here; it is solved by

$$B(v) = \sum_{n=1}^{\infty} a_n v^{\frac{(3n+2)}{3}} .$$

If this series is substituted into equation (2.87), it follows that the potential Φ is of the form

$$\Phi(v) = \sum_{n=1}^{\infty} c_n v^{\left(\frac{3n+1}{3}\right)} \quad .$$

From this series it is seen that the potential and the potential gradient are zero at v = 0. The solution thus describes space-charge-limited flow between two equiangular spiral electrodes.

2:6 Discussion

The electrostatic field of Example #1 has properties which are very similar to those of the electrostatic field of a convergent electron gun with an anode aperture. This similarity may be observed by comparing Figures (2-4) and (3-7). Thus the line x = y in the first quadrant of Figure (2-4) may be considered to be the gun axis, while the cathode coincides with an equipotential such as $\Phi = 1.5$. The constants of Φ can be adjusted so that the cathode is at zero potential, and so that initially the potential increases from the cathode inwards. It is then seen that, as we proceed inwards from the cathode, the equipotential curves first flatten and then reverse in curvature, which is also the case in convergent guns with an anode aperture. Further, by varying the relative magnitudes of the line charge and the double doublet of equation (2.63), the curvature of the equipotentials may be varied over a wide range.

In view of the above-mentioned similarity, further study of Example #1 is warranted. Of particular interest would be the extension of this solution to the space-charge domain, which may be possible by a perturbation method.

Since the number of analytic solutions that are known for

electron motion in electrostatic fields is still relatively small, there is much scope for further work in this area. Two coordinate systems that appear promising in this regard are toroidal and bispherical coordinates, since they are closely related to the Staeckel coordinates.

The metrical coefficients h_i in the previous section of this chapter were taken to be of product form, as described by equations (2.58 and 78). Kirstein[36] showed that the only planar coordinate systems with the h_i of the functional form (2.78) are logarithmic spiral, Cartesian and polar coordinates, and also a coordinate system with h_i of the form

$$h_1 = h_2 = e^{a(g_1^2 - g_2^2)} .$$

This latter coordinate system did not satisfy the separability criteria of either Sub-section 2:5:1 or 2, so no solution was obtained.

The extension of the solutions to three dimensions is in general very difficult, but can in some cases be accomplished. Thus, in logarithmic-spiral cylindrical coordinates (Example #2 extended) the h_i are

$$h_1 = h_2 = e^{b_1 u + b_2 v} , \quad h_3 = 1$$

and it is readily shown that the Hamilton-Jacobi and Laplace equations are separable when W and Φ are of the form

$$W = \frac{\sqrt{\eta k_1}}{2\sqrt{2}} \left(\frac{e^{2(b_1 u + b_2 v)}}{(b_1^2 + b_2^2)} \right) + \int \sqrt{(2\eta)(-\tfrac{1}{2}k_1 z^2 + a_1 z + a_2)}\ dz + k_2$$

$$\Phi = \frac{k_1 e^{2(b_1 u + b_2 v)}}{4(b_1^2 + b_2^2)} - \tfrac{1}{2}k_1 z^2 + a_1 z + a_2 \quad .$$

CHAPTER III - THE ELECTROSTATIC FIELD OF IDEALIZED ANODE STRUCTURES

3:1 Introduction

The electrostatic field distributions of the presently known space-charge-flow solutions are not of the kind that exist in the vicinity of apertured anodes. As a result, these solutions need to be adapted for use in electron gun design. To facilitate this adaptation, it is desirable to know the form of the electrostatic field about various apertured anode shapes. For this purpose, certain assumptions must be made regarding the other gun electrodes, as well as the space-charge distribution.

In this chapter the electrostatic field about four idealized two-dimensional anode geometries will be derived. It will be assumed that the other electrodes are an infinite distance away, and that space-charge effects are negligible. Under these conditions the electrostatic fields can be obtained by a Schwarz-Christoffel transformation[49]:

$$z = z_o + A \int (w - b_o)^{-\frac{\varphi_o}{\pi}} (w - b_1)^{-\frac{\varphi_1}{\pi}} (w - b_2)^{-\frac{\varphi_2}{\pi}} \ldots dw. \tag{3.1}$$

This transformation maps the upper half of the complex w-plane onto the interior of a polygon in the z-plane. The real axis $v = 0$, with points $u = b_o, b_1, b_2, \ldots$, transforms into the boundary of the polygon, having exterior angles $\varphi_o, \varphi_1, \varphi_2, \ldots$ at the corresponding vertices. The complex constants z_o and A

are determined by the origin, scale, and orientation of the polygon.

The boundaries of the polygons to be considered are the projections of the anode surfaces in the z-plane. The anode apertures are of unit width, and provide the reference dimension of distance in this chapter and the next. The potential Φ and flux Ψ will be taken to correspond to v and u respectively in this chapter. By a shift of origin and a change of scale of the w-plane, it is a simple matter to adjust the potential and gradient as needed in Chapter 4.

3:2 Electrostatic Field about a Plane with a Slit

The first and simplest idealized anode to be considered

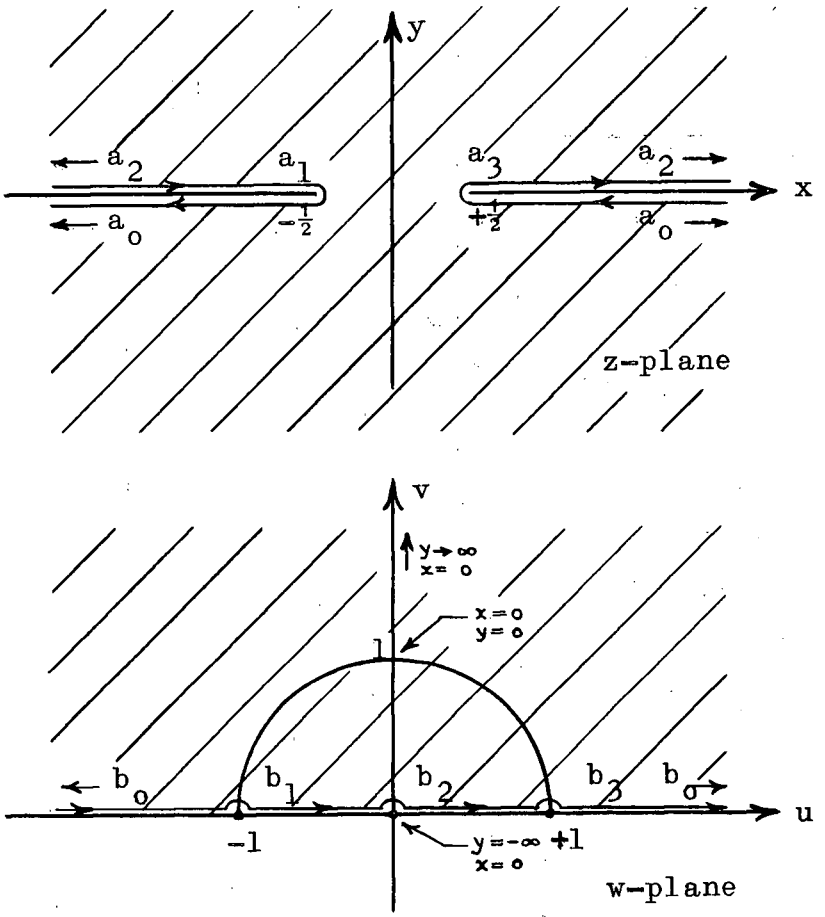

Figure (3-1). Mapping the profile of an infinite plane with a slit onto the u-axis of the w-plane

is an infinite plane with a slit. The Schwarz-Christoffel transformation for this case is well known[49], and is

$$z = z_o + A(w + \frac{1}{w}) \quad . \tag{3.2}$$

The transformation is illustrated in Figure (3-1). To evaluate z_o and A, let $w = \pm 1$. Then it is seen from Figure (3-1) that $z = \mp \frac{1}{2}$ respectively, and it follows from equation (3.2) that $z_o = 0$ and $A = -\frac{1}{4}$. If the latter values for z_o and A are substituted into equation (3.2), and this equation is separated into its real and imaginary parts, there results

$$\left.\begin{aligned} x &= -\frac{1}{4}\left(u + \frac{u}{u^2 + v^2}\right) \\ y &= -\frac{1}{4}\left(v - \frac{v}{u^2 + v^2}\right) \quad . \end{aligned}\right\} \tag{3.3}$$

The electrostatic field described by equations (3.3) is illustrated in Figure (3-2). In Figure (3-9) is shown the potential variation along the axis of symmetry of the anode.

3:3 Electrostatic Field about Two Right-Angled Plates

The polygons in the z-plane projected by two right-angled plates, two parallel semi-infinite plates, and the fictitious "negative thickness" anode of Section 3:5, are degenerate rectangles. A finite embodiment of these rectangles is of the general form as shown in Figure (3-3).

Since the vertices a_1 and a_3 are symmetrically located about a_2 in the z-plane, this symmetry must also pertain to the w-plane for the corresponding points b_1 and b_3 with respect to b_2. Therefore, if the transformed point b_o is placed at

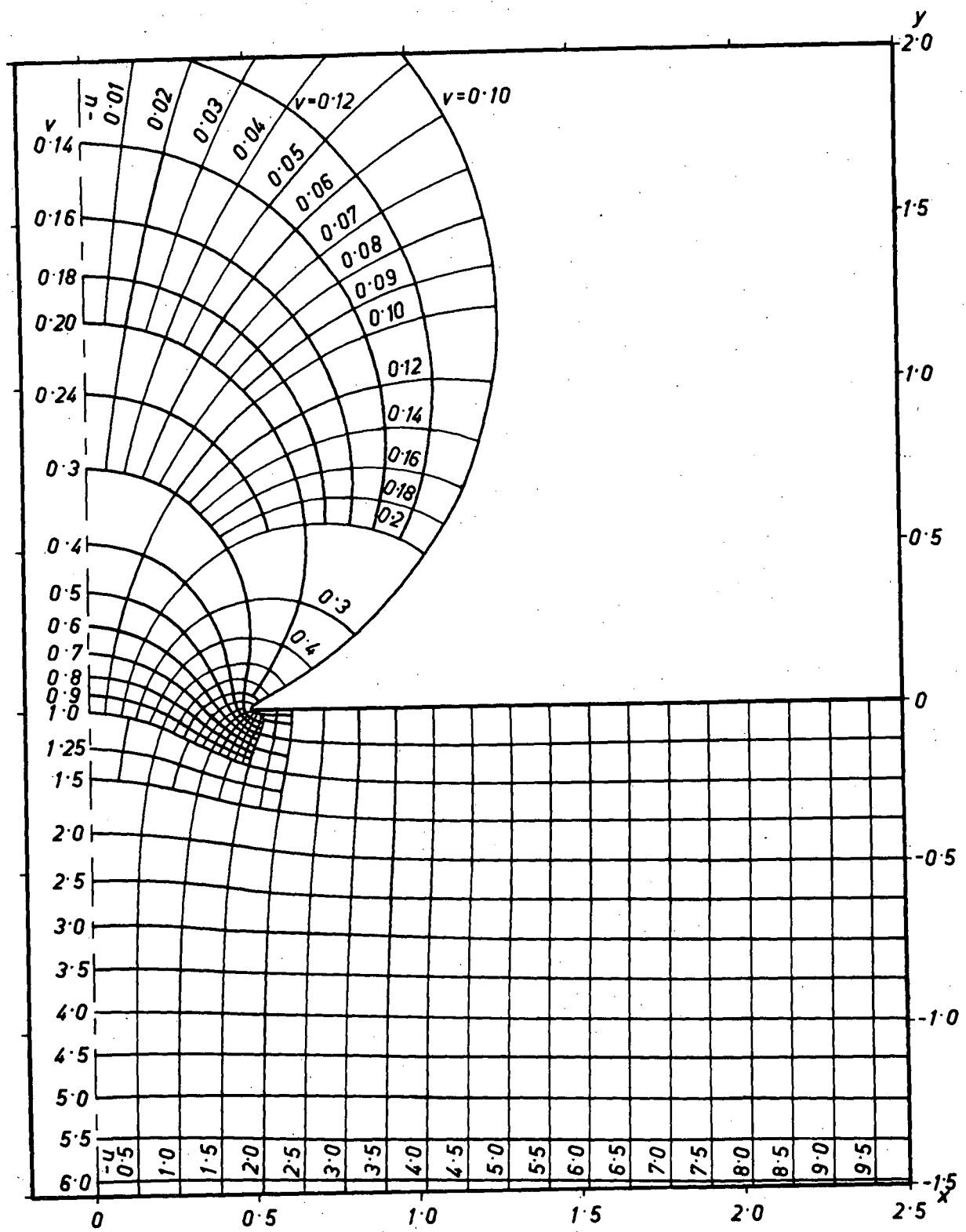

Figure (3-2). Electrostatic field about a plane with a slit

infinity, and $b_1 = -1$ while $b_2 = 0$, then b_3 is at $u = 1$, as shown in Figure (3.3). Under these conditions, equation (3.1) becomes

$$z = z_o + A \int (w + 1)^{\frac{-\varphi_1}{\pi}} \; w^{\frac{-\varphi_2}{\pi}} \; (w - 1)^{\frac{-\varphi_3}{\pi}} \, dw \, . \tag{3.4}$$

When the anode consists of two right-angled plates, the

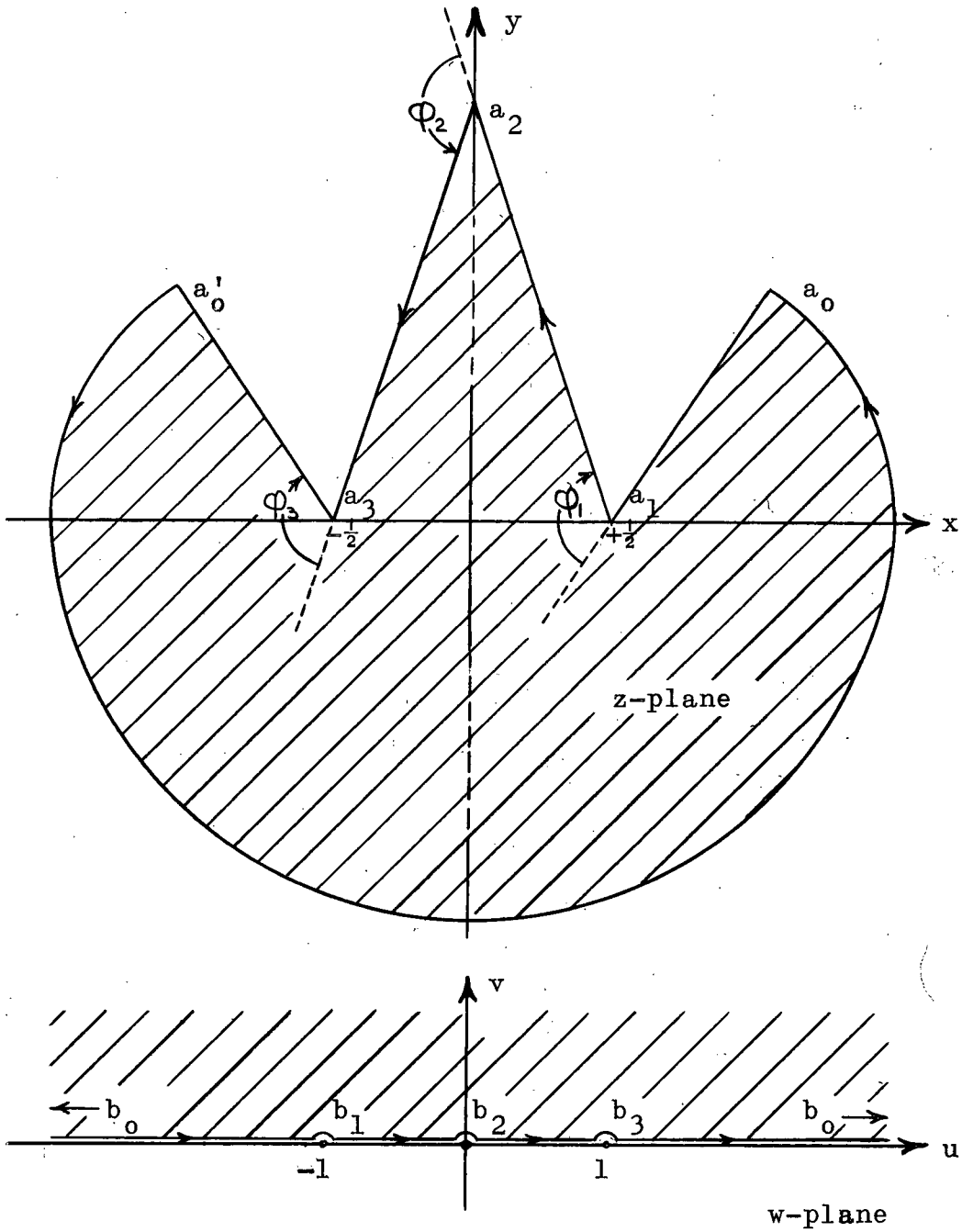

Figure (3-3). Mapping a degenerate rectangle onto the w-plane

angles of the rectangle are $\varphi_0 = 2\pi$, $\varphi_1 = \varphi_3 = -\frac{\pi}{2}$, and $\varphi_2 = \pi$. Equation (3.4) therefore becomes

$$z = z_o + A \int \frac{(w^2 - 1)^{\frac{1}{2}}}{w} \, dw$$

or

$$z = z_o + A \sqrt{w^2 - 1} - A \cos^{-1}\left(\frac{1}{w}\right) . \qquad (3.5)$$

From Figure (3-3), when $w = 1$, $z = -\frac{1}{2}$, so from equation (3.5) it follows that $z_o = -\frac{1}{2}$. Similarly, when $w = -1$, $z = \frac{1}{2}$, and from (3.5) we have $A = -\frac{1}{\pi}$. The transformation is therefore

$$z = -\frac{1}{\pi}\left[\frac{\pi}{2} + \sqrt{w^2 - 1} - \cos^{-1}\left(\frac{1}{w}\right)\right] .$$

When this transformation is separated into its real and imaginary parts, there results

$$\left.\begin{aligned} x &= -\frac{1}{\pi}\left[\frac{\pi}{2} + R^{\frac{1}{2}} \cos\left(\frac{\theta}{2}\right) - \tan^{-1}\left(\frac{B}{\sqrt{1 - B^2}}\right)\right] \\ y &= -\frac{1}{\pi}\left[R^{\frac{1}{2}} \sin\left(\frac{\theta}{2}\right) - \ln\left(A + \sqrt{A^2 + 1}\right)\right] \end{aligned}\right\} \qquad (3.6)$$

where

$$R = \left((u^2 - v^2 - 1)^2 + (2uv)^2\right)^{\frac{1}{2}}$$

$$\theta = \tan^{-1}\left(\frac{2uv}{u^2 - v^2 - 1}\right)$$

$$A = \left[\frac{1}{2}\left(-(1 - a^2 - b^2) + \sqrt{(a^2 + b^2 - 1)^2 + 4b^2}\right)\right]^{\frac{1}{2}}$$

$$B = \left[\frac{1}{2}\left((1 - a^2 - b^2) + \sqrt{(a^2 + b^2 - 1)^2 + 4b^2}\right)\right]^{\frac{1}{2}}$$

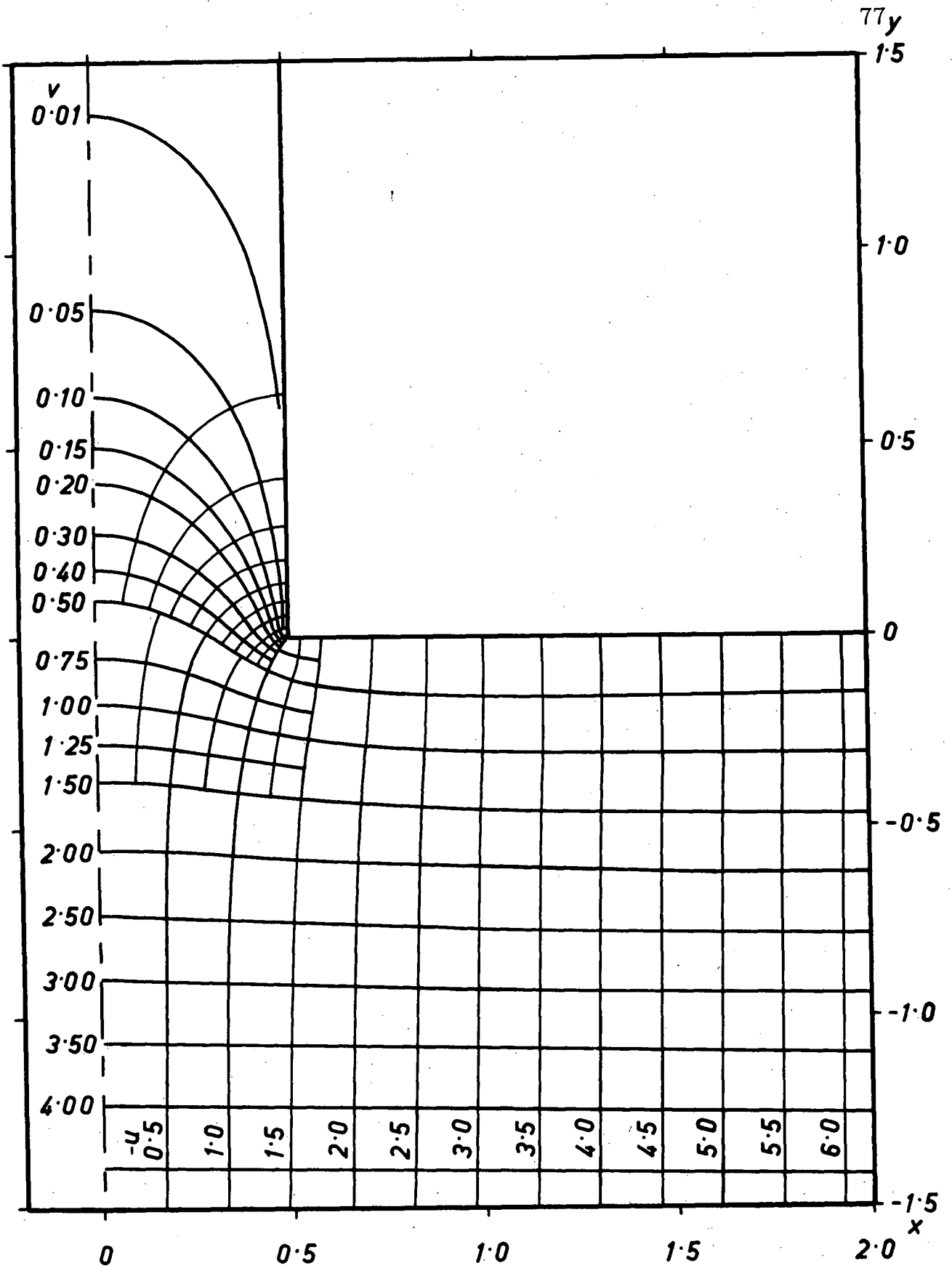

Figure (3-4). Electrostatic field about two right-angled plates

and

$$a = \left(\frac{u}{u^2 + v^2}\right), \quad b = -\left(\frac{v}{u^2 + v^2}\right) .$$

The electrostatic field described by equations (3.6) and its defining relations is shown in Figure (3-4). The potential variation along the axis of symmetry of the right-angled anode is shown in Figure (3-9).

The anode shapes just discussed, the anode consisting of two right-angled plates and the anode consisting of a plane with a slit, represent two extreme cases of a physically more important anode geometry, an anode consisting of a plate of thickness y_1 and having a slit of half-width x_1 (see Figure (3-5)). The computation of the electrostatic field about an apertured

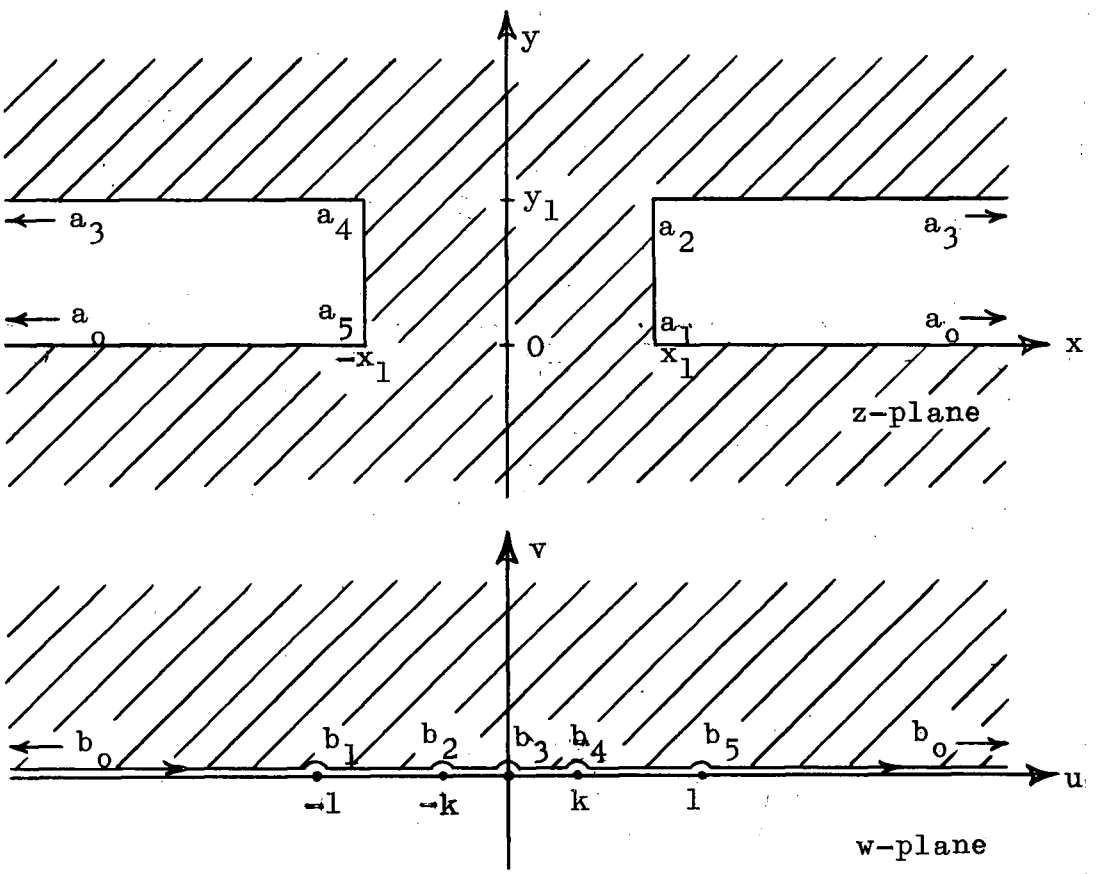

Figure (3-5). Mapping the profile of a plate of thickness y_1, with a slit of half-width x_1, onto the w-plane

plate of finite thickness is more involved than is the case when the plate is of semi-infinite or of vanishing thickness. Fortunately, the field in the region of greatest interest, the region near the anode aperture in the lower-half z-plane, very rapidly approaches the field in the corresponding region near two right-angled plates as the anode thickness is increased. Therefore, the field in the region of interest near an anode of finite thickness can generally be represented accurately by the field about an anode of semi-infinite thickness. This will now be demonstrated.

Consider Figure (3-5). The exterior angles of the polygon in the z-plane are seen to be

$$\varphi_0 = \varphi_3 = 2\pi, \quad \varphi_1 = \varphi_2 = \varphi_4 = \varphi_5 = -\frac{\pi}{2} \quad .$$

The transforms of the vertices of the polygon to the w-plane, b_i, are located as shown, the location of b_2 and b_4 being as yet undetermined except for the fact that they are symmetric about the origin, and lie a distance $0 \leq k \leq 1$ from it. Under these conditions equation (3.1) becomes

$$z = z_0 + A\int \frac{(w^2 - 1)^{\frac{1}{2}}(w^2 - k^2)^{\frac{1}{2}}}{w^2}\, dw \quad .$$

This equation has been integrated by Davy[50], who used the substitution

$$w = \frac{1}{sn(u)}$$

thus making k the modulus of the elliptic function used. The transformation then becomes

$$z = z_o - A\left[\mu\left(k'^2 - \frac{2E}{K}\right) - 2Z(\mu) - \frac{cn(\mu)dn(\mu)}{sn(\mu)}\right] \tag{3.7}$$

where $k'^2 = 1 - k^2$, K and E are, respectively, elliptic integrals of the first and second kind, and $Z(\mu)$ is the Jacobian Zeta-function. The constants z_o and A can be evaluated by substituting the coordinates of b_1 and b_5 into (3.7), giving

$$\left.\begin{aligned} z_o &= 0 \\ A &= \frac{x_1}{Kk'^2 - 2E} \end{aligned}\right\} \tag{3.8}$$

If the coordinates of b_2 and b_4 are substituted into (3.7 and 8), then it is found that

$$\frac{y_1}{x_1} = \frac{(K'k'^2 - 2K' + 2E')}{2E - Kk'^2} \tag{3.9}$$

where K' and E' are, respectively, the elliptic integrals of the first and second kind, in terms of k'.

From equation (3.9) it is observed that the distance k of the points b_2 and b_4 from the origin depends solely on the ratio of the height to the half-width of the anode aperture. Equation (3.9) has been plotted in Figure (3-6). When $y_1 = 0$, then $k = 1$, which represents the case of a plane with a slit. It is seen from Figure (3-6) that when the thickness y_1 is increased, k initially decreases very rapidly; i.e., it rapidly approaches the case of an anode consisting of two right-angled plates. For example, when the thickness of the plate is equal to half the

width of the anode aperture, k has already decreased to about $\frac{1}{10}$.

From Gauss' law it is easily deduced that k is the ratio of the charge on the upper surface $a_2 - a_3$ (or $a_3 - a_4$) to the charge on the surfaces $a_1 - a_2 - a_3$ (or $a_3 - a_4 - a_5$). The physical significance of the rapid decrease of k when y_1 is increased is thus that the proportion of the lines of force entering the anode aperture that terminate on the upper surfaces $a_2 - a_3$ and $a_3 - a_4$ decreases rapidly when the anode thickness is increased. Consequently, the field in the lower-half z-plane converges rapidly to that for an anode consisting of two right-angled plates when the anode thickness y_1 is increased.

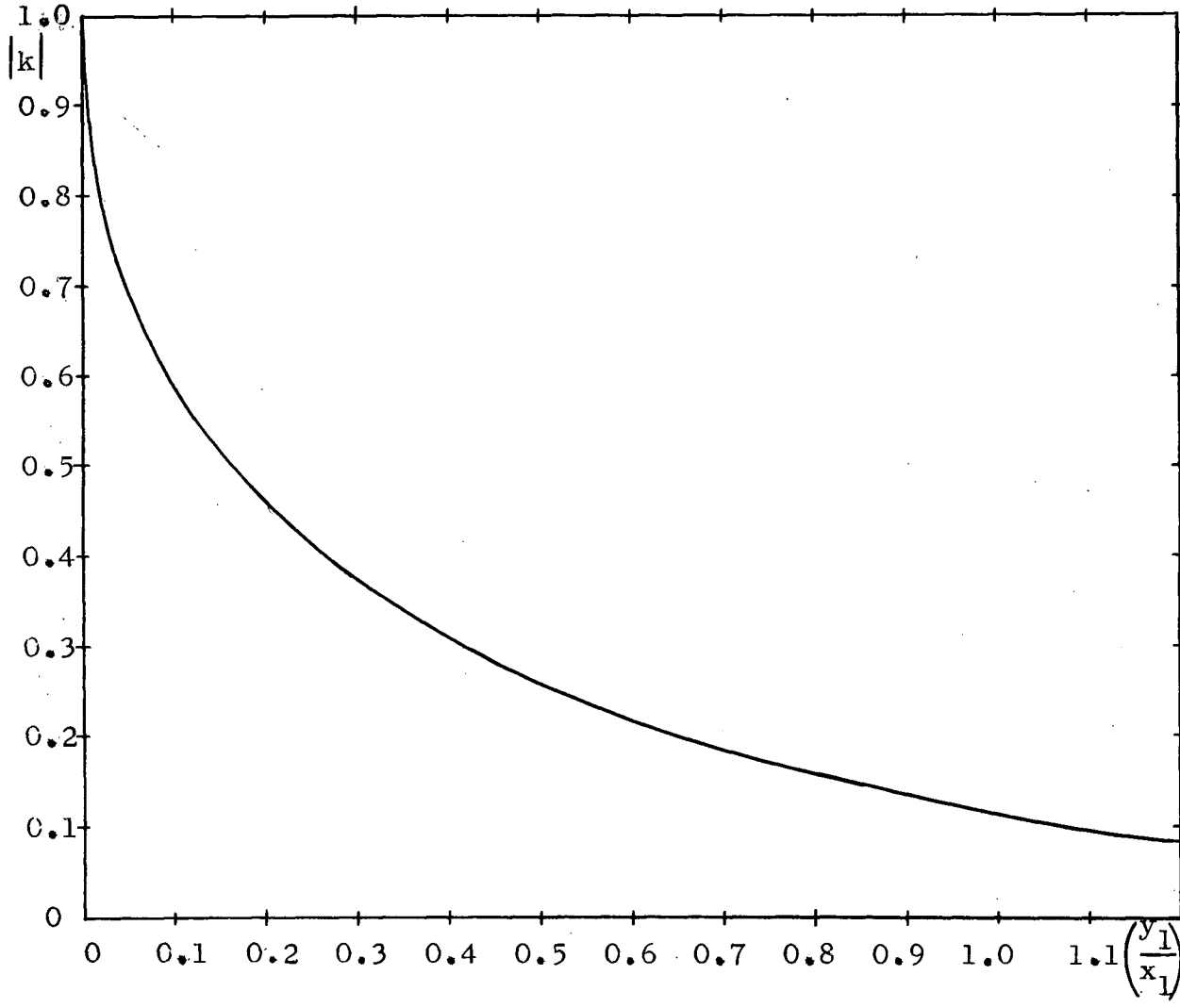

Figure (3-6). Plot of equation (3.9)

3:4 Electrostatic Field about Two Semi-Infinite Parallel Plates

For an idealized anode consisting of two semi-infinite parallel plates, it is seen from Figure (3-3) that the polygon angles are $\varphi_o = 3\pi$, $\varphi_1 = \varphi_3 = -\pi$, and $\varphi_2 = \pi$. The transformation is, therefore, from equation (3.4),

$$z = z_o + A\int\left(\frac{w^2 - 1}{w}\right) dw$$

or

$$z = z_o + A\left(\frac{w^2}{2} + \ln w\right) \quad . \tag{3.10}$$

By referring to Figure (3-3), the constants z_o and A can be evaluated as before, giving

$$z_o = -\frac{1}{2}(1 + i\frac{1}{\pi})$$

$$A = i\frac{1}{\pi} \quad .$$

Equation (3.10) then becomes

$$z = i\left(\frac{1}{2\pi}\right)(-1 + i\pi + w^2 - 2\ln w)$$

or

$$\left.\begin{aligned} x &= \left(\frac{1}{2\pi}\right)\left[-\pi - 2uv + 2\tan^{-1}\left(\frac{v}{u}\right)\right] \\ y &= \left(\frac{1}{2\pi}\right)\left[-1 - v^2 + u^2 - \ln\,(v^2 + u^2)\right]. \end{aligned}\right\} \tag{3.11}$$

Figure (3-7) shows the electrostatic field described by equations (3.11), while the potential variation along the axis of symmetry of the anode is plotted in Figure (3-9).

3:5 The "Wrap-Around Field"

The properties relevant to electron gun design of the three electrostatic fields derived above are studied in the next

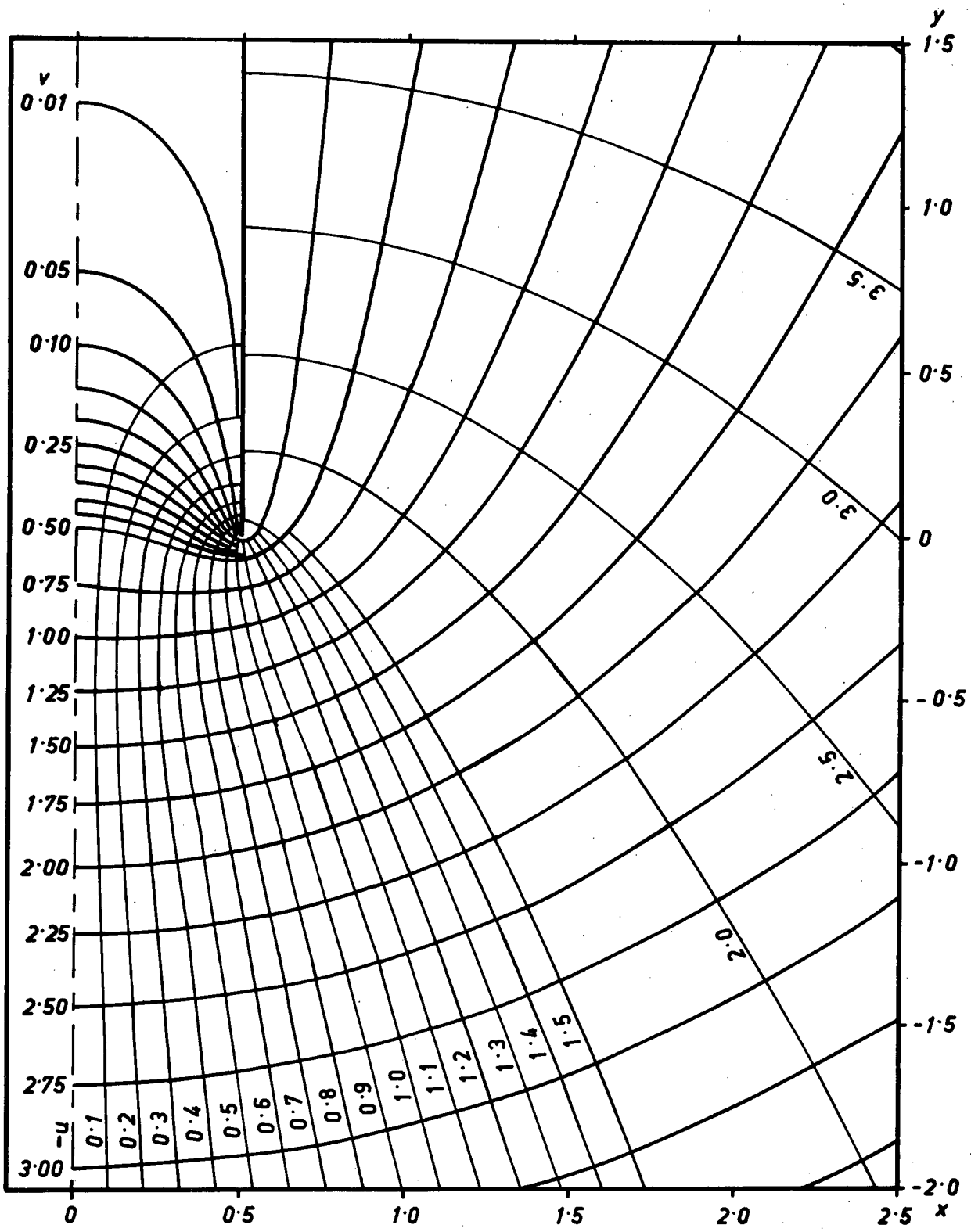

Figure (3-7). Electrostatic field about two semi-infinite parallel plates

chapter, and it is inferred there that the field characteristics improve as the angles φ_1 and φ_3 of Figure (3-3) are made increasingly negative. The limit of physical realizability of the anode is attained when $\varphi_1 = \varphi_3 = -\pi$, as then the anode is of vanishing thickness. Nevertheless, in a Riemann surface the projections $a_o - a_1$ and $a_3 - a'_o$ of the outside anode surfaces can be conceived of as continuing past the respective projections $a_1 - a_2$, and $a_2 - a_3$ of the inside anode surfaces if φ_1 and φ_3 are reduced beyond $-\pi$. The electrostatic field of the resulting fictitious negative thickness electrode will be called the "wrap-around field".

The transformation for the case when $\varphi_1 = \varphi_3 = -\frac{5\pi}{4}$, $\varphi_2 = \pi$, and $\varphi_o = \frac{7\pi}{2}$ will now be derived. Under these conditions, equation (3.4) becomes

$$z = z_o + AI \tag{3.12}$$

where

$$I = \int \frac{(w^2 - 1)^{\frac{5}{4}}}{w}\, dw$$

or

$$I = \left\{ \frac{1}{5}(w^2 - 1)^{\frac{5}{4}} - (w^2 - 1)^{\frac{1}{4}} + \frac{1}{4\sqrt{2}} \left[\ln\left(\frac{(w^2 - 1)^{\frac{1}{2}} + \sqrt{2}(w^2 - 1)^{\frac{1}{4}} + 1}{(w^2 - 1)^{\frac{1}{2}} - \sqrt{2}(w^2 - 1)^{\frac{1}{4}} + 1} \right) + 2\tan^{-1}\left(\frac{\sqrt{2}(w^2 - 1)^{\frac{1}{4}}}{1 - (w^2 - 1)^{\frac{1}{2}}} \right) \right] \right\} .$$

Equation (3.12) can be separated into its real and imaginary components, giving

$$\left.\begin{aligned} x &= x_o + A_R I_R - A_J I_J \\ y &= y_o + A_J I_R + A_R I_J \end{aligned}\right\} \tag{3.13}$$

where

$$z_o = x_o + iy_o$$

$$A = A_R + iA_\mathfrak{I}$$

$$I = I_R + iI_\mathfrak{I}$$

and where

$$I_R = \left(\frac{1}{5}\right)S^{\frac{5}{4}}\cos\left(\frac{5}{4}\alpha\right) - S^{\frac{1}{4}}\cos\left(\frac{\alpha}{4}\right) + \frac{1}{4\sqrt{2}}\left[\ln\sqrt{E^2 + F^2} + \tan^{-1}\left(\frac{2C}{1 - C^2 - D^2}\right)\right]$$

$$I_\mathfrak{I} = \left(\frac{1}{5}\right)S^{\frac{5}{4}}\sin\left(\frac{5}{4}\alpha\right) - S^{\frac{1}{4}}\sin\left(\frac{\alpha}{4}\right) + \frac{1}{4\sqrt{2}}\left[\tan^{-1}\left(\frac{F}{E}\right) + \frac{1}{2}\ln\left(\frac{C^2 + (D + 1)^2}{C^2 + (D - 1)^2}\right)\right]$$

and where

$$S = \left[(u^2 - v^2 - 1)^2 + (2uv)^2\right]^{\frac{1}{2}}$$

$$\alpha = \tan^{-1}\left(\frac{2uv}{u^2 - v^2 - 1}\right)$$

$$C = \left[\frac{\sqrt{2}\,S^{\frac{1}{4}}\cos\left(\frac{\alpha}{4}\right)\left(1 - S^{\frac{1}{2}}\right)}{1 + S - 2S^{\frac{1}{2}}\cos\left(\frac{\alpha}{2}\right)}\right]$$

$$D = \left[\frac{\sqrt{2}\,S^{\frac{1}{4}}\sin\left(\frac{\alpha}{4}\right)\left(1 + S^{\frac{1}{2}}\right)}{1 + S - 2S^{\frac{1}{2}}\cos\left(\frac{\alpha}{2}\right)}\right]$$

$$E = \frac{S^{\frac{1}{2}}\left[S^{\frac{1}{2}} - 2 + 2\cos\left(\frac{\alpha}{2}\right)\right] + 1}{S + 2S^{\frac{1}{2}}\left[1 + \cos\left(\frac{\alpha}{2}\right)\right] - 2\sqrt{2}\,S^{\frac{1}{4}}\cos\left(\frac{\alpha}{4}\right)\left(1 + S^{\frac{1}{2}}\right) + 1}$$

$$F = \frac{2\sqrt{2}\,S^{\frac{1}{4}}\sin\left(\frac{\alpha}{4}\right)\left(1 - S^{\frac{1}{2}}\right)}{S + 2S^{\frac{1}{2}}\left[1 + \cos\left(\frac{\alpha}{2}\right)\right] - 2\sqrt{2}\,S^{\frac{1}{4}}\cos\left(\frac{\alpha}{4}\right)\left(1 + S^{\frac{1}{2}}\right) + 1}\,.$$

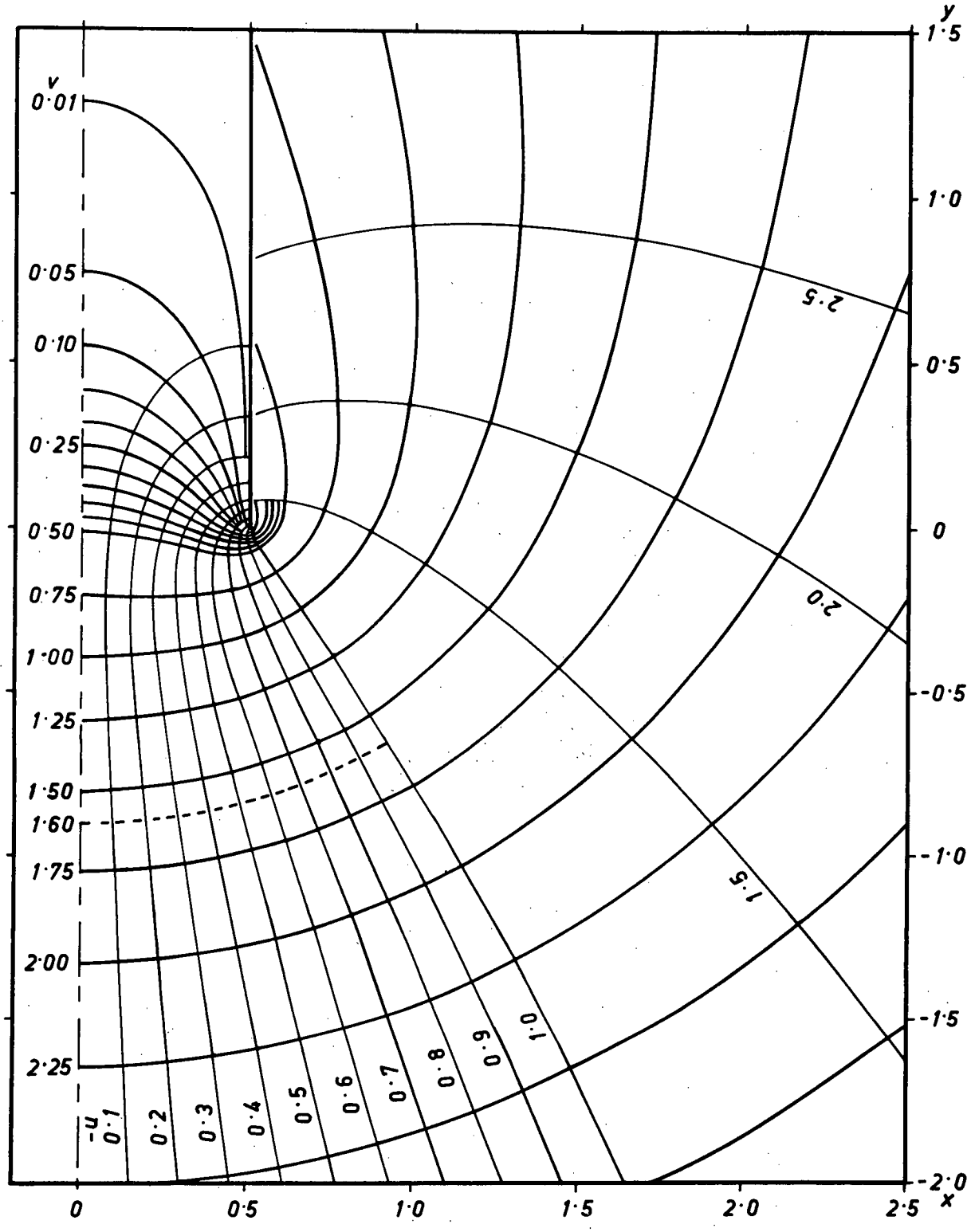

Figure (3-8). The "wrap-around field"

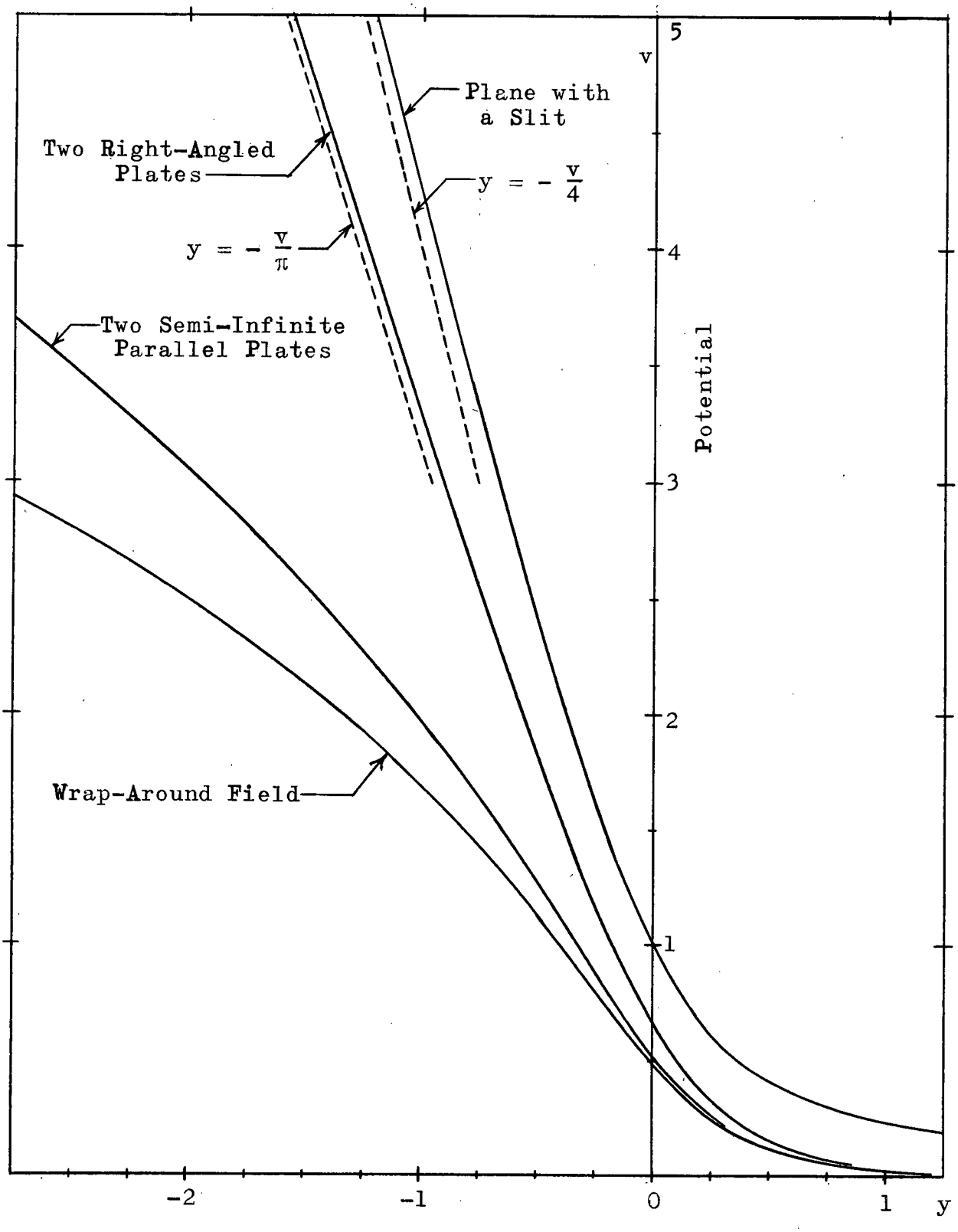

Figure (3-9). Variation of potential along the plane of symmetry of four electrode shapes

The constants z_o and A can be evaluated as before by setting w = 1 and z = $-\frac{1}{2}$, and w = -1 and z = $\frac{1}{2}$. Equations (3.13) then become

$$\left.\begin{aligned} x &= -\frac{1}{2}\ \frac{\sqrt{2}}{\pi}(I_R - I_J) \\ y &= \frac{\sqrt{2}}{\pi}\ (I_R + I_J)\ , \end{aligned}\right\} \qquad (3.14)$$

the desired transformation. The electrostatic field in one half of the first sheet of the Riemann surface is shown in Figure (3-8). The potential variation along the axis of symmetry is plotted in Figure (3-9).

For electron beam design, the region of interest of this electrostatic field lies between the flux lines u = 1 and u = -1, and from about v = 2.75 to v = 0. The field in this region could be approximated by placing electrode sheets along several equipotentials just outside this region, and by maintaining these electrodes at the required potentials.

CHAPTER IV - USE OF SPACE-CHARGE-FREE FIELDS IN ELECTRON GUN DESIGN

4:1 Introduction

In this chapter, the electrostatic field in an electron gun is considered in two parts: the first part is the low-potential region, in which space-charge effects are appreciable, and the second is the high-potential region, in which the effect of space-charge on the electrostatic field is assumed to be negligible.

Consider the electrode configuration of Figure (4-1). The region from the cathode to the auxiliary anode in this figure represents a strip-beam Pierce gun[5]. The upper surface of the auxiliary anode is shaped to coincide with a suitable equipotential of the free-space electrostatic field of the main anode (i.e., an equipotential of the electrostatic field that would exist in an isolated system consisting of the main anode, held at a potential V_k, and a charge located an infinite distance away). The electro-

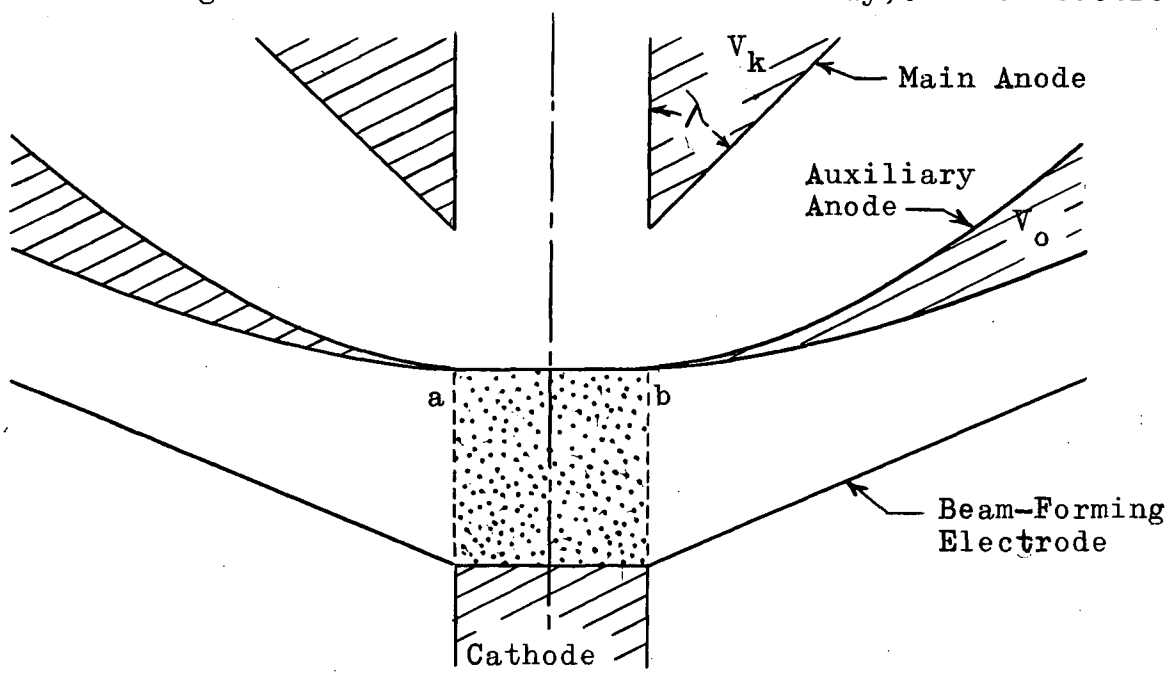

Figure (4-1). Hypothetical electron gun

static field in the auxiliary-main anode region can thus in principle be obtained by a conformal transformation of the space exterior to the main-anode surface, such as was carried out in Chapter III.

Assuming that the Pierce-gun section of the electrode configuration of Figure (4-1) is operating, imagine that the potential of the main anode, V_k, is adjusted so that the potential gradients at the upper and lower surface of the thin section a-b of the auxiliary anode are approximately the same. If section a-b is now removed, the field distribution will therefore be negligibly affected, provided that the potential-depressing effect of the space-charge which will now enter the auxiliary-main anode region can be ignored. If this proviso applies, the electrostatic field in the two-anode gun thus is known.

Van Duzer and Brewer[51] obtained equipotential plots for a Müller-type gun with a perveance of 2.3×10^{-6} by means of an electrolytic tank with provisions for space-charge simulation. Comparison of an equipotential plot taken in the absence of space-charge simulation with a plot taken under conditions of space-charge simulation shows that the equipotentials in the anode region of the second plot have been displaced but have changed little in shape. For the two-anode gun discussed above, the displacement of the equipotentials in the auxiliary-main anode region has largely been taken into account by the gradient-matching procedure used. Van Duzer and Brewer's experimental data thus give an indication of the applicability of the assumption that the electrostatic field in the auxiliary-main anode region can be approximated by a space-charge-free field. This problem is pursued further in the next section. In Sections 4:3 and 4

the gradient-matching procedure is applied to the study of two electron gun configurations.

The auxiliary anode in the hypothetical gun of Figure (4-1) has been inserted only as a temporary measure, to aid the analysis of conditions inside the electron beam. In Chapter 5 it is shown for the electron guns of Sections 4:3 and 4 how this anode can be removed.

4:2 Error Estimate for a Space-Charge-Free Field Approximation in the Anode Region

The error involved in approximating the electrostatic field in the anode region by a space-charge-free field is readily obtained for two space-charge-limited flows of interest in this chapter: flow between two parallel plates and flow between two concentric cylinders.

4:2:1 Flow between Two Parallel Plates

In an ideal planar diode the following relations hold[2]

$$\left.\begin{array}{ll} \text{Potential} & \Phi = Y^{\frac{4}{3}} \\ \text{Electric Intensity} & \mathcal{E} = -\frac{4}{3}Y^{\frac{1}{3}} \\ \text{Electron Velocity} & \dot{Y} = \sqrt{2\eta}\, Y^{\frac{2}{3}} \\ \text{Charge Density} & P = -\left(\frac{4}{9}\,\varepsilon_0\right) Y^{-\frac{2}{3}} \end{array}\right\} \qquad (4.1)$$

where

$$Y = \frac{y}{d} = \frac{\text{distance from cathode}}{\text{cathode-anode distance}}$$

$$\Phi = \frac{V}{V_d} = \frac{\text{potential at } y}{\text{anode potential}} \quad .$$

Equations (4.1) are illustrated in Figure (4-2). It is seen that as Y increases, P decreases monotonically. As a result Φ becomes more linear with increasing Y, tending toward the solution of the Laplace equation,

$$\Phi_L = aY + b \qquad (4.2)$$

where a and b are constants.

Let the potential in the diode be approximated by (4.2) over the interval

$$Y_o < Y \leq 1$$

by matching the gradients of Φ and Φ_L at Y_o, as shown in Figure (4-2). Therefore, at Y_o,

$$\Phi = \Phi_L \text{ and } \frac{d\Phi}{dY} = \frac{d\Phi_L}{dY}$$

and from equation (4.1a) it follows that the constants of equation (4.2) are

$$\left.\begin{aligned} a &= \frac{4}{3} Y_o^{\frac{1}{3}} \\ b &= -\frac{1}{3} Y_o^{\frac{4}{3}} \end{aligned}\right\} .$$

The maximum error incurred by this approximation depends on the value of Y_o. Let the error in potential, e_Φ, be defined as

$$e_\Phi = 100\left(\frac{\Phi - \Phi_L}{\Phi}\right) \%$$

and the error in velocity, $e_{\dot{Y}}$, be defined as

$$e_{\dot{Y}} = 100\left(\frac{\dot{Y} - \sqrt{2\eta\Phi_L}}{\dot{Y}}\right) \% \quad .$$

For the example illustrated in Figure (4-2), $Y_o = 0.75$ and thus

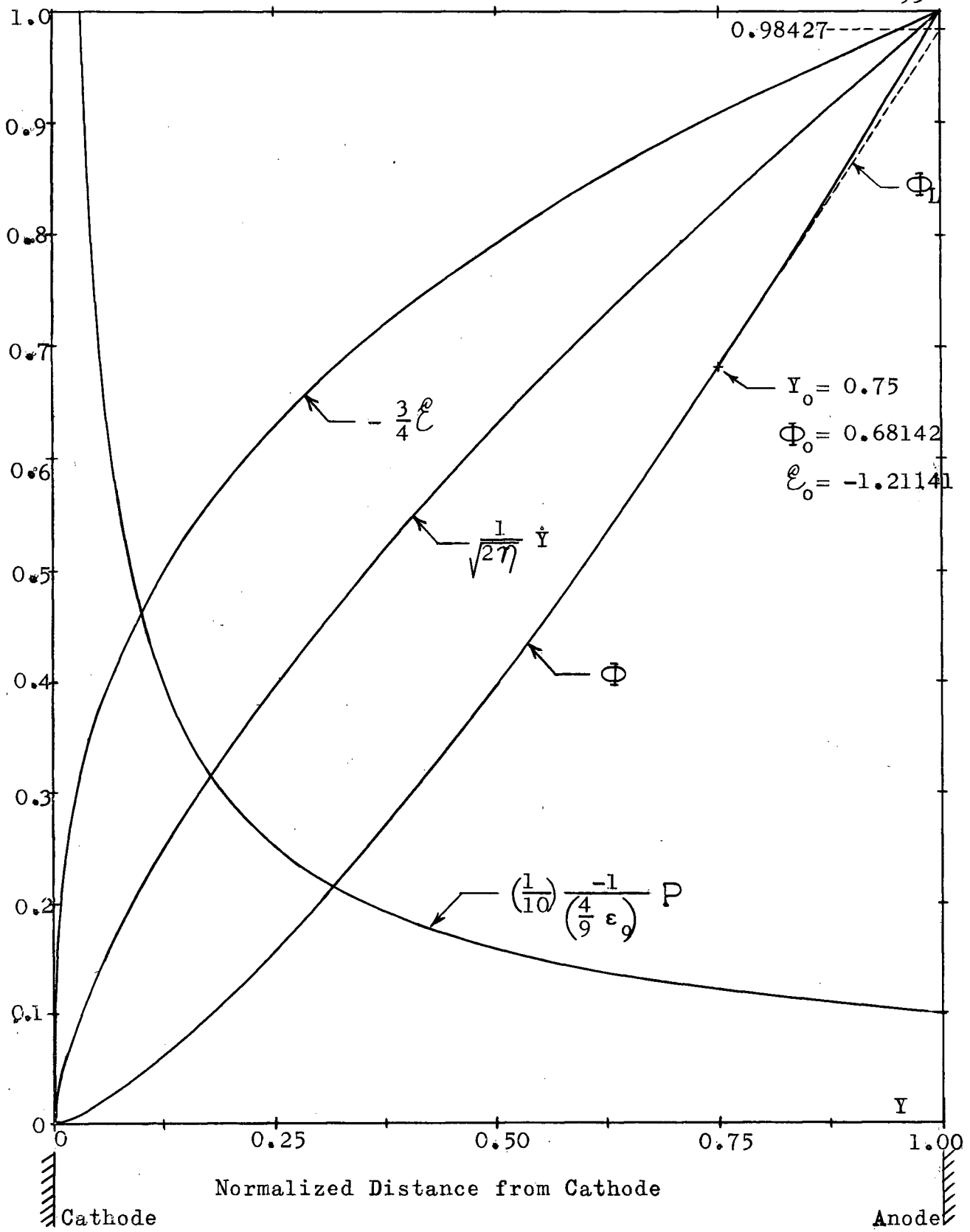

Figure (4-2). Variation of the potential, electric intensity, electron velocity and space-charge density versus distance from the cathode in a parallel plane diode. Also shown is an approximation of the potential in the anode region by $\Phi_L = a\,Y + b$

equation (4.2) is

$$\Phi_L = 1.2114Y - 0.2271$$

while the errors in potential and velocity incurred by this potential approximation are, at the anode,

$$e_\Phi = 1.57\%$$

$$e_{\dot{Y}} = 0.789\% \quad .$$

The values of e_Φ and $e_{\dot{Y}}$ at the anode for other values of Y_o are shown in Figure (4-3).

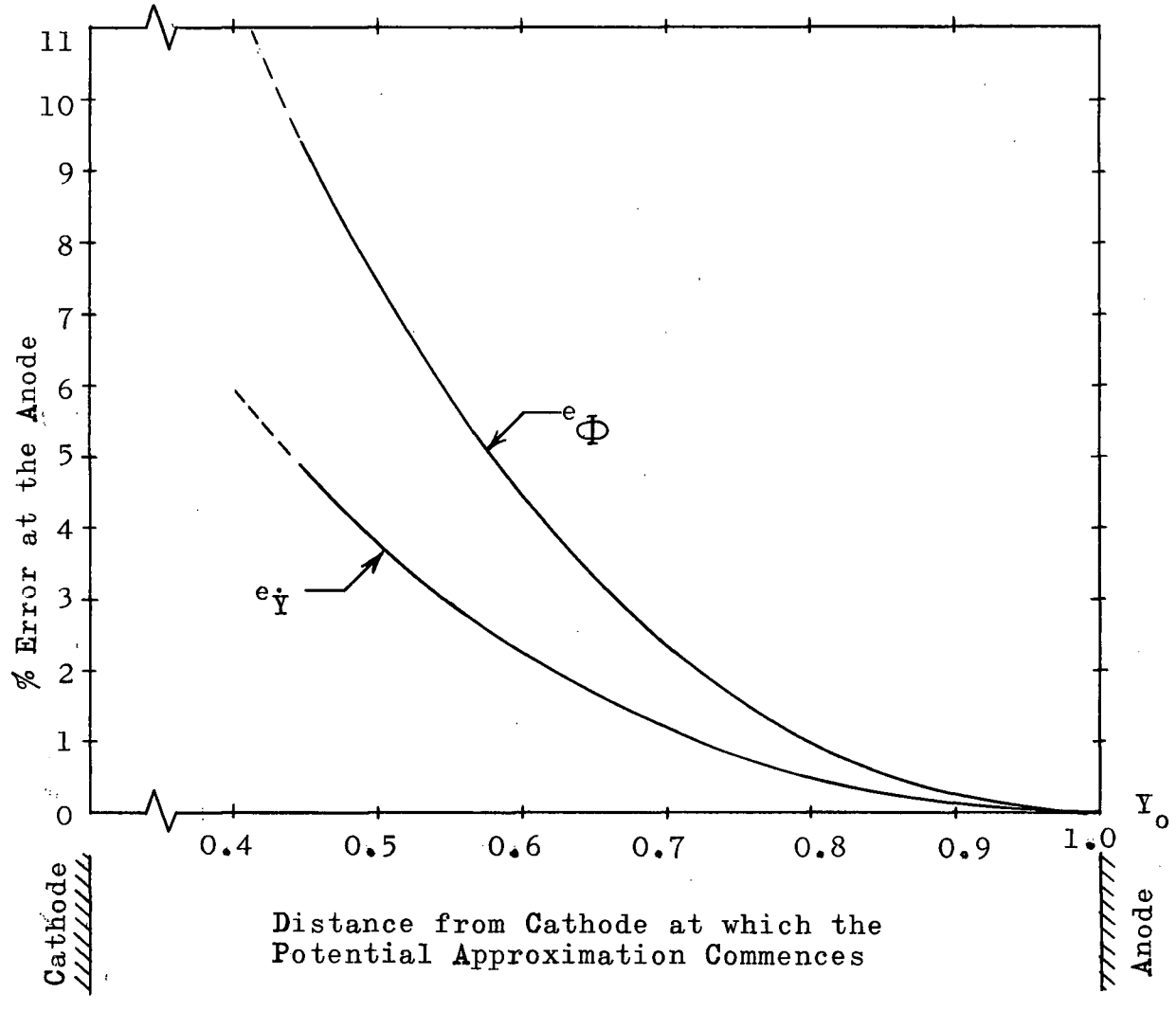

Figure (4-3). Error in potential e_Φ, and in electron velocity $e_{\dot{Y}}$, at the anode of a planar diode when the potential is approximated by $\Phi_L = aY + b$ over the interval $Y_o < Y \leq 1.0$

When the anode has an aperture, the errors incurred by approximating the field in the anode region are no longer readily calculable. However, if the flow being considered is initially parallel and rectilinear, which is the case in Section 4:3, then this analysis is a valuable guide.

4:2:2 Convergent Flow between Two Concentric Cylinders

In an ideal concentric-cylinder diode the following relations apply[3]

$$\left.\begin{aligned}
&\text{Potential} && \Phi = \left(\frac{R\beta^2}{R_a\beta_a^2}\right)^{\frac{2}{3}} \\
&\text{Electric Intensity} && \mathcal{E} = -\frac{2}{3}\left(\frac{1}{R_a\beta_a^2}\right)\left[\frac{\beta^2 + 2\beta\,\frac{d\beta}{d\gamma}}{\left(\frac{R\beta^2}{R_a\beta_a^2}\right)^{\frac{1}{3}}}\right] \\
&\text{Electron Velocity} && \dot{R} = \sqrt{2\eta}\left(\frac{R\beta^2}{R_a\beta_a^2}\right)^{\frac{1}{3}} \\
&\text{Charge Density} && P = -\left(\frac{4}{9}\,\epsilon_o\right)\left(\frac{1}{R_a\beta_a^2}\right)\left[\frac{1}{R\left(\frac{R\beta^2}{R_a\beta_a^2}\right)^{\frac{1}{3}}}\right]
\end{aligned}\right\} \qquad (4.3)$$

where

$$R = \frac{r}{r_c} = \frac{\text{radius}}{\text{cathode radius}}$$

$$\Phi = \frac{V}{V_a} = \frac{\text{potential at } r}{\text{potential at } r_a\text{, the anode}}$$

β = Langmuir parameter, a function of R

$$R_a = \frac{r_a}{r_c} \quad .$$

The radial dependence of the charge-density P is shown in Figure (4-4), while Φ and $\mathcal{E}$ are shown in Figure (4-5) for the case $R_a = 0.25$. Near the cathode, the behaviour of the flow parameters for this case and for the planar diode case is seen to be similar. However, as the flow converges, the parameter behaviour becomes decidedly different. The charge density P attains a minimum and then increases without limit as $R \rightarrow 0$.

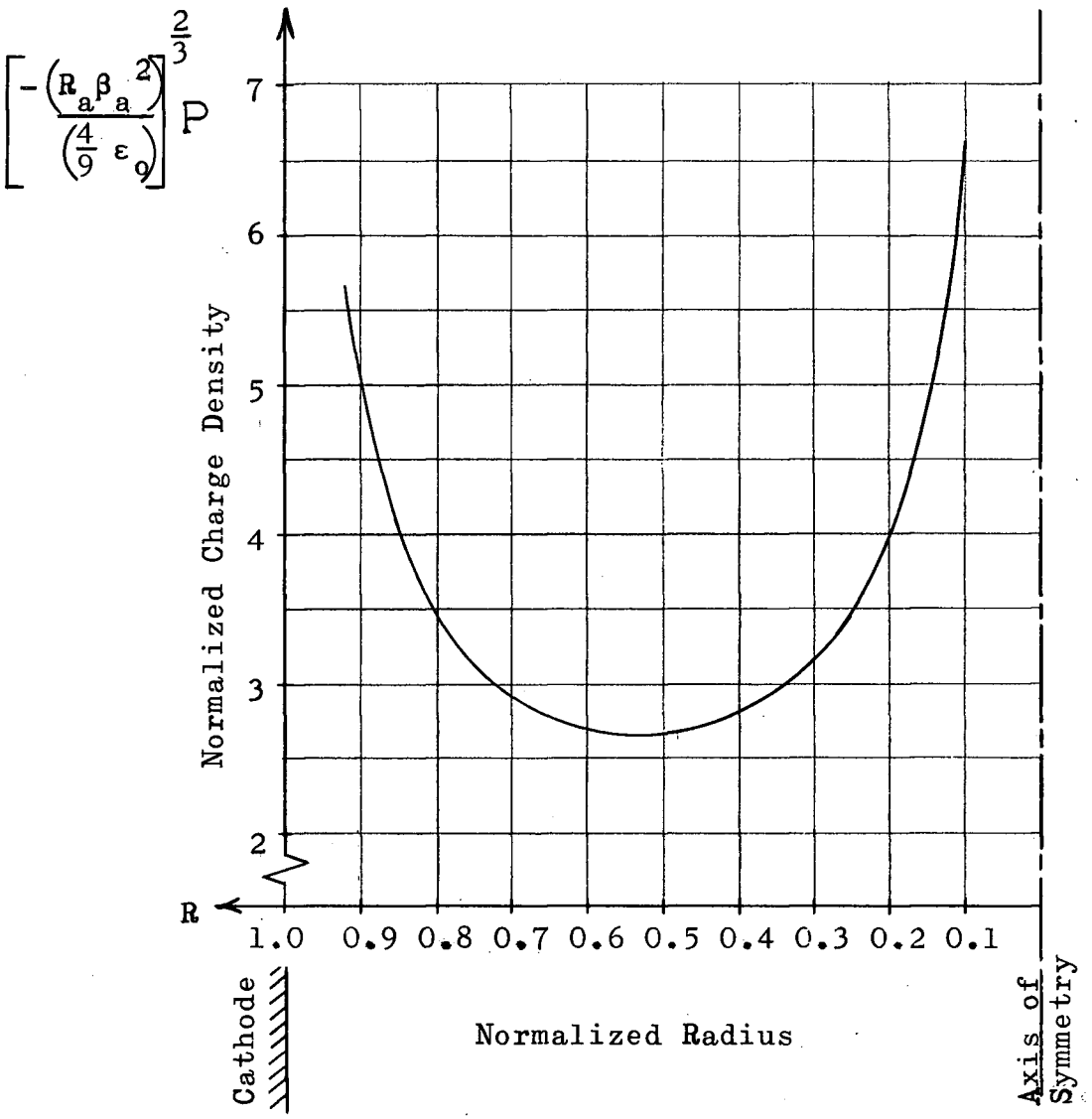

Figure (4-4). Variation of the charge density in rectilinear, convergent electron motion from a cylindrical cathode

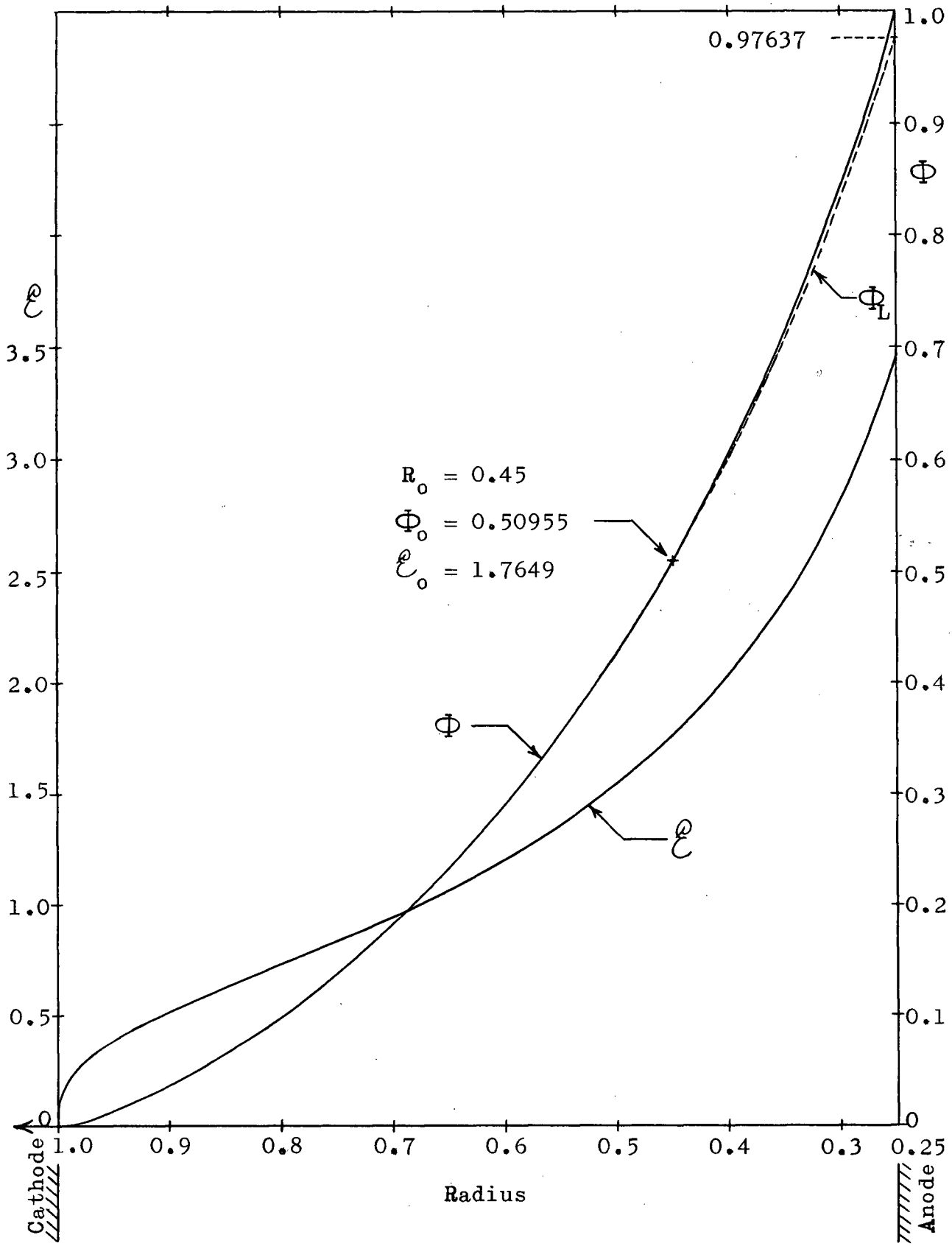

Figure (4-5). Variation of the potential and electric intensity versus distance from the cathode in a concentric-cylinder, convergent-flow diode. Also shown is an approximation of the potential in the anode region by $\Phi_L = a \ln R + b$

Thus, to accurately approximate the electrostatic field in the anode region of a cylindrical diode by a space-charge-free field

$$\Phi_L = a \ln R + b, \qquad (4.4)$$

the anode radius R_a should preferably not be too small. An anode radius of $R_a = 0.25$ was found to be a convenient value.

Let the field be approximated by (4.4 over the range

$$R_o > R \geq 0.25$$

by matching the gradients of Φ and Φ_L at R_o, as shown in Figure (4-5). Therefore, at $R = R_o$,

$$\Phi = \Phi_L \text{ and } \frac{d\Phi}{dR} = \frac{d\Phi_L}{dR}$$

so from equations (4.3a and b) it follows that the constants of equation (4.4) are

$$\left.\begin{aligned} a &= - R_o \mathcal{E}\Big|_{R = R_o} \\ b &= \Phi\Big|_{R = R_o} + R_o \mathcal{E}\Big|_{R = R_o} \ln R_o \end{aligned}\right\} .$$

For the example illustrated in Figure (4-5), $R_o = 0.45$, so equation (4.4) is

$$\Phi_L = -0.79421 \ln R - 0.12463 .$$

Let the error in potential, e_Φ, and the error in velocity, $e_{\dot{R}}$, be defined as in Sub-section 4:2:1, namely

$$\left.\begin{aligned} e_\Phi &= 100\left(\frac{\Phi - \Phi_L}{\Phi}\right) \% \\ e_{\dot{R}} &= 100\left(\frac{\dot{R} - \sqrt{2\eta\Phi_L}}{\dot{R}}\right) \% \end{aligned}\right\} .$$

For a given R_o, the maximum errors occur at the anode. The errors at the anode for the case $R_o = 0.45$ are

$$e_\Phi = 2.36\%$$
$$e_{\dot{R}} = 1.19\% \quad .$$

The errors at the anode incurred by initiating the field approximation at other values of R_o are shown in Figure (4-6). The distance coordinate in this graph is normalized w.r.t. the cathode-anode distance to permit a comparison to be made with the

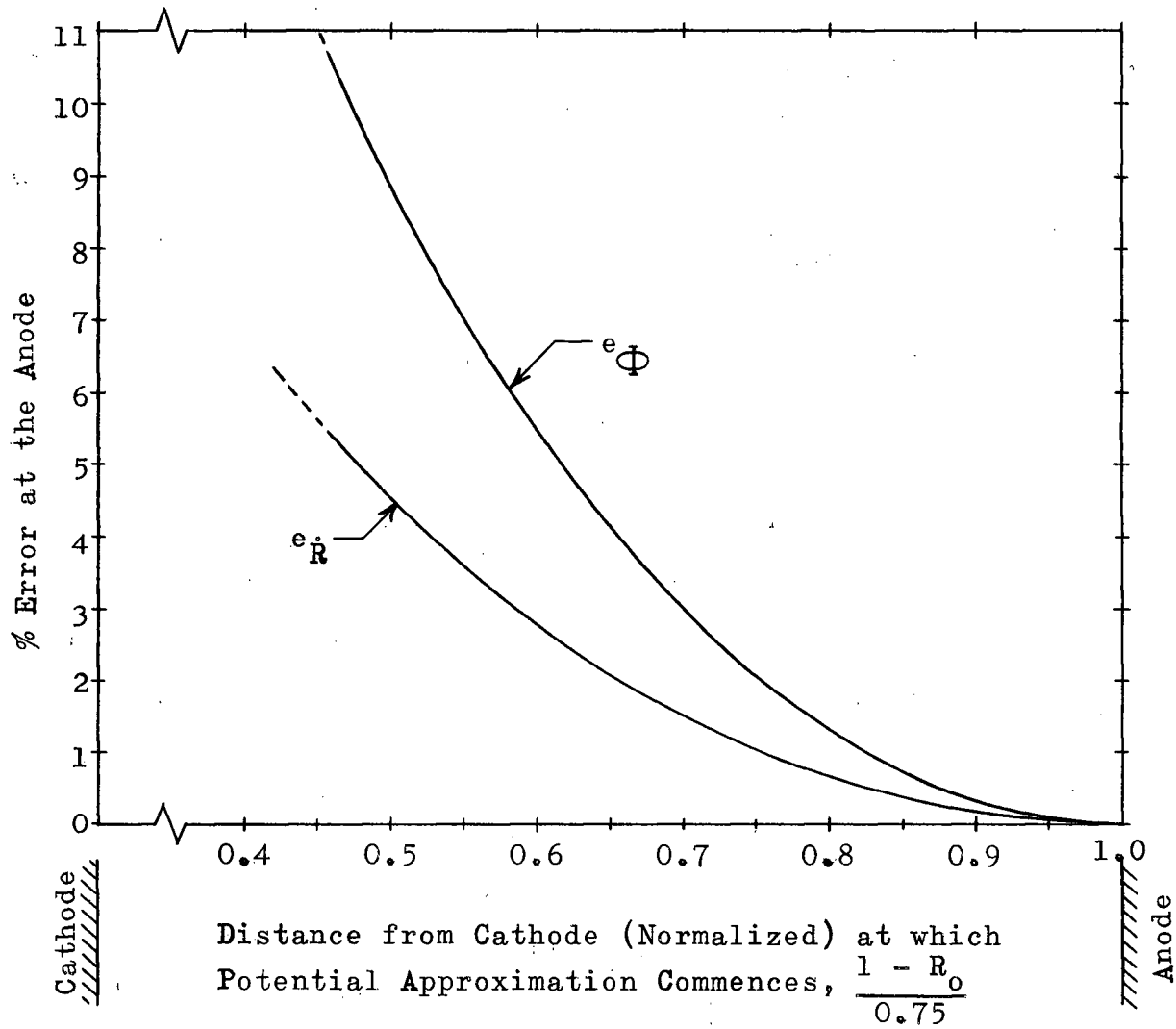

Figure (4-6). Error in potential e_Φ, and in electron velocity $e_{\dot{R}}$, at the anode of a concentric-cylinder, convergent flow diode when the potential is approximated by $\Phi_L = a \ln R + b$ over the interval $R_o > R \geq R_a$, where $R_a = 0.25$

planar diode approximation, Figure (4-3). It is seen that the errors for the cylindrical diode case are higher, as anticipated from the behaviour of P. For example, the field approximations over the intervals $0.75 < Y \leq 1$ and $0.4375 > R \geq 0.25$ for the planar diode and cylindrical diode respectively, both cover one quarter of the cathode-anode distance, and the velocity errors at the anode are $e_{\dot{Y}} = 0.79\%$ and $e_{\dot{R}} = 1.03\%$ respectively.

The space-charge-free potential that we will match to an initially radial, convergent flow is one calculated for an anode with an aperture. In the region of the aperture the beam is defocused due to the combined action of the anode field and the space-charge forces. As a result, the charge density will not follow the theoretical curve of Figure (4-4) beyond the matching radius R_o, but will tend to diverge from it on the low side, which should improve the accuracy of the space-charge-free potential approximation.

4:3 Initially Parallel, Rectilinear Flow to an Apertured Anode

The ideas presented in Sections 4:1 and 2 will now be applied to the study of space-charge-limited flow between a planar cathode and an anode consisting of two right-angled plates, as shown in Figure (4-7). If the anode aperture is taken to be of unit width, then the region of particular interest is $|x| \leq 0.5$. The problem of providing a bounding electrostatic field for a beam within this region is taken up in Chapter V.

It will be assumed that the electron motion in the cathode region, $y_c \leq y \leq y_o$, is parallel and rectilinear, and that the electrostatic field in the anode region, $y > y_o$, can be

represented by the field derived in Section 3:3. The accuracy of these assumptions depends primarily on the ratio of the aperture width to the cathode-anode distance because, if the cathode-anode distance is reduced relative to the aperture width, the perveance is increased and the perturbation of the field due to the anode aperture becomes more severe in the cathode region. The accuracy with which it is desired to satisfy the assumptions thus determines the values of y_o and y_c; y_o must be sufficiently far from the anode that the equipotential Φ_o can be considered to be planar, and y_c must be a sufficient distance beyond y_o so that the electrostatic field in the anode region may be approximated by a space-charge-free field.

From Figure (3-4) it is seen that the equipotential surfaces near y = -1 have become almost planar, varying from the planar by less than .01 or 1% over the distance $|x| \leq 0.5$. Accordingly, y_o will be taken to lie near y = -1, although its value will not be specified at this stage.

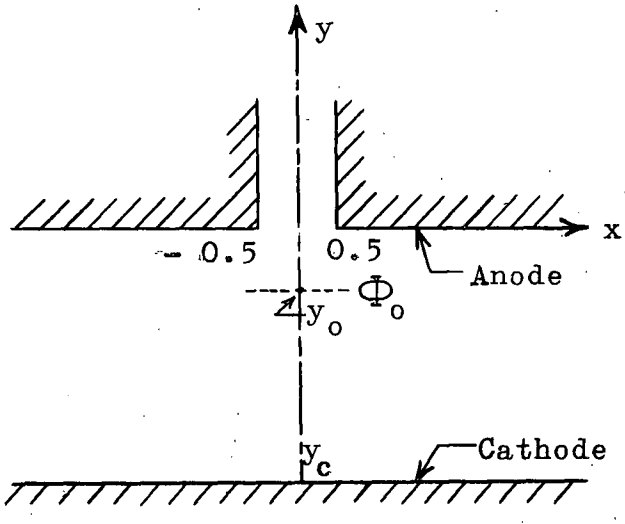

Figure (4-7). Planar diode with an anode aperture

The flow in the cathode region will be taken to be the same as that in the region $0 \leq Y \leq 0.75$ (notation as in Sub-section 4:2:1) of a planar diode. If the anode of the structure in Figure (4-7) had no aperture, the maximum error incurred by approximating the field in the anode region would thus be $e_{\Phi} = 1.57\%$. Furthermore, if in the latter case $y_o = -1$, it follows that $y_c = -4$, so the cathode-anode distance $d = 4$, and y and Y are related by

$$y = -4(1 - Y) \quad .$$

If this equation is substituted into equations (4.1a and b) and evaluated for $y = y_o = -1$, there result

$$\left.\begin{aligned} \Phi_o &= 0.681420 \\ \mathscr{E}_o &= -\left.\frac{d\Phi}{dy}\right|_{y_o} = -0.302853 \quad . \end{aligned}\right\} \tag{4.5}$$

In the actual diode under study an aperture is present. It is mathematically convenient to treat this case by moving the entire cathode region slightly closer to the anode; i.e., the distance between the cathode, $y = y_c$, and the equipotential Φ_o at $y = y_o$ remains

$$y_o - y_c = 3 \tag{4.6}$$

and conditions (4.5) must be satisfied at $y = y_o$. If in addition we specify that the anode potential $\Phi_k = 1$, then the value of y_o, and the space-charge-free field in the anode region, can be calculated from equations (3.6); this will now be done.

The mapping

$$w = \varrho(\eta - \eta_k) \tag{4.7}$$

where

$$w = u + i\,v$$
$$\eta = \Psi + i\,\Phi$$
$$\eta_k = \Psi_k + i\,\Phi_k$$

rescales w by a factor ϱ^{-1}, and shifts the origin of the w-plane a distance η_k. In the z-plane, v = 0 coincides with the anode surface. Since the anode potential is to be unity, we thus must set $\Phi_k = 1$. Further, let $\Psi_k = 0$. Equation (4.7) then becomes

$$\left.\begin{aligned} u &= \varrho\Psi \\ v &= \varrho(\Phi - 1) \quad . \end{aligned}\right\} \tag{4.8}$$

When equations (4.8) are substituted into equations (3.6) and the defining relations following the latter, we obtain

$$\left.\begin{aligned} x &= -\frac{1}{\pi}\left[\frac{\pi}{2} + R^{\frac{1}{2}}\cos\left(\frac{\Theta}{2}\right) - \tan^{-1}\left(\frac{B}{\sqrt{1-B^2}}\right)\right] \\ y &= -\frac{1}{\pi}\left[R^{\frac{1}{2}}\sin\left(\frac{\Theta}{2}\right) - \ln\left(A + \sqrt{A^2+1}\right)\right] \end{aligned}\right\} \tag{4.9}$$

where

$$R = \varrho^2\left\{\left[\Psi^2 - (\Phi-1)^2 - \left(\frac{1}{\varrho^2}\right)\right]^2 + \left[2\Psi(\Phi-1)\right]^2\right\}^{\frac{1}{2}}$$

$$\Theta = \operatorname{Arctan}\left[\frac{2\Psi(\Phi-1)}{\Psi^2 - (\Phi-1)^2 - \left(\frac{1}{\varrho^2}\right)}\right] \quad \text{if} \quad \left[\Psi^2 - (\Phi-1)^2 - \left(\frac{1}{\varrho^2}\right)\right] \geq 0$$

$$= \pi + \operatorname{Arctan}\left[\frac{2\Psi(\Phi-1)}{\Psi^2 - (\Phi-1)^2 - \left(\frac{1}{\varrho^2}\right)}\right] \quad \text{if} \quad \left[\Psi^2 - (\Phi-1)^2 - \frac{1}{\varrho^2}\right] < 0$$

$$A = \left\{ \frac{1}{2} \left[- (1 - a^2 - b^2) + \sqrt{(a^2 + b^2 - 1)^2 + 4b^2} \right] \right\}^{\frac{1}{2}}$$

$$B = \left\{ \frac{1}{2} \left[(1 - a^2 - b^2) + \sqrt{(a^2 + b^2 - 1)^2 + 4b^2} \right] \right\}^{\frac{1}{2}}$$

and

$$a = \frac{\Psi}{\varrho\left[\Psi^2 + (\Phi - 1)^2\right]} \quad , \quad b = \frac{-(\Phi - 1)}{\varrho\left[\Psi^2 + (\Phi - 1)^2\right]} \quad .$$

Along the plane of symmetry of the anode region $\Psi = 0$, so it follows from equation (4.9b) and the defining relations that the potential variation along the plane of symmetry is

$$y\Big|_{x = 0} = - \frac{1}{\pi} \left[\left(\varrho^2 (\Phi - 1)^2 + 1 \right)^{\frac{1}{2}} - \sinh^{-1} \left(\frac{1}{\varrho(\Phi - 1)} \right) \right] \quad . \tag{4.10}$$

The derivative of $y\Big|_{x = 0}$ w.r.t. Φ is

$$\frac{dy}{d\Phi}\Big|_{x = 0} = - \frac{1}{\pi} \left[\varrho^2 + \frac{1}{(\Phi - 1)^2} \right]^{\frac{1}{2}} \quad .$$

The potential gradient along the plane of symmetry in the anode region is therefore

$$\mathcal{E}\Big|_{x = 0} = - \frac{1}{\frac{dy}{d\Phi}\Big|_{x = 0}} = \frac{\pi}{\left[\varrho^2 + \frac{1}{(\Phi - 1)^2} \right]^{\frac{1}{2}}}$$

which can be solved for ϱ:

$$\varrho = - \left[\left(\frac{\pi}{\mathcal{E}\Big|_{x = 0}} \right)^2 - \frac{1}{(\Phi - 1)^2} \right]^{\frac{1}{2}} \quad . \tag{4.11}$$

Equation (4.11) relates the scaling factor Q to the potential and gradient at an arbitrary point on the y-axis. We wish to find the scaling factor when conditions (4.5) are satisfied at y_o. If conditions (4.5) are substituted into equation (4.11), the scaling factor is

$$Q = -9.88700 \quad . \tag{4.12}$$

The value of y_o can now be computed by substituting (4.5a and 12) into (4.10):

$$y_o = -0.952495 \quad . \tag{4.13}$$

The potential in the anode region is described by equations (4.9) and their defining relations, with Q as given by (4.12). The flow parameters in the cathode region can be obtained from equations (4.1) since, from equations (4.6 and 13), y and Y are related by

$$y = -4(1 - Y) + 0.047505 \quad . \tag{4.14}$$

The potential variation along the plane of symmetry is shown in Figure (4.8).

If space-charge forces are neglected, electron trajectories in the anode region can be obtained by a numerical method developed in Appendix C, Section 1. Using this method, trajectories were computed in the region of the anode aperture, $|x| < 0.5$, resulting in the trajectory shapes shown in Figure (4-9a).

For the case when an electron beam enters the anode region over the interval $|x| < 0.5$ only*, the electron trajectories in

*This can be accomplished by, for example, inserting in the structure of Figure (4-7) an intercepting anode which coincides with the equipotential Φ_o over the interval $|x| \geq 0.5$.

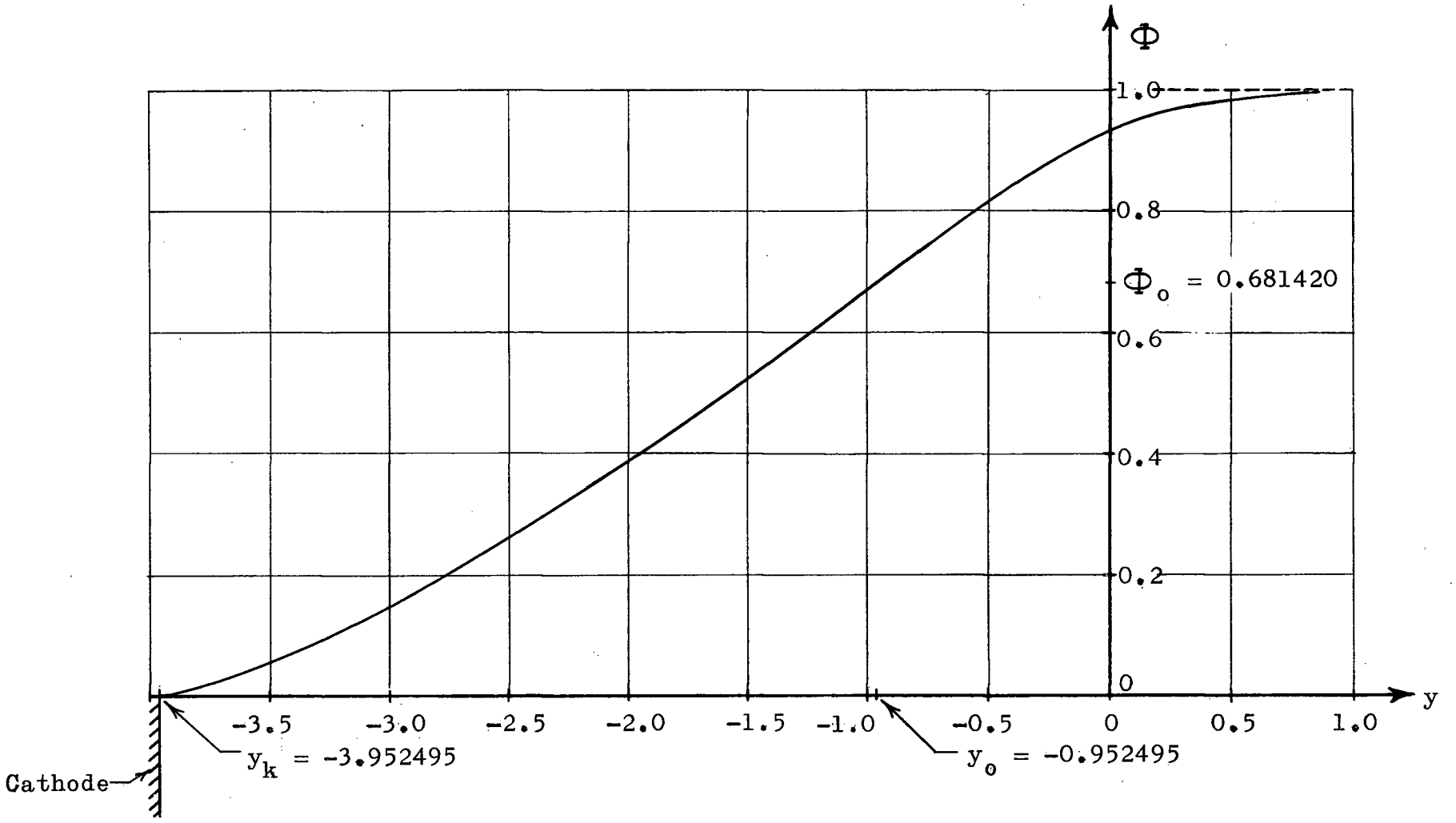

Figure (4-8). Potential variation along the plane of symmetry of an initially parallel, rectilinear flow

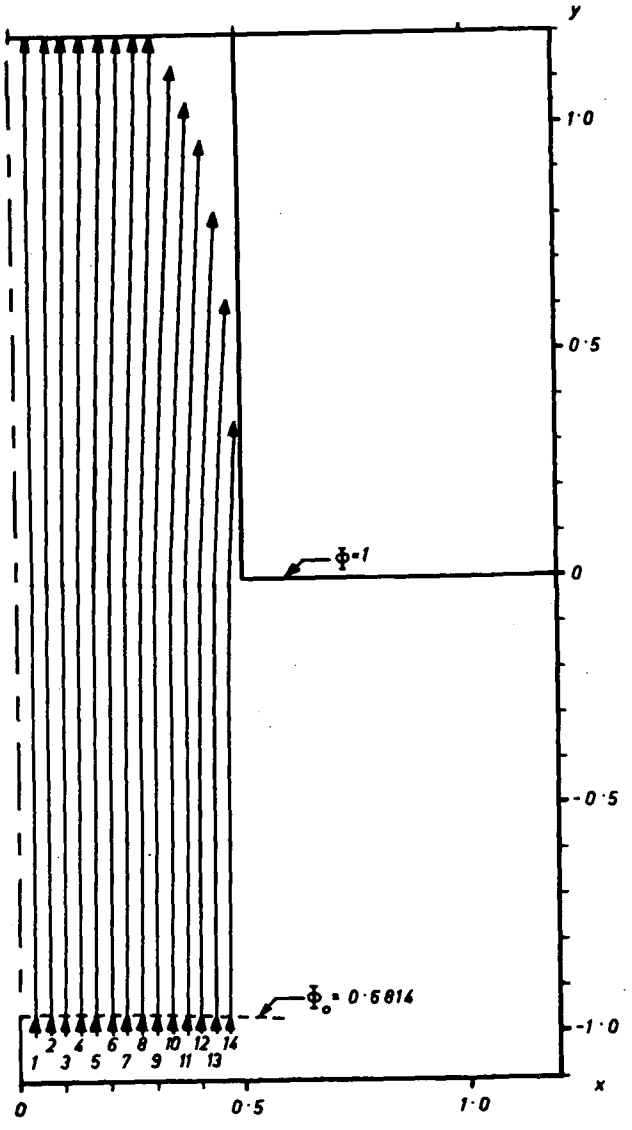

Figure (4-9a). Electron trajectories neglecting space-charge effects

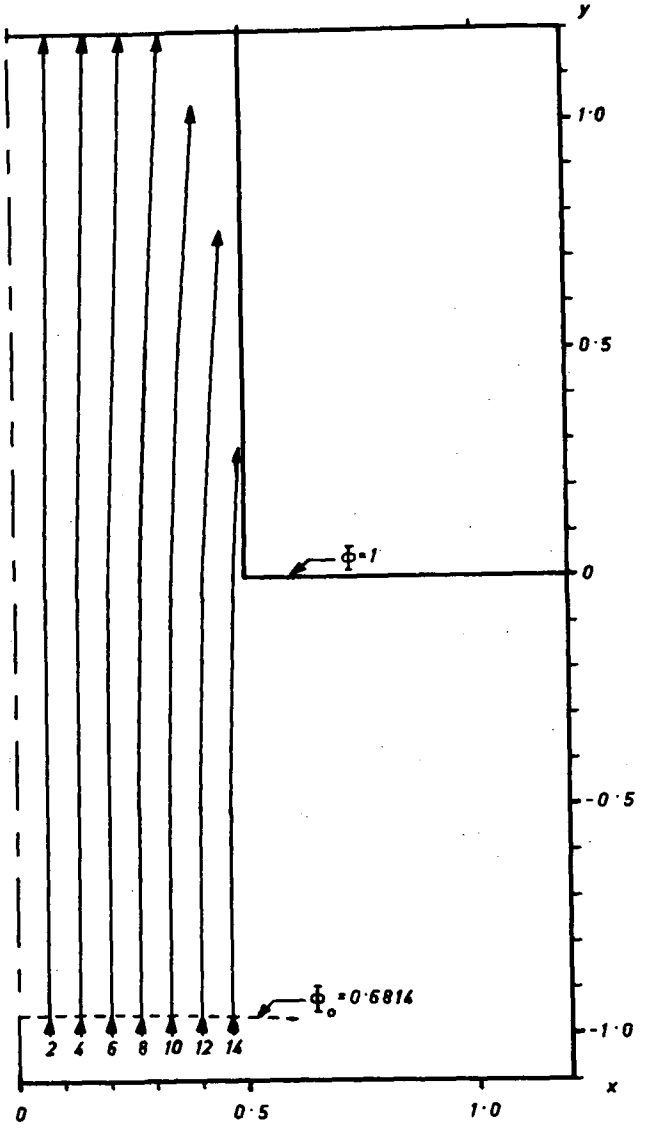

Figure (4-9b). Electron trajectories when space-charge forces are taken into account

the anode region will be the same as those shown in Figure (4-9a), if space-charge forces are neglected. Since the transverse electron velocity of the beam is much less than the axial velocity, a first-order correction can be made for the transverse space-charge forces. This correction is made in Appendix C, Section 2, and space-charge-corrected electron trajectories obtained by this method are shown in Figure (4-9b). The difference between the trajectory shapes of Figures (4-9a and b) is seen to be slight.

The perveance of the beam in the region $|x| < 0.5$ is approximately equal to the perveance of an equivalent planar diode with cathode-anode distance d = 4, because the cathode was moved closer to the anode to maintain the perveance in the region $|x| < 0.5$ when an aperture was cut in the anode. From equation (1.1) and the Langmuir-Child law[2] it is readily found that the perveance per unit distance perpendicular to the x-y plane is

$$\frac{K}{\ell} = \frac{2k_1 x}{d^2} \qquad (4.15)$$

where

$$k_1 = \frac{4}{9}\varepsilon_o\sqrt{2\eta} \quad .$$

Referring to Figure (4-9b), it is observed that a trajectory with coordinate x = 0.4641 in the initially parallel part of the beam has diverged to x = 0.4752 at the plane y = 0. An electron beam with an initial half-width of 0.4641 would therefore be suitable for this anode aperture. Setting x = 0.4641 and d = 4 in equation (4.15), the perveance of the resultant beam is thus

$$\frac{K}{\ell} = 0.14 \times 10^{-6} \text{ amp/volt}^{\frac{3}{2}} \text{ meter.}$$

4:4 Initially Radial, Convergent Flow to an Apertured Anode

As a second illustration of the usefulness of the "two-region concept" for electron gun studies, a case of great practical interest is considered next: convergent flow from a cathode that is a section of a cylinder. It will be assumed that the flow in the cathode region is radial and space-charge limited, and that the field in the anode region can be approximated by a space-charge-free field. To this end a study will first be made of pertinent characteristics of the anode fields derived in the third chapter to determine their suitability for this electron motion.

4:4:1 Analysis of Anode Fields

Consider Figure (4-10). For electron motion in the cathode region, $r_c \geq r \geq r_o$, to be rectilinear and convergent toward a common axis (x_c, y_c), it is clear that the equipotentials in the cathode region must be cylindrical sections with a common centre of

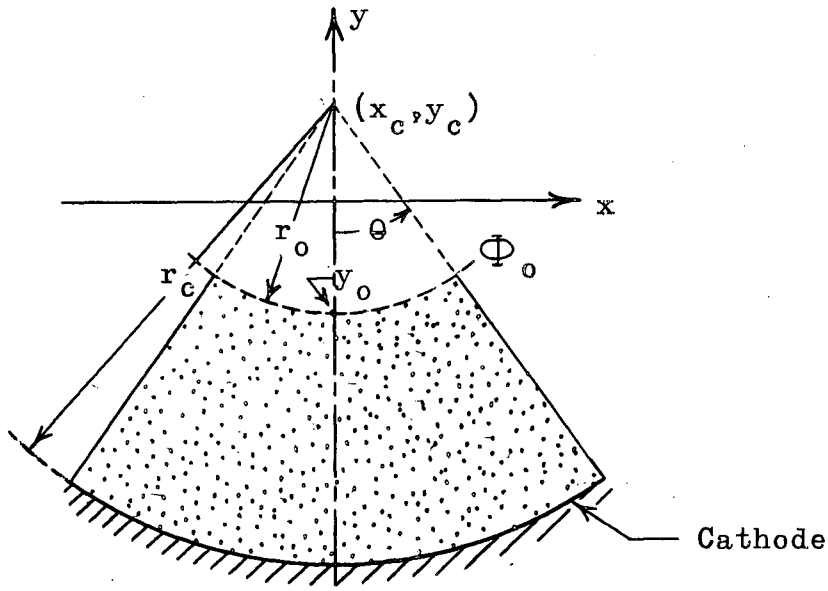

Figure (4-10). Cathode region of an initially radial, convergent flow

curvature (x_c, y_c). The basic conditions that must thus be met by the equipotential Φ_o at $r = r_o$ are that over the width of the beam (a) Φ_o be a section of a cylinder and (b) the gradient at Φ_o be independent of θ. In addition, it is desirable that Φ_o be close to the anode aperture and that Φ_o have a short radius of curvature, because this improves the beam perveance.

It is clear from Figures (3-2 and 4) that an anode consisting of a plate with a slit, or consisting of two right-angled plates, is not suitable for an initially radial, convergent flow, because no equipotential in front of their anode apertures satisfies the basic requirements for Φ_o. However, the field surrounding an anode consisting of two semi-infinite parallel planes, which is illustrated in Figure (3-7), is seen to exhibit the required behaviour. The variation of the radius of curvature and of the centre of curvature along the equipotentials of this field were obtained by a method presented in Appendix D, and are shown in Figures (4-11 and 12). For example, the radius of curvature of the equipotential $v = 2.50$ in Figure (3-7) at $u = 1.0$ is, from Figure (4-11), $r = 3.164$, and the angle between the radius of curvature and the plane of symmetry is $\theta = 16.85^{\circ}$; the centre of curvature of the above equipotential at $u = 1.0$ is, from Figure (4-12), $(x_c, y_c) = (-7.496 \times 10^{-4}, 1.718)$. Also shown in Figure (4-11) is a curve that is indicative of the maximum half-angle θ that can be occupied by the electron beam. This curve, which will be called the "maximum line", was obtained by determining, for each of several equipotentials, the point on the equipotential from which an electron, travelling along the radius of curvature and continuing in a straight line, will graze

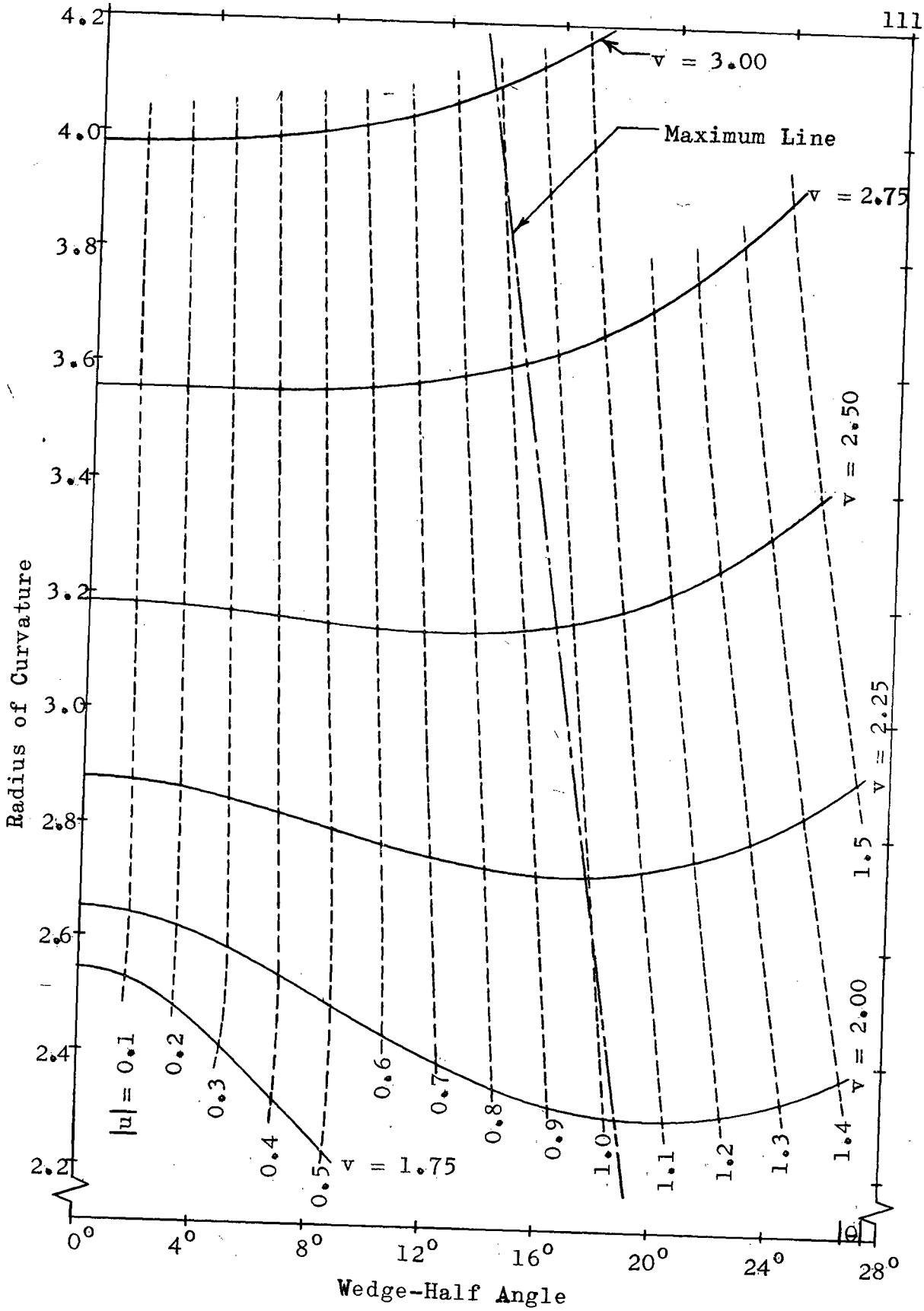

Figure (4-11). Radius of curvature of equipotentials in the field about two semi-infinite parallel plates

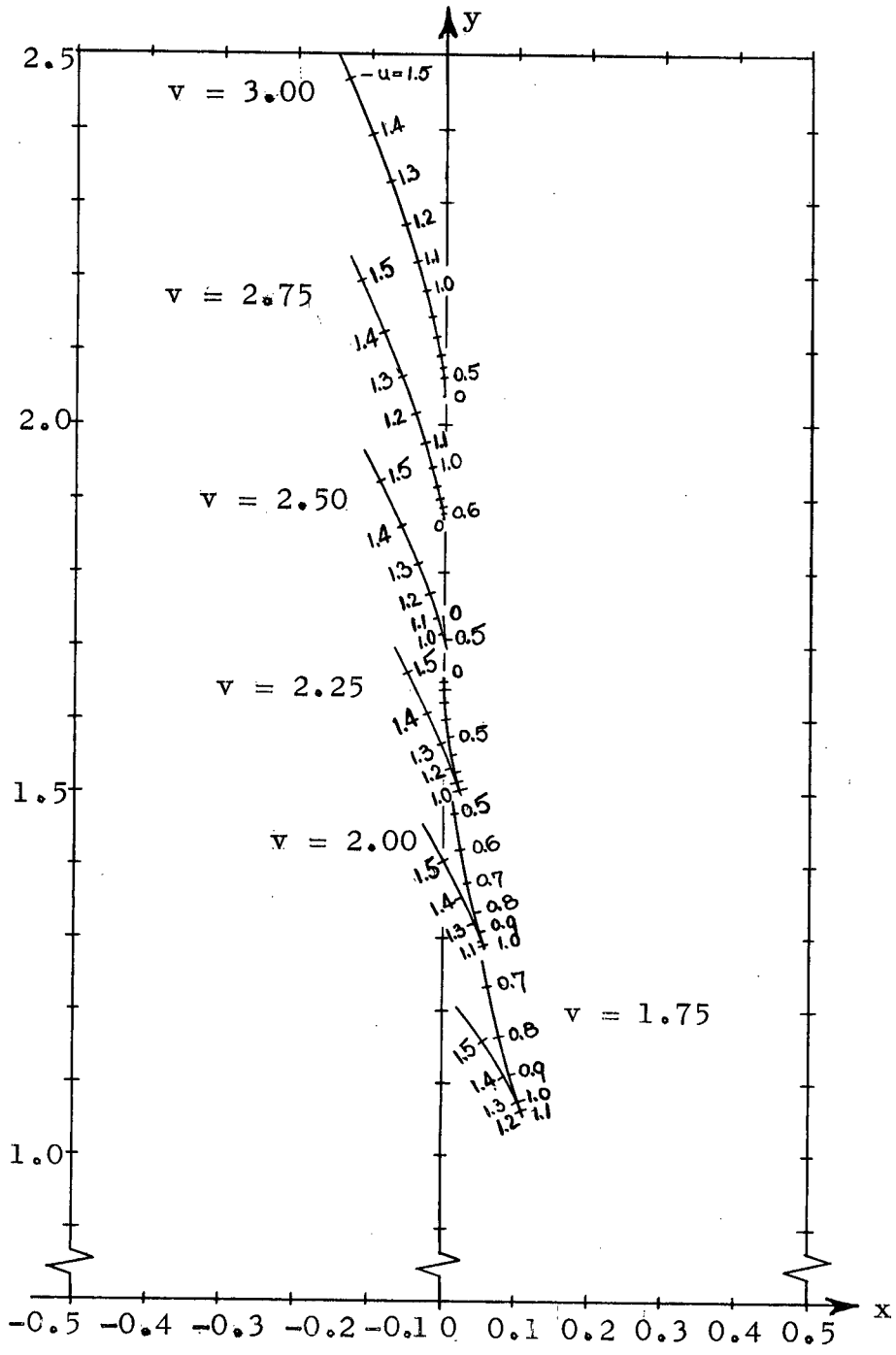

Figure (4-12). Position of the centre of curvature of equi-potentials in the field about two semi-infinite parallel plates

the mouth of the anode. For example, the maximum half-angle determined by the maximum line criterion for the equipotential $v = 2.50$ is $\theta = 16.25^{\circ}$.

From Figures (4-11 and 12) it is seen that the equipotential $v = 2.75$ in Figure (3-7) has a radius of curvature and a centre of curvature that are almost constant over the interval $|u| = 0.6$. This equipotential crosses the y-axis at $y = -1.6848$ and the half-angle at $|u| = 0.6$ is $\theta = 11.6^{\circ}$. Therefore, although the shape of this equipotential makes it ideal for use as the matching equipotential Φ_o, the relatively large distance of this equipotential from the anode aperture and the relatively small half-angle would result in a flow that would have neither a high perveance nor a high convergence.

The equipotentials $v < 2.75$ have radii of curvature that first decrease and then increase again with increasing $|u|$; the centres of curvature simultaneously move towards the equipotentials when the radii of curvature decrease, and move away from them again when the radii of curvature increase. When these variations in the curvature are not excessive, the equipotentials can be approximated accurately over the region of interest by sections of a cylinder. For example, a section of a cylinder with centre of curvature at

$$(x_c, y_c) = (0, 1.51714)$$

and having a radius of curvature $r = 2.5343$, coincides with the equipotential $v = 2.00$ at $|u| = 1.0$ and deviates from this equipotential by less than 0.0008, or 0.032% of the radius. Since this equipotential crosses the y-axis at $y = -1.0164$, and since the maximum half-angle determined by the maximum line criterion for

this equipotential is $\theta = 18.9^{\circ}$, this equipotential is obviously much more desirable for use as the matching equipotential Φ_o than the equipotential $v = 2.75$.

For equipotentials $v < 2$ the variation in curvature and of the gradient along the equipotentials increase rapidly for decreasing v, which makes them unsatisfactory for use as Φ_o.

The question that arises next is if the outside surfaces of a semi-infinite parallel-plane anode can be changed in shape in such a way that the desired field characteristics are improved; i.e., the equipotential that is suitable for use as the matching equipotential Φ_o occurs closer to the anode aperture and has a shorter radius of curvature. It is apparent from Figure (3-7) that to effect this improvement it is necessary to make the lines of force that issue from the aperture (the curves u = constant, where $|u| < 1$) spread out more rapidly. Now the semi-infinite parallel-plane anode is a special case of the anode geometry of Figure (3-3), with $\varphi_1 = \varphi_3 = -\pi$. Furthermore, the lines of force $u = \pm 1$ that leave the anode at the intersection of the inside and outside surfaces bisect the exterior angles between these surfaces. The magnitude of the angle that the flux lines $u = \pm 1$ make initially with both surfaces is thus $\frac{|\varphi_1| + \pi}{2}$. Clearly, the way to increase this angle, and hence the spreading of the flux lines, is by making φ_1 and φ_3 more negative. However, the case of an anode consisting of two semi-infinite parallel planes is already the limiting case of physical realizability and any attempt to make the angles φ_1 and φ_3 more negative would require the outside surfaces to pass through the inside surfaces, creating electrodes of "negative thickness", a physical impossibility. Mathematically

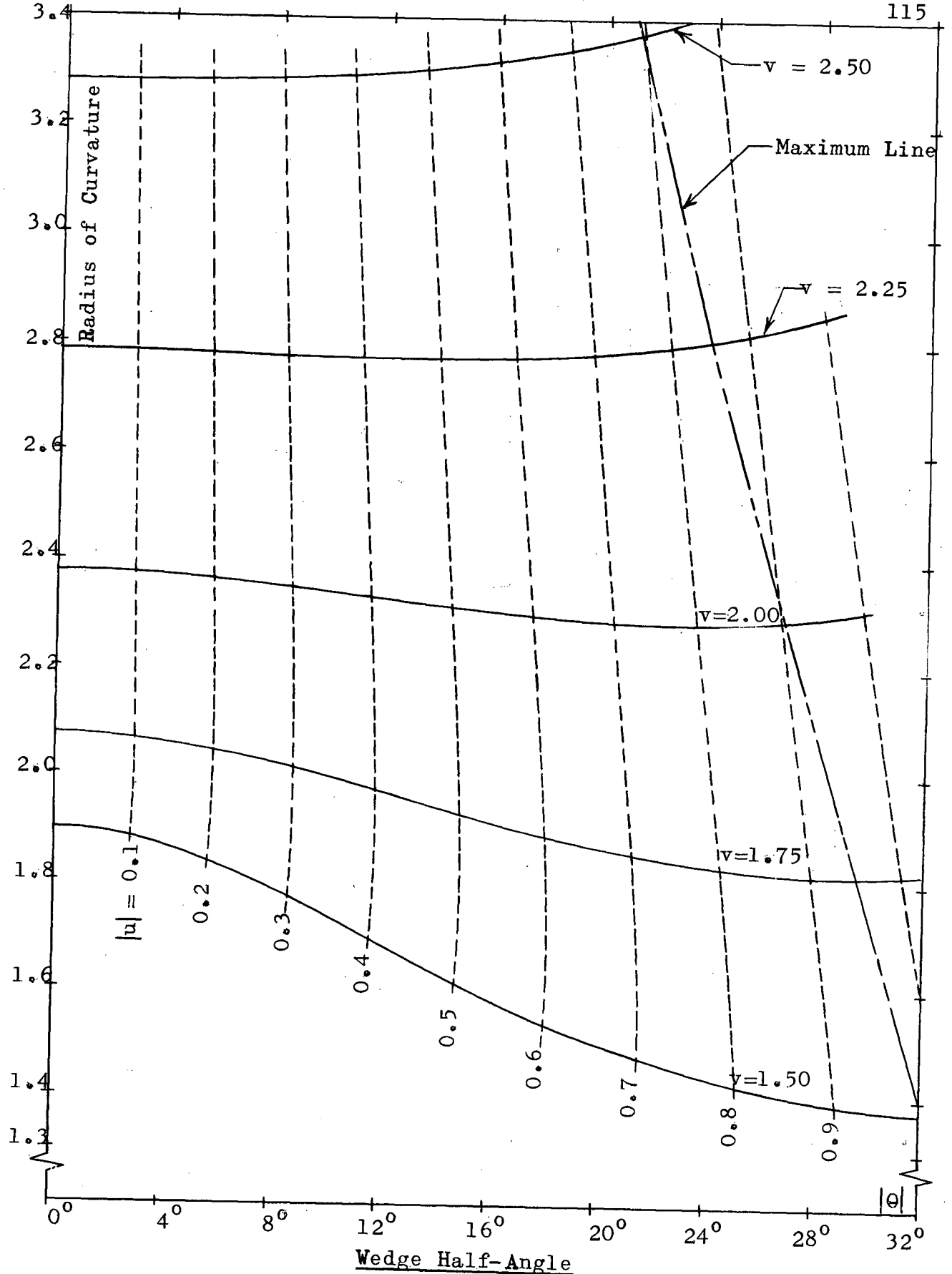

Figure (4-13). Radius of curvature of equipotentials in the wrap-around field

this is still possible, and has been discussed in Section 3:5 for the case $\varphi_1 = \varphi_3 = -\frac{5\pi}{4}$. Since the region of interest in this "wrap-around field" is the anode-aperture region, in which the potential is single valued, the field in this region can be realized by providing the required potential distribution at its boundary.

The variation of the radius of curvature and of the centre of curvature along the equipotentials of this wrap-around field were obtained by the method of Appendix D, and are shown in

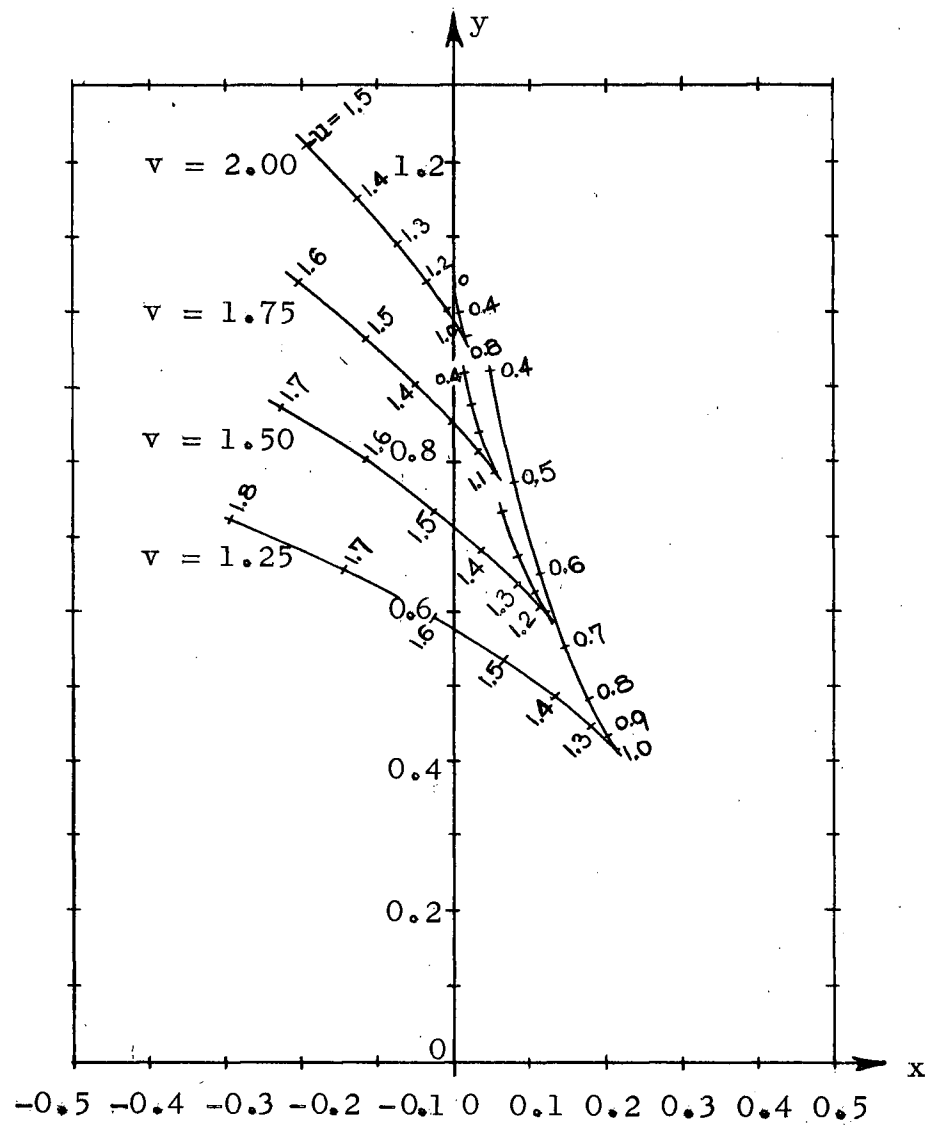

Figure (4-14). Centre of curvature of equipotentials in the wrap-around field

Figures (4-13 and 14). The variation of the potential gradient along the equipotentials is shown in Figure (4-15). For equipotentials far from the anode, the magnitude of the potential gradient is seen to decrease with increasing distance from the axis of symmetry. For equipotentials closer to the anode, the anode aperture causes an initial drop in the potential gradient near the axis of symmetry. As a result, the potential gradient at the surface v = 1.60 is almost constant to $|u| = 0.9$, varying by less than $\frac{1}{2}\%$ from the average gradient over this interval.

Comparison of the characteristics of the wrap-around field with those of the semi-infinite parallel-plane field reveals that the radii of curvature of the equipotentials of the wrap-around field are shorter and more constant. For example, the equipotentials v = 1.75 in the wrap-around field and v = 2.00 in the parallel-plane field, which are approximately the same distance from their respective anode apertures,* have radii of curvature that compare as follows:

Wrap-Around Field	Semi-Infinite Parallel Plane Field
v = 1.75	v = 2.00
$r_{max} = 2.074$	$r_{max} = 2.651$
$r_{min} = 1.816$	$r_{min} = 2.298$
$\Delta r = 0.258$	$\Delta r = 0.353$

The above change in radius for the wrap-around field occurs over a half-angle of $\theta = 29.5^{\circ}$, whereas the larger change of radius for the parallel plane field occurs over a half-angle of only $\theta = 18.9^{\circ}$. Clearly, the desired characteristics of the wrap-around

*Both equipotentials pass through the points $(x,y) = (\pm 0.860, -0.866)$.

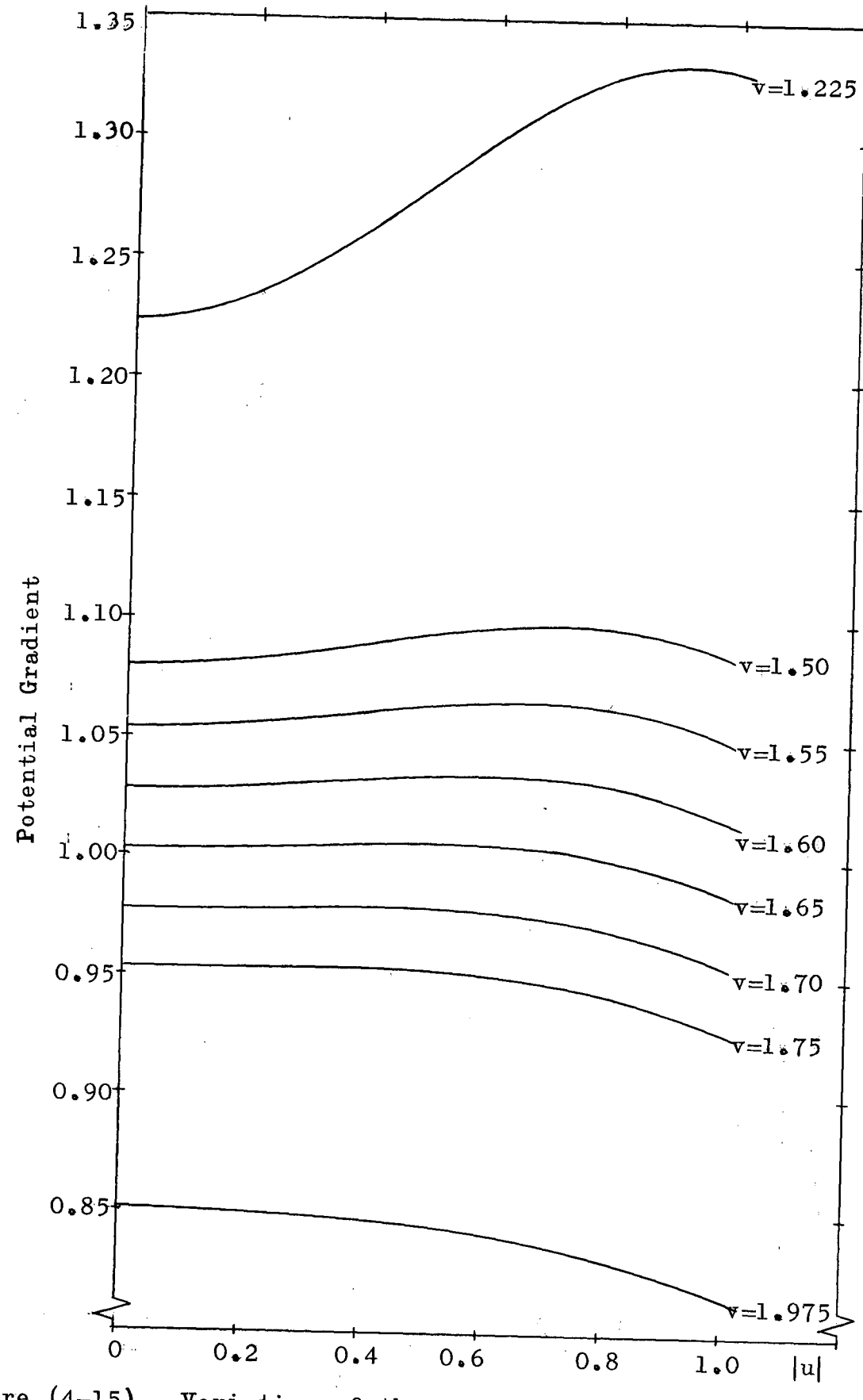

Figure (4-15). Variation of the potential gradient along equi-potentials of the wrap-around field

field are superior to those of the field about two semi-infinite parallel planes.

4:4:2 Electrostatic Field in the Anode Region Approximated by a Wrap-Around Field

A study will now be made of the initially radial, convergent flow of Figure (4-10) for the case when the field in the beam part of the anode region can be represented by the wrap-around field shown in Figure (3-8). The procedure to be used parallels that of Section (4:3).

The initial task in this study is to determine in the wrap-around field an equipotential surface that is suitable for use as the matching equipotential surface at potential Φ_o. The equipotential $v = 1.60$ is seen to be suitable for this purpose, because the potential gradient along the equipotential is almost constant and because the equipotential surface can be approximated accurately over the region of interest by a section of a cylinder with centre of curvature at

$$(x_c, y_c) = (0,\ 0.900000)$$

and with radius $r_o = 1.806283$. This cylindrical section coincides with the equipotential $v = 1.60$ at $|u| = 0.9$, and deviates from this equipotential by less than 0.0032, or about $\frac{1}{3}\%$ of the radius. The cylindrical section thus crosses the plane of symmetry $x = 0$ at $\overline{y}_o = y_c - r_o$; i.e., $\overline{y}_o = -0.906283$. The equipotential $v = 1.60$ crosses the plane of symmetry at $y_o = -0.903119$.

The flow in the cathode region will be taken to be the same as that in the region $1 \geq R \geq 0.45$ of a concentric cylinder diode with $R_a = 0.25$ (notation as in Sub-section 4:2:2); i.e., $R_o = 0.45$.

From the definition of R it follows that the cathode radius r_c can now be evaluated:

$$r_c = \frac{r_o}{R_o} = 4.013962$$

and hence the anode radius r_a of the equivalent concentric cylinder diode is

$$r_a = R_a r_c = 1.003491 \quad .$$

Using these values of r_a and r_c, the parameters of the electron motion in the cathode region, equations (4.3), become

$$\left.\begin{aligned} &\text{Potential} && \Phi = 0.300150(r\beta^2)^{\frac{2}{3}} \\ &\text{Electric Intensity} && \mathscr{E} = -.200100\left[\frac{\beta^2 + 2\beta\frac{d\beta}{d\gamma}}{(r\beta^2)^{\frac{1}{3}}}\right] \\ &\text{Electron Velocity} && \dot{r} = 3.2494 \times 10^5 (r\ \beta^2)^{\frac{1}{3}} \\ &\text{Charge Density} && P = -1.18115 \times 10^{-11}\left[\frac{1}{r(r\ \beta^2)^{\frac{1}{3}}}\right] \end{aligned}\right\} \quad (4.16)$$

where $4.013962 \geq r \geq 1.806283$.

When equations (4.16a and b) are evaluated at $r = r_o$, there result

$$\left.\begin{aligned} &\Phi\Big|_{r = r_o} = \Phi_o = 0.509549 \\ &\text{and} \\ &\mathscr{E}\Big|_{r = r_o} = \mathscr{E}_o = 0.439692 \quad . \end{aligned}\right\} \quad (4.17)$$

Equations (3.13), describing the potential in the anode region, must next be rescaled so that they attain the potential Φ_o and gradient $\mathscr{E}_o$ at $r = r_o$. For this purpose the mapping

$$w = \varrho(\eta - \eta_k) \tag{4.7}$$

is again required. Let $\Psi_k = 0$ as before; equation (4.7) then becomes

$$\left.\begin{aligned} u &= \varrho\Psi \\ v &= \varrho(\Phi - \Phi_k) \end{aligned}\right\} \tag{4.18}$$

When equations (4.18) are substituted into equations (3.11) and the defining relations of the latter, it is seen that only the parameters S and α are affected:

$$\left.\begin{aligned} S &= \varrho^2\left\{\left[\Psi^2 - (\Phi - \Phi_k)^2 - \left(\frac{1}{\varrho^2}\right)\right]^2 + \left[2\Psi(\Phi - \Phi_k)\right]^2\right\}^{\frac{1}{2}} \\ \alpha &= \tan^{-1}\left[\frac{2\Psi(\Phi - \Phi_k)}{\Psi^2 - (\Phi - \Phi_k)^2 - \left(\frac{1}{\varrho^2}\right)}\right]. \end{aligned}\right\} \tag{4.19}$$

Along the plane of symmetry of the anode region $\Psi = 0$, so it follows from equations (3.13b and 4.19) that the potential variation along the plane of symmetry is

$$y\Big|_{x=0} = \frac{2}{\pi}\left\{\frac{\pi}{4} - S^{\frac{1}{4}}\left(\frac{S}{5} + 1\right) + \frac{1}{4}\left[\tan^{-1}\left(\frac{2S^{\frac{1}{4}}(1-S^{\frac{1}{2}})}{S^{\frac{1}{2}}(S^{\frac{1}{2}} - 2)+1}\right) + \tanh^{-1}\left(\frac{2S^{\frac{1}{4}}(1+S^{\frac{1}{2}})}{S^{\frac{1}{2}}(S^{\frac{1}{2}}+2)+1}\right)\right]\right\} \tag{4.20}$$

where $S = Q^2(\Phi - \Phi_k)^2 + 1$.

The derivative of $y\Big|_{x = 0}$ w.r.t. Φ is

$$\left.\frac{dy}{d\Phi}\right|_{x = 0} = - \frac{\left[Q^2(\Phi - \Phi_k)^2 + 1\right]^{\frac{5}{4}}}{\pi(\Phi - \Phi_k)} \quad .$$

The potential gradient along the plane of symmetry in the anode region is therefore

$$\mathcal{E}\Big|_{x = 0} = - \frac{1}{\left.\frac{dy}{d\Phi}\right|_{x = 0}} = \frac{\pi(\Phi - \Phi_k)}{\left[Q^2(\Phi - \Phi_k)^2 + 1\right]^{\frac{5}{4}}}$$

which becomes, when solved explicitly for Q,

$$Q = - \left[\left(\frac{\pi}{\mathcal{E}\Big|_{x = 0}}\right)^{\frac{4}{5}} \frac{1}{(\Phi - \Phi_k)^{\frac{6}{5}}} - \frac{1}{(\Phi - \Phi_k)^2}\right]^{\frac{1}{2}} \quad . \qquad (4.21)$$

At this point the procedure used to obtain the potential in the anode region of the flow differs from that used in Section 4:3. In Section 4:3, the anode potential was set equal to unity by letting $\Phi_k = 1$ in equation (4.11); the analogous equation in the present problem is equation (4.21). Upon substitution of $\mathcal{E}_o$ and Φ_o into equation (4.11), the scaling constant Q, and subsequently y_o were obtained. In the present case we cannot follow this procedure, because it was necessary to specify r_o, and hence y_o, in order to determine $\mathcal{E}_o$ from the cylindrical-diode equation (4.3b). Therefore, it is not permissible to specify Φ_k in equation (4.21), otherwise too many

constraints are placed on the anode field. The two quantities to be solved for in the present case are thus Q and Φ_k. If conditions (4.17) are substituted into equation (4.21), there results

$$Q = -\left[4.821709(0.509549 - \Phi_k)^{-\frac{6}{5}} - (0.509549 - \Phi_k)^{-2}\right]^{\frac{1}{2}} . \tag{4.22}$$

Further, if the values of y_o and Φ_o are substituted for y and Φ respectively in equation (4.20), we obtain

$$0 = 1.4031189 + \frac{2}{\pi}\left\{-S^{\frac{1}{4}}\left(\frac{S}{5}+1\right) + \frac{1}{4}\left[\tan^{-1}\left(\frac{2S^{\frac{1}{4}}(1-S^{\frac{1}{2}})}{S^{\frac{1}{2}}(S^{\frac{1}{2}}-2)+1}\right) + \tanh^{-1}\left(\frac{2S^{\frac{1}{4}}(1+S^{\frac{1}{2}})}{S^{\frac{1}{2}}(S^{\frac{1}{2}}+2)+1}\right)\right]\right\} \tag{4.23}$$

where $S = Q^2(0.509549 - \Phi_k)^2 + 1$.

The solution of simultaneous equations (4.22 and 23) is

$$\left.\begin{aligned} Q &= -2.337807 \\ \Phi_k &= 1.193951 \quad . \end{aligned}\right\} \tag{4.24}$$

The potential in the anode region of the electron beam is described by equations (3.13) and their defining relations (4.19), with Q and Φ_k as given by (4.24). The potential variation along the plane of symmetry of the gun has been calculated by using equation (4.16a) for the cathode region and using (4.20 and 24) for the anode region; this potential variation is shown in Figure (4-16).

The maximum value of the wedge half-angle θ of the beam in the cathode region is limited by considerations of beam

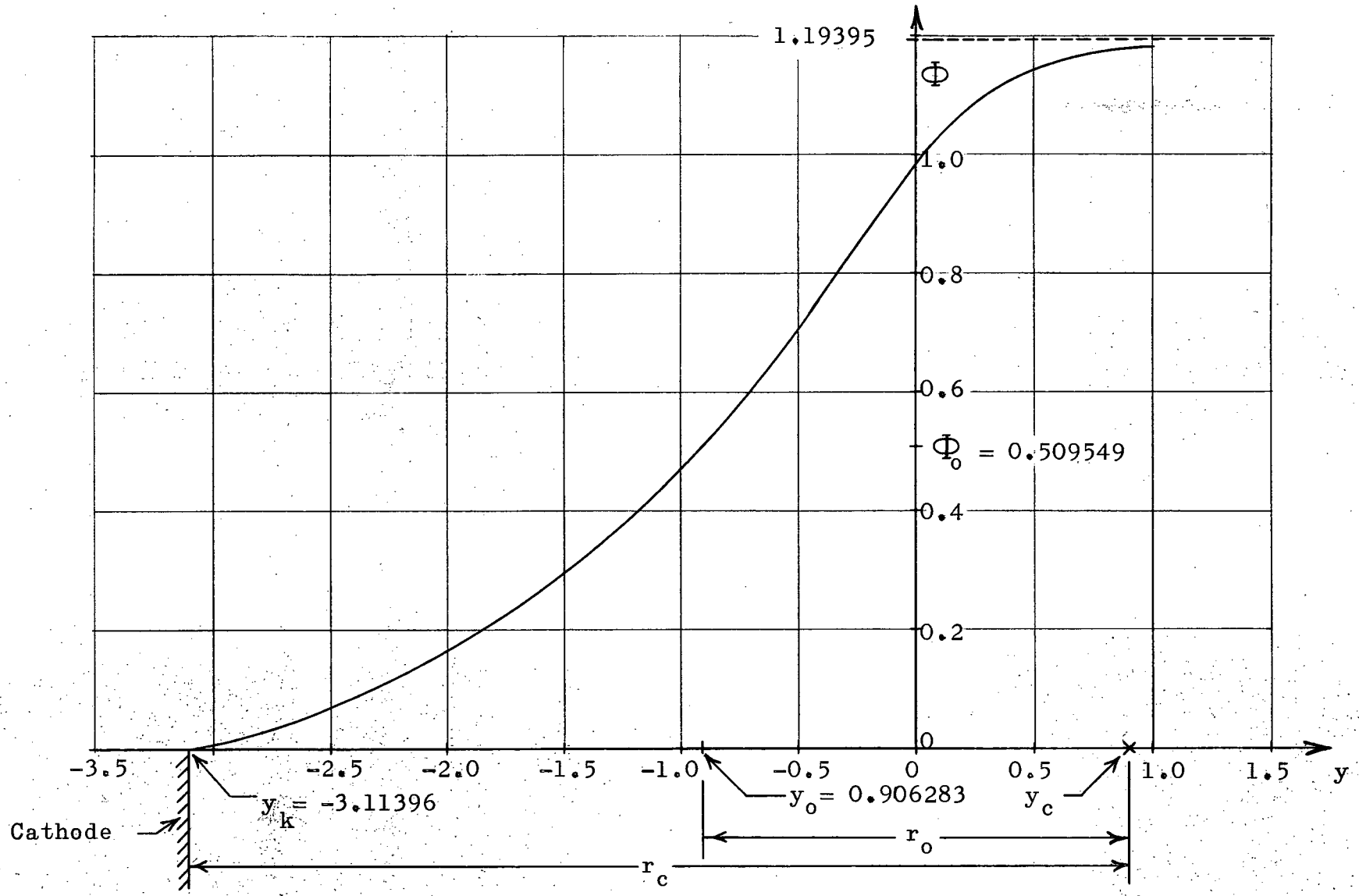

Figure (4-16). Potential variation along the plane of symmetry of an initially radial, convergent electron beam

interception by the anode. If the trajectories near the beam boundary continued onward in a straight line from the equipotential Φ_o, the angle at which electrons would graze the mouth of the anode would be 29.05°. In an actual electron gun, the beam boundary will be indistinct due to initial thermal velocities of the electrons. The beam boundary in the anode region is also broadened by the beam space-charge. The maximum value that can be used for the half-angle θ of the cathode is thus a few degrees less than 29°; the actual value of θ is probably best found by experimentation, although valuable guidance in this regard can be obtained from a preliminary study of the trajectories by analogue or by numerical methods.

Let θ arbitrarily be taken at 25°, so that an estimate of the gun perveance can be made. Since the flow in the cathode region of the gun is, by hypothesis, the same as that occurring in the corresponding region of an equivalent concentric-cylinder diode with $r_c = 4.01396$ and $r_a = 1.00349$, the beam current per unit length is[3]

$$\frac{I}{\ell} = \left[\frac{k_2 V_a^{\frac{3}{2}}}{r_a \beta_a^2}\right]\left(\frac{\theta}{180}\right) \qquad (4.25)$$

where

$$k_2 = \left[\frac{8\pi}{9}\,\varepsilon_o\sqrt{2\eta}\right]$$

and where V_a is the anode potential of the equivalent diode. To maintain the original conditions in the cathode region when a wrap-around field was used in the anode region, a normalized anode potential greater than unity was found to be required: $\Phi_k = 1.19395 = \frac{V_k}{V_a}$. On combining this with equations (1.1 and

4.25), the perveance per unit length is

$$\frac{K}{\ell} = \frac{k_2 \theta}{180\, r_a \beta_a^{\,2} \Phi_k^{\frac{3}{2}}}$$

or

$$\frac{K}{\ell} = 0.26 \times 10^{-6} \text{ amp/volt}^{\frac{3}{2}} \text{ meter.}$$

4.5 Discussion

The method employed in this chapter to adapt space-charge free anode fields and space-charge-limited flow solutions to electron gun design can be used for other anode fields and flow solutions. For example, the solution for space-charge-limited flow from a cathode consisting of two inclined plates[36] could be used; this solution has properties that make it desirable for use in electron gun design. With appropriate modifications, the method of this chapter could also be used for the design of axially-symmetric guns.

CHAPTER V - THE DETERMINATION OF BEAM-FORMING ELECTRODES

Little has been said so far about the electrodes required to produce the desired field conditions at beam boundaries. In particular, it is desired to determine beam-forming electrodes for the two examples in the previous chapter. To this end, a brief account will first be given of the physical considerations which apply to this problem.

5:1 Physical Considerations

The "engineering problem" of determining the shape of electrodes that will produce prescribed field conditions at the boundary of an electron beam is not a problem that arises in a natural or a direct way; rather, it is an inverse problem. Implicit in this problem are the assumptions that (a) such physically realizable electrode shapes exist, and (b) the electron beam is in a stable configuration. Neither assumption is necessarily warranted. For example, it has been shown[52,53] that a hollow beam confined by an axial magnetic field is in an unstable configuration. An example of a case where the prescribed boundary conditions cannot be met by beam-forming electrodes is the case of two parallel, space-charge-limited strip beams (see Appendix E).

If analogue equipment, such as an electrolytic tank, is used to obtain the shape of the beam-forming electrodes, then the procedure involved is generally one of trial and error, with some guidance from theory; i.e., the electrode shapes of the analogue model are adjusted until the boundary conditions are

satisfied to a sufficient accuracy.

If analytic methods or if numerical methods are employed to obtain the shape of the beam-forming electrodes, then the procedure generally followed is: (a) Laplace's equation is solved exterior to the beam surface — an open boundary — subject to Cauchy-type boundary conditions, and (b) beam-forming electrodes are arranged along equipotential surfaces exterior to the beam, generally and preferably only along the equipotentials at cathode and at anode potential. Success in part (b) of the procedure is contingent upon the solution being well-behaved in the vicinity of the beam. The remainder of this section will be devoted to part (a) of the procedure, the nature of the solution.

A boundary-value problem is properly set "if and only if its solution exists, is unique and depends continuously on the data assigned"[54]. A Cauchy problem for Laplace's equation on an open boundary is an improperly set problem, because the solution does not depend continuously on the boundary conditions[55]. That this is so can be readily demonstrated with an example contrived by Hadamard[54]. Consider the Laplace equation in two dimensions,

$$\frac{\partial^2 \Phi}{\partial x^2} + \frac{\partial^2 \Phi}{\partial y^2} = 0 \qquad (5.1)$$

which is to be solved subject to the Cauchy conditions

$$\Phi(0,y) = 0, \quad \left.\frac{\partial \Phi}{\partial x}\right|_{x=0} = \frac{1}{n}\sin(ny) \qquad (5.2)$$

where n is a large number. Equations (5.1 and 2) are solved by

$$\Phi(x,y) = \frac{1}{n^2} \sin(ny)\sinh(nx) \quad . \tag{5.3}$$

It is seen that by increasing the value of n, the Cauchy conditions (5.2) can be made as close to zero as desired. The solution of (5.1) when the Cauchy conditions are identically zero is $\Phi \equiv 0$. However, the solution (5.3) is by no means identically zero; for large x, sinh(nx) grows as e^{nx}, so that (5.3) oscillates with an amplitude that increases indefinitely. Any attempt to approximate zero Cauchy conditions more closely by increasing the value of n will increase the amplitude of the oscillation.

The solution exhibits the same discontinuous dependence on the boundary conditions when, instead of the Cauchy conditions (5.2) chosen by Hadamard, the Cauchy conditions

$$\Phi(0,y) = \frac{1}{n} \sin(ny) \quad , \quad \left.\frac{\partial \Phi}{\partial x}\right|_{x = 0} = 0 \tag{5.4}$$

are specified. In this case (5.1 and 4) are solved by

$$\Phi(x,y) = \frac{1}{n} \sin(ny)\cosh(nx) \tag{5.5}$$

which, for large x, again grows as e^{nx}.

The above examples illustrate that if the potential or the gradient or both are not prescribed exactly (i.e., are prescribed by analytic functions) on the boundary surface, then the error in the data, no matter how small it may be, can cause an error in the field which increases exponentially with distance from the boundary. The rate of error growth is discussed in more

detail in Appendix F.

Conversely, the sensitivity of the field conditions at the beam boundary to errors in the field conditions elsewhere decreases at an exponential rate with increasing distance from the beam boundary. The converse result has two most important consequences already mentioned; namely, that the electrodes can be truncated at a reasonable distance from the beam*, and that some degree of variation is possible in the electrode shapes.

5:2 Design Procedure

An electrolytic-tank procedure for obtaining beam-forming electrodes for the initially radial, convergent flow of Section 4:4 and for the initially parallel, rectilinear flow of Section 4:3 will now be considered. The latter case will be taken first.

It will be recalled that the electron motion in the cathode region was assumed to be the same as that occurring in a strip-beam Pierce gun. The shapes of the beam-forming electrode at cathode potential and of the equipotential surface Φ_0 are thus prescribed (the outward analytic continuation of equations (E.2 and 3)).

In Chapter 4, the potential and the potential gradient of the fields in the cathode and in the anode region were matched inside the beam at the equipotential Φ_0. The field conditions outside the beam were assumed to be satisfied by the use of an auxiliary anode, as shown in Figure (4-1). It is now desired

---

*In some exceptional cases, the beam-forming electrodes may completely enclose the space exterior to the beam, making truncation of the electrodes unnecessary(56).

to eliminate the need for this auxiliary anode by altering the main anode surface in such a way that the potential and the potential gradient are sufficiently well-matched along the equipotential surface Φ_0 so that the field in the beam region is negligibly affected by the removal of the auxiliary anode.

From the earlier treatment of the field at the anode it can be shown that an adjustment of the angle λ alone, keeping the anode faces plane, could not be expected to provide the desired result. A more promising approach would be to keep the angle λ fixed at $\frac{\pi}{2}$, whereby it is already known that a good match occurs in the beam region at the surface Φ_0. By curving the anode away from the cathode it should be possible to improve the match at points on Φ_0 further removed from the beam without seriously affecting conditions at the beam. It is a difficult problem to determine the required anode shape analytically, but an analogue method, utilizing an electrolytic tank or a resistor network could be used. An electrolytic tank model of the electron gun is shown in Figure (5-1). An electrode which coincides with the equipotential Φ_0 has been inserted. The required anode shape is obtained by adjusting the contour of the electrode representing the anode until the potential gradient on either side of Φ_0, measured by probing points as indicated, becomes approximately equal, and the potential gradient inside the beam boundary at Φ_0 remains approximately constant.

The determination of beam-forming electrodes for the radially convergent flow is more difficult analytically, since electrode shapes must first be found which will realize the wrap-around field inside the beam. The main problem to be solved in this regard

involves the termination of the field before it becomes multi-valued.

The determination of the beam-forming electrodes can be carried out in two steps; namely, (a) by designing a gun with a two-potential main anode and an auxiliary anode, and (b) by subsequent alteration of the shape of the main anode to eliminate the auxiliary anode.

(a) Since the electron motion in the cathode region is by hypothesis the same as the convergent electron motion in a concentric-cylinder diode, the shape of the beam-forming electrode at cathode potential and that of the lower surface of

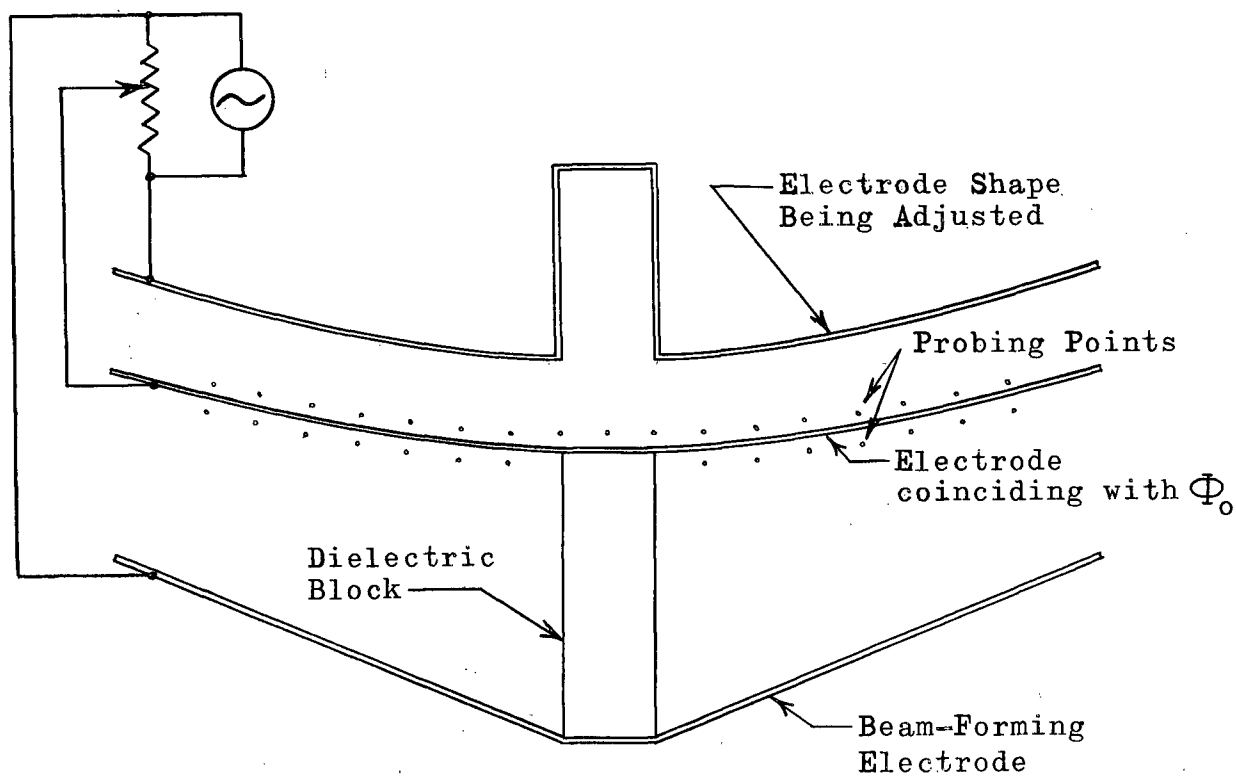

Figure (5-1). Electrolytic tank model of an initially parallel, rectilinear-flow electron gun

the auxiliary anode are thus prescribed*. The shape of the upper surface of the auxiliary anode is also known, since by hypothesis it coincides with the equipotential v = 1.60 of the wrap-around field. The determination of the shape of the main anode is more difficult, involving some approximations.

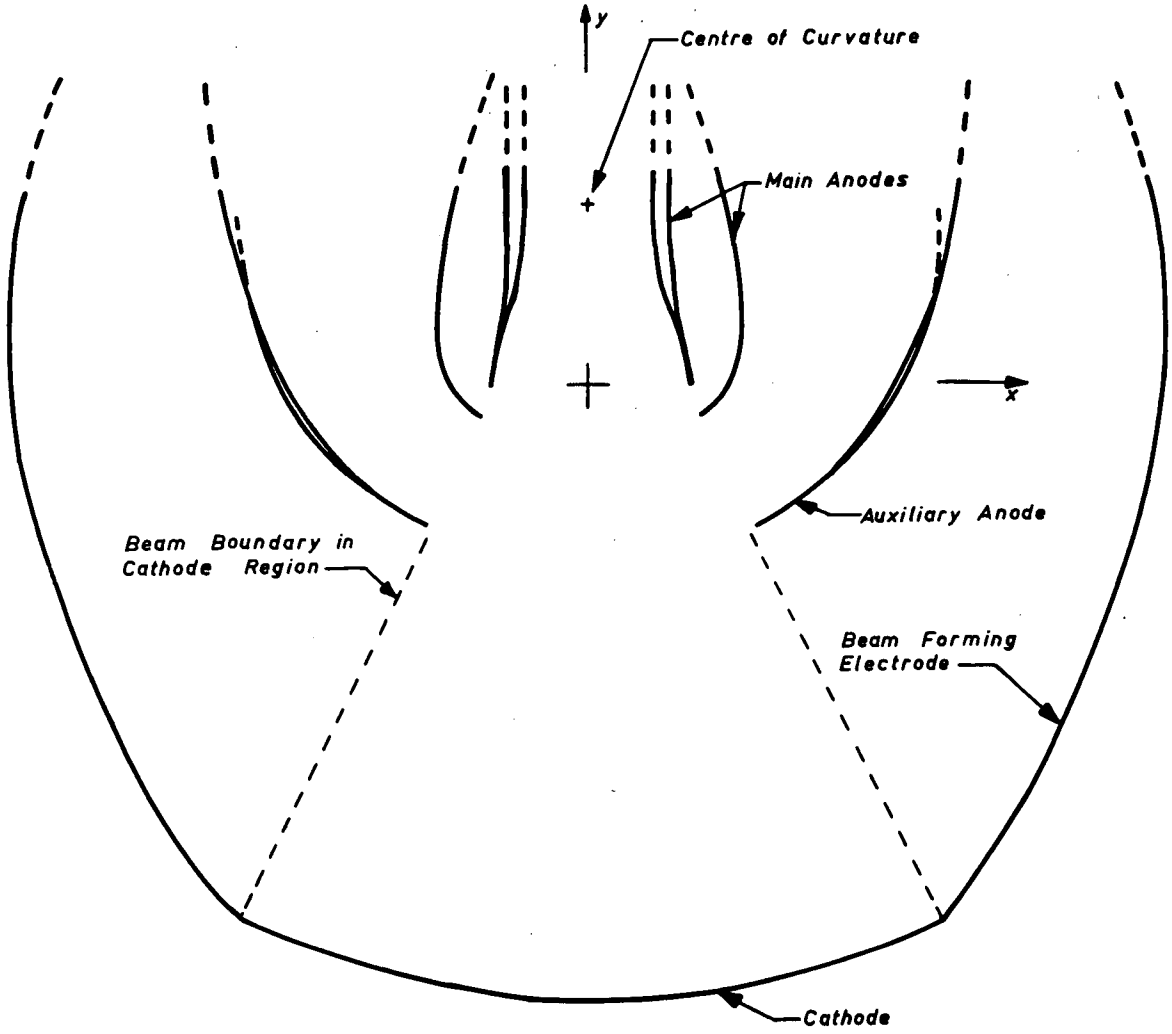

Figure (5-2). Initially radial, convergent-flow electron gun with an auxiliary anode and a two-potential main anode

* The field outside a wedge beam has been found by the use of an electrolytic tank analogue by Pierce[5], and by the use of an analytic method by Radley[7].

It can be seen by referring to Figure (3-8) that the field at the mouth of the anode aperture is very intense. To reduce the danger of arcing to other electrodes, and to aid the physical realization of the wrap-around field in the beam region, it is desirable to choose for the anode surface, in the region of the mouth of the aperture, an equipotential other than v = 0. The equipotential surface v to be chosen for this purpose is a compromise because, although equipotentials with a larger value of v have more rounded corners at the mouth of the anode aperture, these equipotentials are also more prone to intercept the electron beam. The equipotential v = 0.05 appears to be a suitable compromise. By referring to Figure (3-8) it is observed that nine-tenths of the lines of force that enter the anode aperture intersect the equipotential v = 0.05 in the interval between the mouth of the anode aperture and y = 0.5. For values of y greater than 0.5, the field is thus very weak, and the field will be relatively unaffected if the anode wall deviates from this equipotential as shown in Figure (5-2), so that electron-beam interception is avoided.

It remains to satisfy the field conditions on the outside of the main anode. This can be accomplished to a good approximation by inserting a second anode along an equipotential of the wrap-around field that lies close to the mouth of the main anode, yet is far enough away that at the upper end this equipotential does not cross over into the multivalued region until it is well away from the mouth of the main anode. From Figure (3-8) it is seen that the equipotential v = 0.75 is well suited for this purpose. The complete electrode configuration is shown in

Figure (5-2).

(b) To permit the auxiliary anode to be removed, it would be necessary to reshape the contour of the main anode. An electrolytic tank procedure similar to that described for the parallel beam case could be used for this purpose. Such a model is shown in Figure (5-3).

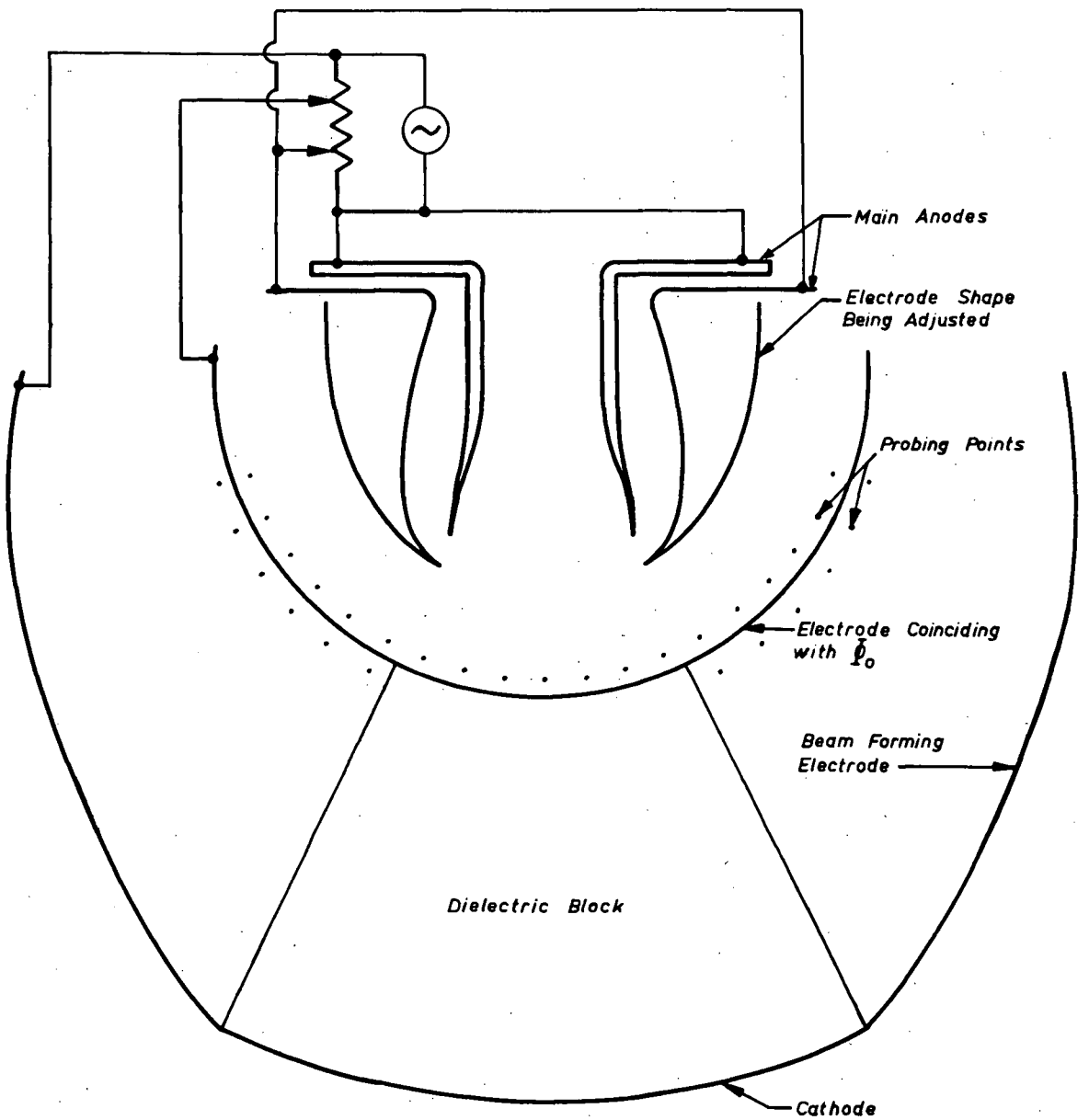

Figure (5-3). Electrolytic tank model of an initially radial, convergent-flow electron gun

5:3 Discussion

There is scope for further work on this approach to gun design. The consideration of axially symmetric guns, particularly convergent ones in which the field in the anode region is similar to the wrap-around field, is very desirable. To optimize the electrode shapes, an experimental investigation of prototypes of these gun structures is essential; in this way also, guns with higher perveances than the theoretical figures obtained above can no doubt be attained.

In the initially radial, convergent flow gun described above, the use of the wrap-around field in the anode region has the effect of reducing the field distortion, due to the anode aperture, in the cathode region. This effect has been obtained by the use of an intensifying electrode by Müller[17] and Brewer[12], and by altering the shape of the cathode by other investigators. Other means that could be employed to reduce or compensate for the field distortion in the cathode region are: (a) dielectrics between the beam-forming electrodes, and (b) non-unipotential cathodes.

A dielectric block of suitable shape and dielectric constant, placed near the beam-forming electrode at cathode potential, could be used to alter the shape of the equipotentials in the cathode region in such a way as to neutralize the field distortion due to the anode aperture. A more exotic but impractical example is the problem of bounding the field in a strip beam by dielectric material placed outside the beam. Since the potential along the trajectories of this beam varies as $y^{\frac{4}{3}}$ and since the normal gradient along them is zero, the

dielectric material would need to have an anisotropic dielectric constant varying as $y^{-\frac{1}{3}}$ in the y-direction, and remaining constant at ε_o in the x-direction. For current-type analogues of electrostatic fields the resistivity at a particular location in the model is proportional to the dielectric constant of the actual medium in which the field is being studied. An analogue study of the effect of the shape and dielectric constant of a dielectric block between the beam-forming electrodes on the field in a proposed gun structure is thus quite feasible. If a network analogue is used, the dielectric block can be represented by suitably changing the values of the resistors; if Teledeltos paper is used, the resistivity can be adjusted by using several layers of paper.

By the use of a non-unipotential cathode, the off-cathode gradient can be made more uniform, thus improving the uniformity of emission when the field distortion due to the anode aperture is severe. Although a laminated cathode with insulated laminae could be used for this purpose, a more practical embodiment would probably be a cathode made of a resistive material. By appropriately adjusting the thickness of the cathode, the desired potential variation along the cathode surface could then be attained.

CHAPTER VI - CONCLUSION

By choosing certain convenient functional forms of the action function, potential and metrical coefficients, some new solutions have been obtained for electron motion in electrostatic fields, by the method of separation of variables. A study of the fields and of the electron trajectories of these solutions has revealed some interesting properties.

The electrostatic field about three idealized two-dimensional anode geometries has been derived. These geometries are: (a) a plane with a slit, (b) two right-angled plates, and (c) two semi-infinite parallel plates. The wrap-around field, an anode field with improved characteristics, has resulted from a study of the characteristics of the above three fields.

It has been shown how use may be made of the above space-charge-free anode fields in the design of electron guns. An estimate has been made of the error introduced by approximating the field in the anode region by a space-charge-free field. An initially parallel, rectilinear flow gun and an initially radial, convergent flow gun have been designed as examples.

The instability of the Pierce-Cauchy problem has been discussed, and an estimate has been made of the rate at which errors in the Cauchy data are propagated when the beam boundaries are axially symmetric.

An electrolytic tank method has been suggested for the determination of beam-forming electrodes for the two above guns that obviates the need for an auxiliary anode.

APPENDIX A - ESTIMATE OF SELF MAGNETIC FORCES AND RELATIVISTIC EFFECTS

Both self-magnetic forces and relativistic effects depend on the electron velocity. The theory of Chapter II assumes that the electron mass is constant; however, according to relativity theory it is given by

$$m = m_o \frac{1}{\sqrt{1 - \frac{v^2}{c^2}}} ,$$

where m_o is the rest mass of the electron, and c is the velocity of light. An electron that, starting from rest, has been accelerated through 20 kV will have a velocity of 0.28c. From the above equation, the increase in electron mass is thus 3.93%, which generally can be ignored.

To study the validity of the neglect of self-magnetic forces, consider the case of a parallel cylindrical electron beam of radius R, constant charge density ρ, and travelling at constant velocity v_z. The electric intensity E_r due to the space charge of the beam is directed radially inward and at a radius $r \leq R$ it is

$$E_r = \frac{\rho r}{2\varepsilon_o} .$$

The electrostatic force F_{re} experienced by an electron at radius $r \leq R$ is thus

$$F_{re} = -eE_r = -\left(\frac{e}{2\varepsilon_o}\right) \rho r ,$$

and is directed radially outward. The magnetic induction B_θ due to the beam current is, at a radius $r \leq R$,

$$B_\theta = \frac{\mu r \rho v_z}{2} \quad .$$

The magnetic force F_{rm} experienced by an electron at radius $r \leq R$ is thus

$$F_{rm} = +e\, v_z B_\theta = + \left(\frac{e\mu_o}{2}\right) v_z^2 \rho\, r \quad ,$$

and is directed radially inward. The ratio of the magnitudes of the two forces is

$$\left| \frac{F_{rm}}{F_{re}} \right| = \mu_o \varepsilon_o v_z^2 = \frac{v_z^2}{c^2} \quad .$$

At 20 kV the ratio of the forces is 0.078. It is apparent that for electron energies greater than 20 keV the self-magnetic forces generally need to be taken into account. At 10 kV the ratio of the forces is $\frac{1}{25}$.

In evaluating the self-magnetic forces in electron beams of actual electron guns, other considerations are involved besides the one obtained for the above idealized beam model. Some of these considerations are discussed in reference (57).

APPENDIX B - DEMONSTRATION OF THE EXISTENCE OF $W(q_1, q_2, q_3) = c_1$ WHEN THE CONDITION $\nabla \times \vec{v} = 0$ IS SATISFIED

For electron motion occurring in an electrostatic field and starting from rest at a zero-potential cathode, the condition $\nabla \times \vec{v} = 0$ is satisfied, by Lagrange's invariant theorem[35,39]. Therefore we may write

$$\vec{v} = \nabla W$$

or

$$dW = \vec{v} \cdot \vec{ds} \quad .$$

It is seen that W is constant when $\vec{ds}$ is normal to $\vec{v}$. Let us call this normal differential vector $\vec{dn}$. We then have

$$dW = 0$$

for

$$\vec{v} \cdot \vec{dn} = 0 \quad .$$

But the Pfaffian differential equation $\vec{v} \cdot \vec{dn} = 0$ is integrable because by hypothesis $\vec{v}$ satisfies the condition $\nabla \times \vec{v} = 0$, and therefore it follows that there exists between the space-coordinates q_1, q_2, and q_3 a one-parameter family of surfaces

$$W(q_1, q_2, q_3) = c_1$$

normal to the trajectories[34].

APPENDIX C - NUMERICAL METHOD FOR OBTAINING ELECTRON TRAJECTORIES IN ELECTROSTATIC FIELDS

C:1 Space-Charge Effects Neglected

Consider the motion of an electron entering a uniform electric field $\vec{E}$ at (x_o, y_o) with initial velocity $(\dot{x}_o, \dot{y}_o)$, as illustrated in Figure (C-1). From equation (2.8) the equations of motion are

$$\left.\begin{aligned} \ddot{x} &= -\eta E_x \\ \ddot{y} &= -\eta E_y \quad . \end{aligned}\right\} \qquad (C.1)$$

Integration of these equations w.r.t. time results in

$$\left.\begin{aligned} \dot{x} &= -\eta E_x t + \dot{x}_o \\ \dot{y} &= -\eta E_y t + \dot{y}_o \end{aligned}\right\} \qquad (C.2)$$

and

$$\left.\begin{aligned} x &= -\eta \frac{E_x}{2} t^2 + \dot{x}_o t + x_o \\ y &= -\eta \frac{E_y}{2} t^2 + \dot{y}_o t + y_o \end{aligned}\right\} \qquad (C.3)$$

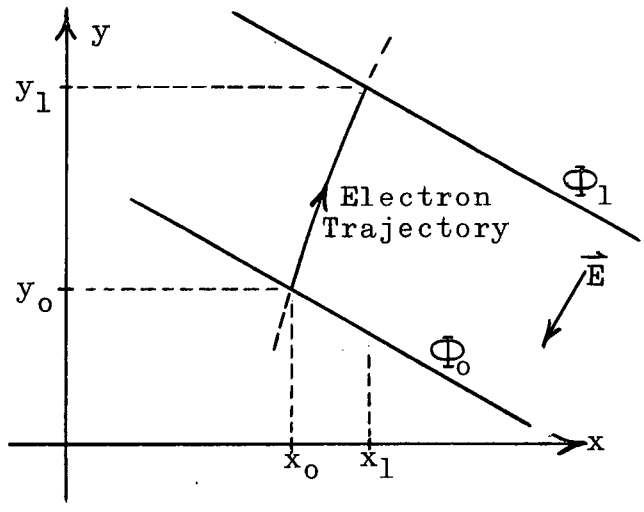

Figure (C-1). Motion of an electron in a uniform electric field

The parameter t in equations (C.3) can be eliminated by the use of equations (C.2); taking the sum of the squares of the latter, we obtain

$$v^2 = \eta^2 E^2 t^2 - 2\eta(E_x \dot{x}_o + E_y \dot{y}_o)t + v_o^2 \quad . \qquad (C.4)$$

It will be assumed that the total electron energy is zero; therefore, from (2.13),

$$v^2 = 2\eta\Phi \quad . \qquad (C.5)$$

Upon substitution of equation (C.5) into (C.4) and solving the latter for t, there results

$$t = \frac{1}{\eta E^2}\left[(E_x \dot{x}_o + E_y \dot{y}_o) + \sqrt{2\eta\Phi E^2 - (E_x \dot{y}_o - E_y \dot{x}_o)^2}\right] . \qquad (C.6)$$

Equations (C.3 and 6) describe the parabolic trajectory in a uniform field in terms of the parameter Φ, of the electric intensity components, and of the initial velocity components and position coordinates.

In electrostatic fields that are not uniform but that are slowly varying in space, electron trajectories can be obtained by considering the electrostatic field to be uniform over short intervals, and applying equations (C.2, 3 and 6) to plot the trajectory in each interval. The size of interval to be used in a particular region of a field depends on the desired accuracy of the trajectories, on the degree of non-uniformity of the field, and on the round-off errors in the computations.

Let j be an index denoting the interval number along an electron trajectory. Thus (x(j), y(j)) are the coordinates of

the j'th point on this trajectory. The equipotential passing through the j'th point is $\Phi(j)$. If the electrostatic field over the j'th interval of the trajectory is approximated by a uniform field, conditions will be as illustrated in Figure (C-2). In particular, it is seen that the equipotentials $\Phi(j-1)$ and $\Phi(j)$ are distorted to the parallel straight lines $\Phi(j-1)_u$ and $\Phi(j)_u$ respectively, so that the trajectory obtained by using the uniform-field assumption crosses the line $\Phi(j)_u$ at $(j)_u$. A first-order correction will be made by extrapolating the trajectory to the point where it intersects the equipotential $\Phi(j)$; this point will be taken to be the j'th point on the trajectory.

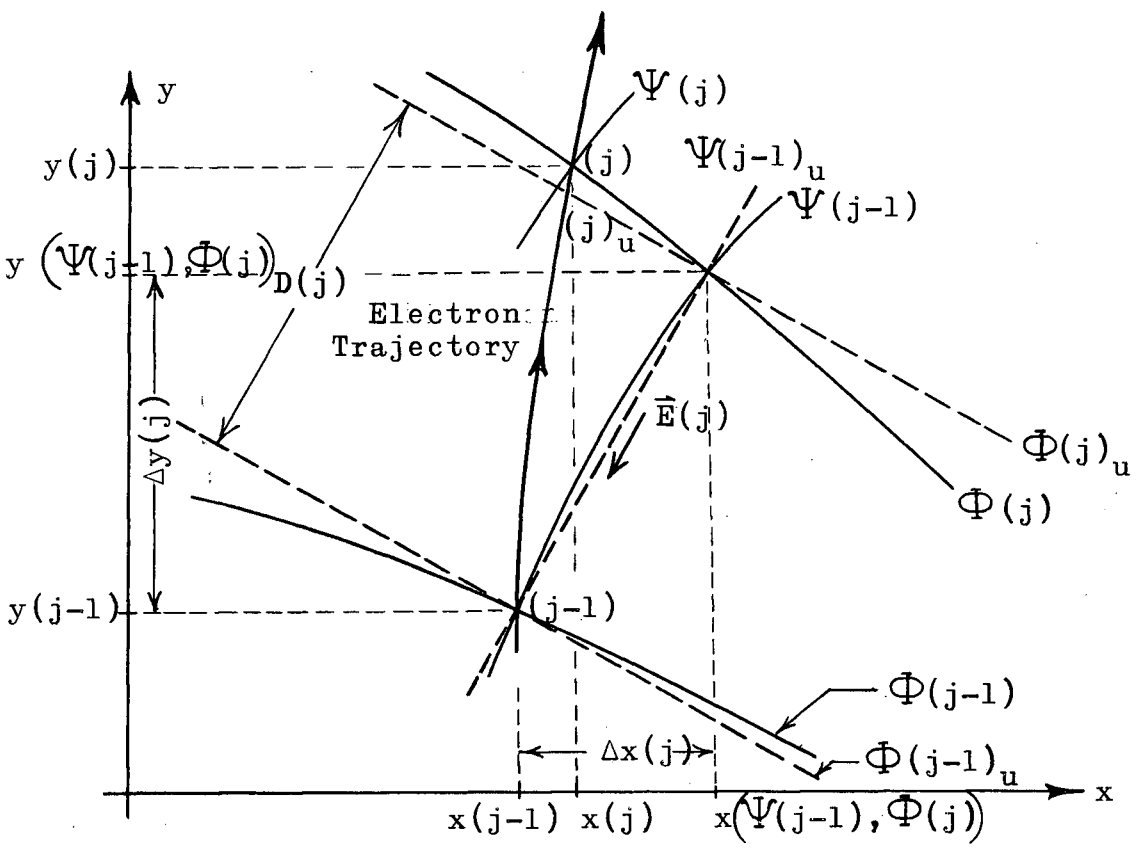

Figure (C-2). Electron path in the j'th interval of a non-uniform field, showing the effect of a uniform-field approximation. The interval size is greatly exaggerated.

The velocity components and the coordinates of the electron at the point $(j)_u$ are, from equations (C.2, 3 and 6)

$$\left.\begin{aligned} \dot{x}(j)_u &= -\eta E_x(j)t(j) + \dot{x}(j-1) \\ \dot{y}(j)_u &= -\eta E_y(j)t(j) + \dot{y}(j-1) \end{aligned}\right\} \qquad (C.7)$$

$$\left.\begin{aligned} x(j)_u &= t(j)\left[-\frac{\eta}{2}E_x(j)t(j) + \dot{x}(j-1)\right] + x(j-1) \\ y(j)_u &= t(j)\left[-\frac{\eta}{2}E_y(j)t(j) + \dot{y}(j-1)\right] + y(j-1) \end{aligned}\right\} \qquad (C.8)$$

where

$$t(j) = \frac{1}{\eta E^2(j)}\left\{\left[E_x(j)\dot{x}(j-1) + E_y(j)\dot{y}(j-1)\right] + \left[2\eta\Phi(j)E^2(j) - \left(E_x(j)\dot{y}(j-1) - E_y(j)\dot{x}(j-1)\right)^2\right]^{\frac{1}{2}}\right\} \qquad (C.9)$$

and where the electric intensity components are as described below in equations (C.11 and 14).

The electrostatic fields in which it is desired to obtain electron trajectories are described by equations of the form

$$\left.\begin{aligned} x &= x(\Psi,\Phi) \\ y &= y(\Psi,\Phi) \end{aligned}\right\} \qquad (C.10)$$

where the curves Ψ = constant are lines of force. The magnitude of the electric intensity in the j'th interval can therefore conveniently be taken as

$$E(j) = \frac{\left|\Phi(j) - \Phi(j-1)\right|}{D(j)} \qquad (C.11)$$

where D(j) is the distance along the secant line joining the point (j-1) and the point marking the intersection of $\Psi(j-1)$ and $\Psi(j)$, as shown in Figure (C-2). It follows that

$$D(j) = \sqrt{\Delta x^2(j) + \Delta y^2(j)} \qquad (C.12)$$

where

$$\left.\begin{aligned} \Delta x(j) &= x(\Psi(j-1),\ \Phi(j)) - x(\Psi(j-1),\ \Phi(j-1)) \\ \Delta y(j) &= y(\Psi(j-1),\ \Phi(j)) - x(\Psi(j-1),\ \Phi(j-1)) \end{aligned}\right\} . \qquad (C.13)$$

From equations (C.11-13) it is readily seen that

$$\left.\begin{aligned} E_x(j) &= -\frac{E(j)\Delta x(j)}{D(j)} \\ E_y(j) &= -\frac{E(j)\Delta y(j)}{D(j)} \end{aligned}\right\} \qquad (C.14)$$

for $\Phi(j) \geq \Phi(j-1)$.

To extrapolate the trajectory from the point $(j)_u$ to its intersection with the equipotential $\Phi(j)$ we shall approximate the trajectory between these two points by a straight line whose slope is the same as the slope of the trajectory at $(j)_u$. The straight-line trajectory is thus

$$y = ax + b \qquad (C.15)$$

where

$$a = \frac{\dot{y}(j)_u}{\dot{x}(j)_u} \quad \text{and} \quad b = y(j)_u - \frac{\dot{y}(j)_u}{\dot{x}(j)_u}\, x(j)_u \quad .$$

The remaining problem is to determine the coordinates of the intersection of equation (C.15) with the equipotential $\Phi(j)$; the latter is seen from equations (C.10) to be described by equations of the form

$$\left.\begin{aligned} x &= x\left(\Psi, \Phi(j)\right) \\ y &= y\left(\Psi, \Phi(j)\right) \end{aligned}\right\} . \qquad (C.16)$$

The following iterative procedure can be used to determine the coordinates of the intersection:

(1) Solve equations (C.16) with a suitable initial guess for $\Psi(j)$. For the first interval in a trajectory a suitable value for $\Psi(j)$ is generally the value of $\Psi(j-1)$ (i.e., when $j = 1$, use the value of $\Psi(0)$ as an initial guess for $\Psi(1)$). For subsequent intervals, better initial guesses of $\Psi(j)$ can be made by noting how Ψ varies along the trajectory from interval to interval. If the initial guess is denoted by $\Psi_1(j)$, equations (C.16) become

$$\left.\begin{aligned} x_1(j) &= x(\Psi_1(j), \Phi(j)) \\ y_1(j) &= y(\Psi_1(j), \Phi(j)) \end{aligned}\right\} \qquad (C.17)$$

where $(x_1(j), y_1(j))$ are the corresponding initial guesses of the desired coordinates $(x(j), y(j))$.

(2) Substitute (C.17a) into (C.15) to determine the value of the initial estimate of the y-coordinate, $\overline{y}_1(j)$, on the straight line trajectory; i.e.,

$$\overline{y}_1(j) = ax_1(j) + b \quad .$$

(3) Define an error function ε_1 as

$$\varepsilon_1 = \overline{y}_1(j) - y_1(j) \quad .$$

(4) If $|\varepsilon_1| \leq |\varepsilon_o|$, where ε_o is a predetermined error bound, then $(x_1(j), y_1(j))$ are taken to be the coordinates of the j'th point on the trajectory, and the computations for the j'th interval are completed.

(5) If $|\varepsilon_1| > |\varepsilon_o|$, subtract an increment $\Delta\Psi$ from $\Psi_1(j)$,

obtaining

$$\Psi_2(j) = \Psi_1(j) - \Delta\Psi$$

and repeat steps (1) - (4) above:

$$\left.\begin{aligned} \text{(a)}\quad x_2(j) &= x(\Psi_2(j), \Phi(j)) \\ y_2(j) &= y(\Psi_2(j), \Phi(j)) \end{aligned}\right\}$$

$$\text{(b)}\quad \overline{y}_2(j) = a x_2(j) + b$$

$$\text{(c)}\quad \varepsilon_2 = \overline{y}_2(j) - y_2(j)$$

$$\text{(d)}\quad |\varepsilon_2| \overset{?}{\leq} |\varepsilon_o| \quad .$$

(6) If $|\varepsilon_2| > |\varepsilon_o|$, the iteration must be repeated. Since from the first two iterations two values on the curve of ε vs. $\Psi(j)$ are known, the third value of $\Psi(j)$ to be used for the iteration can be predicted from a straight line approximation (see Figure (C-3)). Thus

$$\Psi_3(j) = \frac{\varepsilon_2 \Psi_1(j) - \varepsilon_1 \Psi_2(j)}{(\varepsilon_2 - \varepsilon_1)} \quad .$$

(7) In general, after n iterations, the curve $\Psi(j) = f(\varepsilon)$ can be approximated by a (n-1)'th degree polynomial:

$$\Psi(j) = a_o + a_1\varepsilon + a_2\varepsilon^2 + a_3\varepsilon^3 + \ldots + a_{n-1}\varepsilon^{n-1} \quad .$$

The coefficients a_i can be determined from the set of equations:

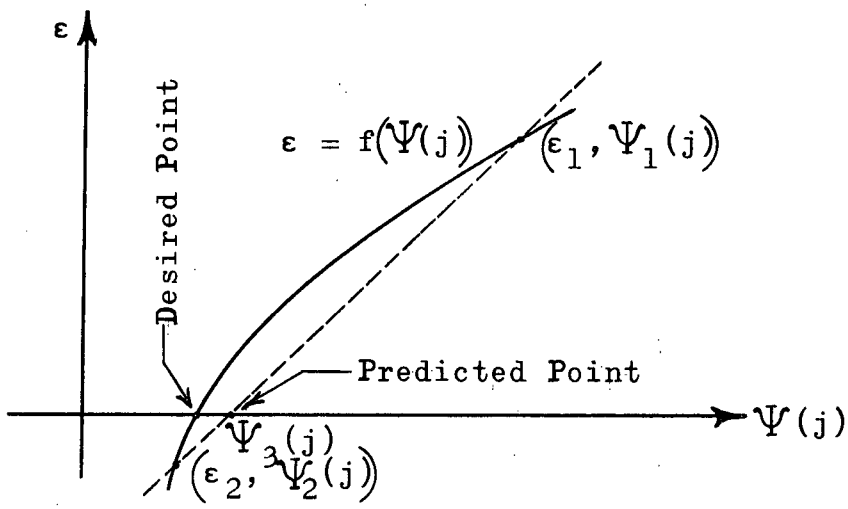

Figure (C-3). Prediction of $\Psi_3(j)$ in the iterative process

$$\begin{aligned}
\varepsilon_1 a_1 + \varepsilon_1^2 a_2 + \varepsilon_1^3 a_3 + \cdots + \varepsilon_1^{n-1} a_{n-1} + a_o &= \Psi_1(j) \\
\varepsilon_2 a_1 + \varepsilon_2^2 a_2 + \varepsilon_2^3 a_3 + \cdots + \varepsilon_2^{n-1} a_{n-1} + a_o &= \Psi_2(j) \\
\varepsilon_3 a_1 + \varepsilon_3^2 a_2 + \varepsilon_3^3 a_3 + \cdots + \varepsilon_3^{n-1} a_{n-1} + a_o &= \Psi_3(j) \\
\vdots \qquad \vdots \qquad \vdots \qquad\qquad \vdots \qquad \vdots \qquad \vdots & \\
\varepsilon_n a_1 + \varepsilon_n^2 a_2 + \varepsilon_n^2 a_3 + \cdots + \varepsilon_n^{n-1} a_{n-1} + a_o &= \Psi_n(j)
\end{aligned}$$

and thus

$$\Psi_{n+1}(j) = f(\varepsilon)\Big|_{\varepsilon = 0} = a_o = \frac{1}{\Delta} \begin{vmatrix} \varepsilon_1 & \varepsilon_1^2 \cdots \varepsilon_1^{n-1} & \Psi_1(j) \\ \varepsilon_2 & \varepsilon_2^2 \cdots \varepsilon_2^{n-1} & \Psi_2(j) \\ \varepsilon_3 & \varepsilon_3^2 \cdots \varepsilon_3^{n-1} & \Psi_3(j) \\ \vdots & \vdots \qquad \vdots & \vdots \\ \varepsilon_n & \varepsilon_n^2 \qquad \varepsilon_n^{n-1} & \Psi_n(j) \end{vmatrix} .$$

where Δ is the determinant of the coefficients a_i.

The trajectories shown in Figure (4-9a) were obtained by

the above method. It was found that in most cases only four iterations were required for an error bound of $|\varepsilon_o| = 10^{-6}$.

C:2 Correction for Space-Charge Forces

Some useful approximations can be made for the beam discussed in Section 4:3 to take into account spreading of the beam due to space-charge forces. This beam and the electrostatic field are symmetric about the plane $x = 0$, the transverse velocity of the beam is small compared to its axial velocity ($\dot{x} << \dot{y}$) and, in the cathode region, conditions in the beam are assumed to be independent of the transverse direction. If image charge effects due to the electrodes are ignored, it is therefore not unreasonable to assume that in the anode region the flux due to the beam itself is transversely directed, whence by Gauss' law

$$E_s = \frac{\lambda}{2\varepsilon_o} \qquad (C.18)$$

where E_s = electric intensity due to the electrons only, at a point (x,y) in the beam

λ = charge/unit length/unit depth contained by an incremental beam section of width $2x$ at (x,y).

It follows from the definition of λ, and equation (2.6) that

$$\lambda = \int_{-x}^{x} \frac{J(x,y)}{\mathcal{V}(x,y)}\, dx \quad . \qquad (C.19)$$

In the beam under study in Section 4:3, we shall not be far wrong if it is assumed that the electron velocity is constant across the beam because, by the time the field becomes markedly

non-uniform, the electrons are all travelling near terminal velocity. Rewriting equation (C.19) and combining it with (C.18) results in

$$E_s(x,y) = \frac{x_o J(y_o)}{\varepsilon_o \sqrt{2\eta}\, \overline{\Phi}^{\frac{1}{2}}(x,y)} \qquad (C.20)$$

where (see Figure (C-4))

$E_s(x,y)$ = electric intensity due to the electrons only, at a point (x,y) on the trajectory that had coordinates (x_o,y_o) when it passed through Φ_o

$J(y_o)$ = current density of the beam at the equipotential Φ_o

$\overline{\Phi}(x,y) = \frac{1}{2}\left[\Phi(0,y) + \Phi(x,y)\right]$, an approximate average of the potential across a beam cross-section of width 2x at (x,y).

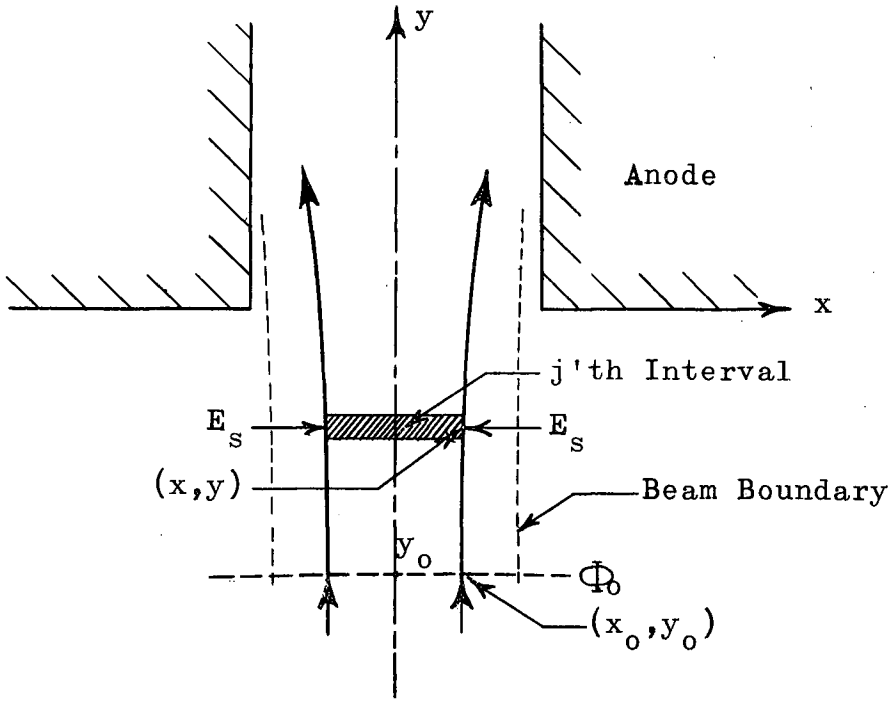

Figure (C-4). Space-charge effects in the anode region

The contribution of space-charge to the electrostatic field in the anode region can be incorporated into the trajectory calculation procedure of Section C:1 by evaluating equation (C:20) at each trajectory interval and adding it to $E_x(j)$ in equations (C.7-9). The trajectories shown in Figure (4-9b) were obtained by this modified method.

APPENDIX D - ANALYSIS OF THE CURVATURE OF AN EQUIPOTENTIAL

Consider a continuous curve v_1 which is described in terms of the parameter u by the equations

$$\left.\begin{aligned} x &= x(u) \\ y &= y(u) \end{aligned}\right\} \quad . \qquad \text{(D.1)}$$

We wish to determine the radius of curvature and the centre of curvature of v_1 at u_i, as shown in Figure (D-1). For this purpose, consider in addition two nearby points u_{i-1} and u_{i+1} on v_1. The centre of curvature of v_1 at u_i is then obtained by the following procedure:

(1) Join the points u_{i-1} and u_i, and u_i and u_{i+1} on v_1 by two secant lines.

(2) Bisect the secant lines and erect lines perpendicular to them passing through the bisect points.

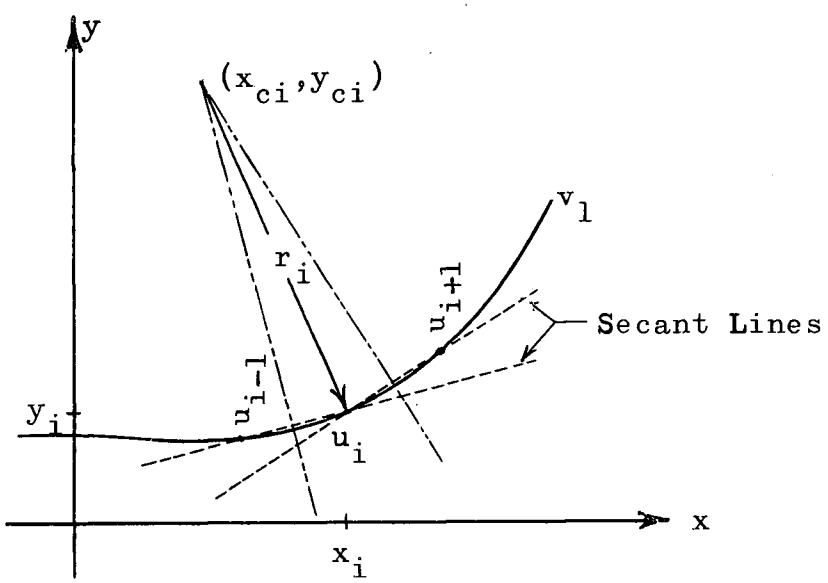

Figure (D-1). Centre of curvature of v_1 at u_i

(3) The intersection of the two perpendiculars is then, in the limit as u_{i-1} and $u_{i+1} \longrightarrow u_i$, at the centre of curvature of v_1 at the point u_i.

Algebraically this is accomplished as follows:

The slope of the secant line passing through u_{i-1} and u_i is

$$m_i = \frac{y_i - y_{i-1}}{x_i - x_{i-1}} \tag{D.2}$$

while the slope of the line passing through u_i and u_{i+1} is

$$m_{i+1} = \frac{y_{i+1} - y_i}{x_{i+1} - x_i} \quad . \tag{D.3}$$

Thus the slopes of the lines perpendicular to these are

$$s_i = -\left(\frac{1}{m_i}\right) = -\left(\frac{x_i - x_{i-1}}{y_i - y_{i-1}}\right) \tag{D.4}$$

and

$$s_{i+1} = -\left(\frac{1}{m_{i+1}}\right) = -\left(\frac{x_{i+1} - x_i}{y_{i+1} - y_i}\right) \tag{D.5}$$

respectively.

The bisecting point on the line $u_{i-1} - u_i$ has coordinates

$$\left.\begin{aligned} x_{bi} &= x_{i-1} + \left(\frac{x_i - x_{i-1}}{2}\right) \\ y_{bi} &= y_{i-1} + \left(\frac{y_i - y_{i-1}}{2}\right) \quad . \end{aligned}\right\} \tag{D.6}$$

The bisecting point on the line $u_i - u_{i+1}$ has coordinates

$$\left.\begin{aligned} x_{b(i+1)} &= x_i + \left(\frac{x_{i+1} - x_i}{2}\right) \\ y_{b(i+1)} &= y_i + \left(\frac{y_{i+1} - y_i}{2}\right) \quad . \end{aligned}\right\} \tag{D.7}$$

Thus the equation of the perpendicular bisector of $u_{i-1} - u_i$ is

$$(y - y_{bi}) = s_i(x - x_{bi}) \qquad (D.8)$$

and the equation of the perpendicular bisector of $u_i - u_{i+1}$ is

$$\left(y - y_{b(i+1)}\right) = s_{i+1}\left(x - x_{b(i+1)}\right) \quad . \qquad (D.9)$$

Substituting equations (D.4 and 6) into (D.8), and (D.5 and 7) into (D.9), we obtain

$$y + A_i x = B_i \qquad (D.10)$$

and

$$y + A_{i+1} x = B_{i+1} \qquad (D.11)$$

respectively, where

$$A_i = \frac{x_i - x_{i-1}}{y_i - y_{i-1}}$$

and

$$B_i = \frac{1}{2}\left[(y_i + y_{i-1}) + \frac{\left(x_i^2 - x_{i-1}^2\right)}{(y_i - y_{i-1})}\right] .$$

Equations (D.10 and 11) intersect at

$$\left.\begin{aligned} x_{ci} &= \left[\frac{B_{i+1} - B_i}{A_{i+1} - A_i}\right] \\ y_{ci} &= \left[\frac{B_i A_{i+1} - B_{i+1} A_i}{A_{i+1} - A_i}\right] \end{aligned}\right\} \qquad (D.12)$$

and in the limit, as u_{i-1} and $u_{i+1} \longrightarrow u_i$, (x_{ci}, y_{ci}) is the centre of curvature of the curve v_1 at (x_i, y_i). For computational purposes, we need to retain the small increments $u_{i-1} - u_i$ and

$u_i - u_{i+1}$, the size of the increments depending on the behaviour of v_1, and the accuracy to which (x_{ci}, y_{ci}) is desired.

From Figure (D-1) the radius of curvature is readily seen to be

$$r_i = \sqrt{(x_i - x_{ci})^2 + (y_i - y_{ci})^2} \qquad (D.13)$$

while the angle with which r_i intersects the y-axis (the slope of v_1 at u_1) is

$$\theta_i = \tan^{-1}\left[\frac{x_i - x_{ci}}{y_{ci} - y_i}\right] \quad . \qquad (D.14)$$

Equations (D.12, 13 and 14) were used to compute the centre of curvature (x_{ci}, y_{ci}), the radius of curvature r_i, and the angle θ_i for a series of points u_i on equipotentials in the field about two semi-infinite parallel planes and in the wrap-around field (see Figures (4-11 to 15)).

APPENDIX E - ELECTROSTATIC FIELD REQUIRED TO MAINTAIN TWO PARALLEL, SPACE-CHARGE-LIMITED STRIP BEAMS

For simplicity the strip beams will be assumed to be of vanishing thickness; no generality is lost by this assumption, since the field required outside two beams of finite thickness is the same as that required for the case to be discussed.

In Figure (E-1) are shown two strip beams, which are a distance 2h apart. The potential variation along these beams is, from the Langmuir-Child law[2],

$$\left.\begin{aligned} V(h,y) &= A_1 y^{\frac{4}{3}} \\ V(-h,y) &= A_2 y^{\frac{4}{3}} \end{aligned}\right\} \qquad (E.1)$$

where

$$A_i = \left(\frac{J_i}{k_1}\right)^{\frac{2}{3}}$$

and J_1 and J_2 are the current densities in the right and in the left beam, respectively.

If the Laplace equation is solved subject to (E.1) by analytic continuation, in the manner of Pierce[5], it is found that the electrostatic field required to maintain the right beam is

$$V(x,y) = A_1\left[(x-h)^2 + y^2\right]^{\frac{2}{3}} \cos\left[\frac{4}{3}\tan^{-1}\left(\frac{x-h}{y}\right)\right] \qquad (E.2)$$

while the field required to maintain the left beam is

$$V(x,y) = A_2\left[(x+h)^2 + y^2\right]^{\frac{2}{3}} \cos\left[\frac{4}{3}\tan^{-1}\left(\frac{x+h}{y}\right)\right] . \qquad (E.3)$$

If $J_1 = J_2$, then the fields described by (E.2) and (E.3)

are observed to be the same and to be spatially displaced from each other a distance 2h; further, the potential variation along the y-axis described by (E.2) and (E.3) is then the same.

Since the fields described by equations (E.2) and (E.3) overlap, they cannot simultaneously be realized physically, as this would require multivalued potentials in the overlapping regions. However, by suitably terminating the fields in the region between the two beams, this overlapping of the fields can be avoided. The fields can be terminated by various means. For example, for the case when $J_1 = J_2$, a resistive strip of thickness 2s could be inserted midway between the two beams, as shown in Figure (E-1). If the resistivity of this strip varies as

$$R \propto \left[(s - h)^2 + y^2\right]^{\frac{2}{3}} \cos \frac{4}{3}\left[\tan^{-1}\left(\frac{s - h}{y}\right)\right]$$

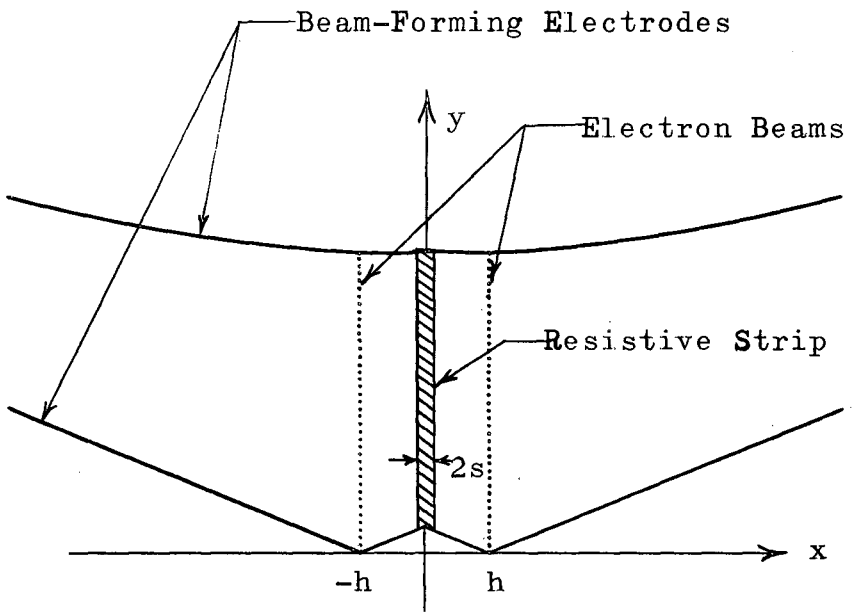

Figure (E-1). Electrodes and resistive strip to maintain two parallel strip-beams

and the ends of the strip are electrically connected to the beam-forming electrodes, the desired field conditions are attained, because the resistive strip divides the region between the beam-forming electrodes — which theoretically should extend to infinity — into two closed regions (the potential in a closed region is specified uniquely once the potential is known on the boundary).

APPENDIX F - ON THE STABILITY OF THE PIERCE-CAUCHY PROBLEM

If the beam boundary as well as the Cauchy boundary conditions are prescribed by analytic functions, then, by the Cauchy-Kowalewski theorem[58], a unique solution of the electrostatic field exists, at least in the neighbourhood of the beam surface. Several exact, stable methods, based on solving the Laplace equation by analytic continuation, have been developed in the past. Pierce[5] used analytic continuation to determine the plane electrostatic field required outside a strip beam with a rectilinear boundary. Lomax[56] and Kirstein[59] used this process for plane fields outside planar flows with curvilinear boundaries, and Harker[60] applied it to the axially symmetric case for beams with curvilinear boundaries.

When "marching-type" numerical procedures are used to solve the Laplace equation outside the beam boundary, errors are inevitably introduced by the finite-difference approximation of the Laplace equation and by the limited precision of the numerical computations. It has already been shown in Section 5:1 that these errors can grow at an exponential rate. Sugai[61] and Meltzer[62] found an upper limit of 5.828 for the growth of the error per step when the five-point star formula

$$\Phi_{k+1,n} = 4\,\Phi_{k,n} - \Phi_{k-1,n} - \Phi_{k,n+1} - \Phi_{k,n-1} \qquad \text{(F.1)}$$

is used to solve (5.1), the Laplace equation for plane electrostatic fields.

For axially symmetric fields, the Laplace equation to be solved is

$$\frac{\partial^2\Phi}{\partial r^2} + \frac{1}{r}\frac{\partial\Phi}{\partial r} + \frac{\partial^2\Phi}{\partial z^2} = 0 \qquad \text{(F.2)}$$

so the five-point star formula is

$$\Phi_{m+1,n} = \left(\frac{4m-1}{m}\right)\Phi_{m,n} - \left(\frac{m-1}{m}\right)\Phi_{m-1,n} - \Phi_{m,n+1} - \Phi_{m,n-1} \qquad \text{(F.3)}$$

where the notation is as illustrated in Figure (F-1). The upper limit of the growth rate of the error per step for equation (F.3) is the same as that for (F.1); this is clear if it is considered that when "m" is large in equation (F.3), the latter approaches the functional form of (F.1). For finite "m", however, the maximum growth rate of the error of (F.3) is always somewhat smaller than that of the error of (F.2), as will be demonstrated.

Let $\varepsilon_{m,n}$ be the error in the value of the potential Φ at $(r,z) = (m\Delta r, n\Delta z)$. Since equation (F.3) is linear, it can be used to describe the propagation of initial errors in potential, as well as to compute the potential itself. Therefore,

$$\varepsilon_{m+1,n} = \left(\frac{4m-1}{m}\right)\varepsilon_{m,n} - \left(\frac{m-1}{m}\right)\varepsilon_{m-1,n} - \varepsilon_{m,n+1} - \varepsilon_{m,n-1} \qquad \text{(F.4)}$$

For simplicity, let it be assumed that the beam boundary coincides with the line $m = m_o$, so that the Cauchy conditions specify the values of potential at mesh points of the lines $m = m_o$ and $m = m_1$ (see Figure (F-1)). It will further be convenient to define a new index "k", which is zero at the beam boundary, so that

$$k = m - m_o \quad .$$

As an example, the case $m_o = 10$ will be taken. Using equation (F.4), errors in potential at the mesh points of the lines $m_o = 10$ and $m_1 = 11$ are found to propagate as follows:

$$\varepsilon_{12,n} = \left[-\frac{10}{11}\,\varepsilon_{10,n}\right] + \left[-\varepsilon_{11,n-1} + \frac{43}{11}\,\varepsilon_{11,n} - \varepsilon_{11,n+1}\right]$$

$$\varepsilon_{13,n} = \left[+\frac{10}{11}\,\varepsilon_{10,n-1} - 3\,\frac{37}{66}\,\varepsilon_{10,n} + \frac{10}{11}\,\varepsilon_{10,n+1}\right] +$$

$$\left[\varepsilon_{11,n-2} - 7\,\frac{109}{132}\,\varepsilon_{11,n-1} + 16\,\frac{13}{33}\,\varepsilon_{11,n} - 7\,\frac{109}{132}\,\varepsilon_{11,n+1} + \varepsilon_{11,n+2}\right]$$

etc.

In general,

$$\varepsilon_{m,n} = \sum_{p=n-(m-12)}^{p=n+(m-12)} a_{10,p}\varepsilon_{10,p} + \sum_{q=n-(m-11)}^{q=n+(m-11)} a_{11,q}\,\varepsilon_{11,q} \qquad \text{(F.5)}$$

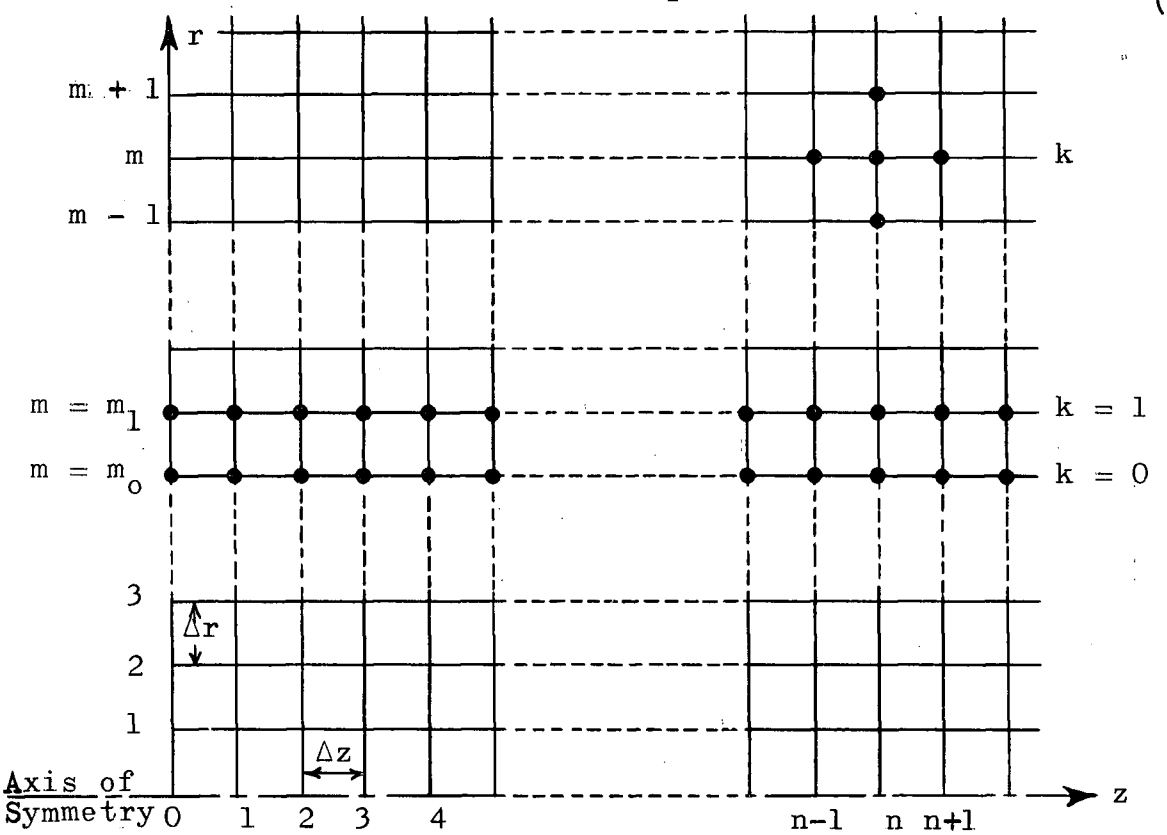

Figure (F-1). Square lattice ($\Delta r = \Delta z$) used for solving equation (F.3)

where $a_{10,p}$ and $a_{11,q}$ are coefficients. Since the potentials at the mesh points of the line $m_1 = 11$ depend both on the prescription of the potential at mesh points of $m_o = 10$ and on a finite-difference approximation of the normal gradient, the errors on the line $m_1 = 11$ will in general be greater than the errors on the line $m_o = 10$. The second summation of equation (F.5) is thus the dominant part of $\varepsilon_{m,n}$. Values of the coefficients $a_{11,q}$ are shown in Table (F-1) for values of m up to 17; this table illustrates the rapid rate of growth of the initial errors. The worst case occurs when the potentials at each mesh point on the two starting lines m_o and m_1 have the maximum allowed initial error, and this error alternates in sign for consecutive mesh points. The rate of growth of $\varepsilon_{11,q}$ will then be the sum of the magnitudes of the coefficients; it is seen from Table (F-1) that upon reaching a mesh on the line $k = 7$ the initial errors $\varepsilon_{11,q}$ already will have grown to 37,700 times their original value.

Since the dominant coefficient is $a_{11,n}$, its rate of growth has been taken to give a more valid indication of the rate of growth of the initial errors to be expected in the general case. This procedure was also followed by Sugai[61]. In Figure (F-2) have been plotted the ratios of adjacent central column coefficients of $\varepsilon_{m_1,q}$ for the cases when $m_o = 10$ and when $m_o = 0$. The curve obtained by Sugai for plane electrostatic fields, when equation (F.1) applies, is also shown. As m_o is increased, the growth of the initial error per step is seen to approach the curve for the plane case.

$a_{11,q}$ \ m	11	12	13	14	15	16	17
$a_{11,n\pm6}$							1
$a_{11,n\pm5}$						-1	-23.548
$a_{11,n\pm4}$					1	19.611	232.41
$a_{11,n\pm3}$				-1	-15.677	-155.13	-1,254.0
$a_{11,n\pm2}$			1	11.749	93.399	638.24	4,055.8
$a_{11,n\pm1}$		-1	-7.8257	-47.172	-266.15	-1,475.2	-8,148.1
$a_{11,n}$	1	3.$\dot{9}\dot{0}$	16.$\dot{3}\dot{9}$	76.358	378.89	1,951.4	10,279
Ratio of adjacent central-column coefficients	3.$\dot{9}\dot{0}$	4.194	4.658	4.962	5.150	5.267	

Table (F-1). Coefficients of $\varepsilon_{11,q}$ in equation (F.5)

In view of the high instability of these marching-type methods, the best procedure to follow is, in general, to start with a fine lattice between m_o and m_1 (to keep the initial errors low), but to enlarge the lattice as rapidly as possible when working away from the beam boundary. For example, for plane fields, to obtain the value of $\Phi_{14,n}$, the equation

$$\Phi_{14,n} = 4\,\Phi_{12,n} - \Phi_{12,n-2} - \Phi_{12,n+2} - \Phi_{10,n}$$

would be preferable to the equation

$$\Phi_{14,n} = 4\,\Phi_{13,n} - \Phi_{13,n-1} - \Phi_{13,n+1} - \Phi_{12,n}\ .$$

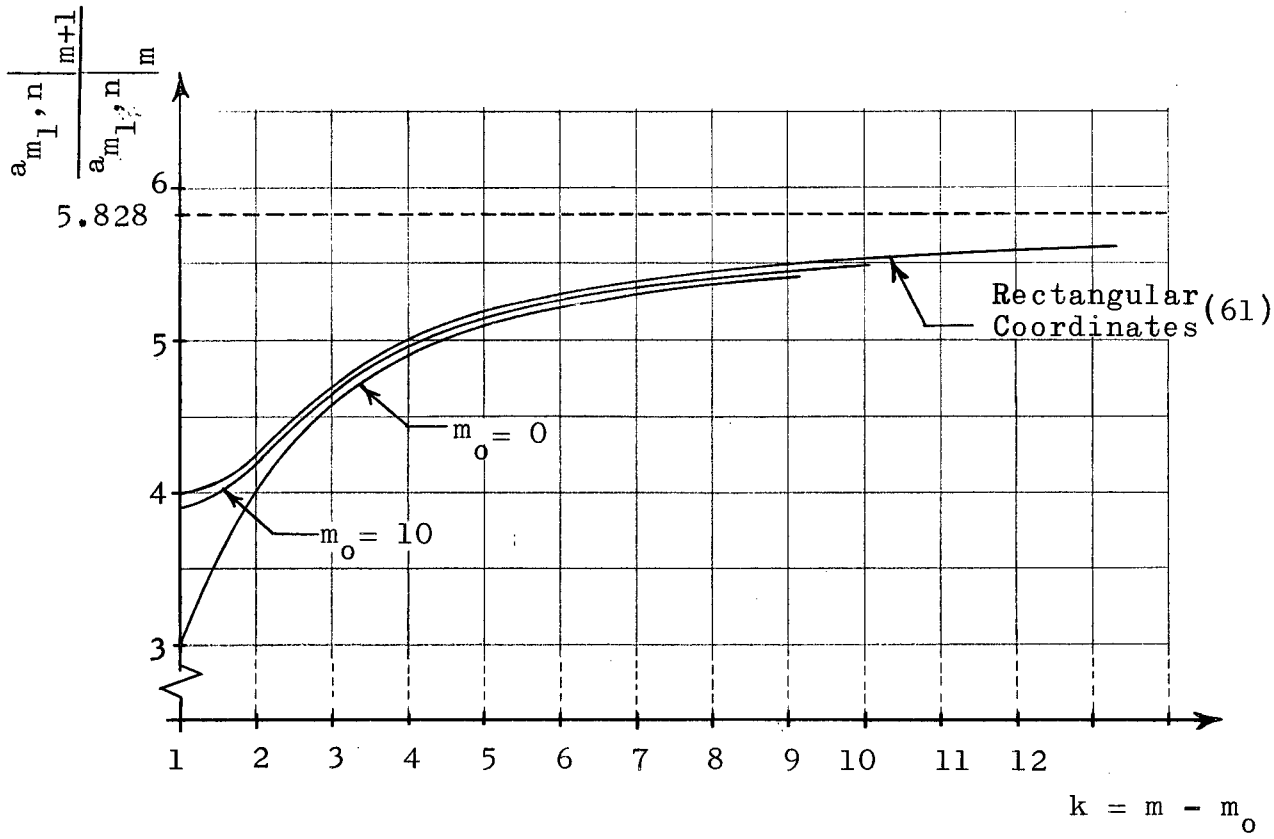

Figure (F-2). Ratio of the adjacent central-column coefficients $a_{m_1,n}$ versus distance from the beam boundary

REFERENCES

1. O'Neill, G.D., "The Unit of Perveance", Proc. IRE, 37:11:1295, (November 1949)

2. Langmuir, I., "The Effect of Space-Charge and Residual Gases on Thermionic Currents in High Vacuum", Phys. Rev., 2:450-486, (1913)

3. Langmuir, I., and K. Blodgett, "Currents Limited by Space-Charge between Coaxial Cylinders", Phys. Rev., 22:347-356, (1923)

4. Langmuir, I., and K. Blodgett, "Currents Limited by Space-Charge between Concentric Spheres", Phys. Rev., 24:49-59, (1924)

5. Pierce, J.R., "Rectilinear Electron Flow in Beams", J. Appl. Phys., 11:7:548-554, (August 1940)

6. Morse, P.M., and H. Feshback, Methods of Theoretical Physics, vol. 1, McGraw-Hill, New York, 1953, ch. 6

7. Radley, D.E., "The Theory of the Pierce Type Electron Gun", J. Electron. Contr., 4:2:125-148, (February 1958)

8. Davisson, C.J., and C.J. Calbick, "Focal Length of Anode Apertures", Phys. Rev., 38:585, (1931), and 42:580, (1932)

9. Birdsall, C.K., "Aperture Lens Formula Corrected for Space Charge in the Electron Stream", IRE Trans. on Electron Devices, ED-4:2:132-134, (April 1957)

10. Pöschl, K., and W. Veith, "Die Brennweite einer Lochblende von endlicher Offnung für Elektronenstrahlen endlicher Raumladung", Arch. elektr. Übertr., 12:1:45-48, (January 1958)

11. Bevc, V., and C. Süsskind, "Corrections of Davisson-Calbick Aperture-Lens Formula for Space-Charge and Magnetic Field", Proc. IRE, 47:2:336-337, (February 1959)

12. Brewer, G.R., "Formation of High-Density Electron Beams", J. Appl. Phys., 28:1:7-15, (January 1957)

13. Harris, L.A., "A Study of Aperture-type Electron Lenses with Space Charge", J. Electron. Contr., 8:4:241-265, (April 1960)

14. Stuart, G.A., and B. Meltzer, "Perturbation Analysis of Stationary Dense Electron Flow in a Space-Charge-Limited Triode", J. Electron. Contr., 3:1:51-62, (July 1957)

15. Danielson, W.E., J.L. Rosenfeld, and J.A. Saloom, "A Detailed Analysis of Beam Formation with Electron Guns of the Pierce Type", Bell Sys. Tech. J., 35:2:375-420, (March 1956)

16. Brown, K.L., and C. Süsskind, "The Effect of the Anode Aperture on Potential Distribution in a 'Pierce' Electron Gun", Proc. IRE, 42:3:598, (March 1954)

17. Müller, M., "New Points of View in the Design of Electron Guns for Cylindrical Beams of High Space Charge", J. Brit. IRE, 16:83-94, (February 1956)

18. Amboss, K., "The Effect of the Anode Aperture in Conical Flow Pierce Guns", J. Electron. Contr., 13:7:545-572, (July 1962)

19. Süsskind, C., "Electron Guns and Focusing for High-Density Electron Beams", Advances in Electronics and Electron Physics", ed. L. Marton, N.Y., Academic Press, vol. 8, 1956, pp. 363-402

20. Hechtel, J.R., and J.A. Seeger, "Accuracy and Limitations of the Resistor Network Used for Solving Laplace's and Poisson's Equations", Proc. IRE, 49:5:933-940, (May 1961)

21. Hechtel, J.R., "Electron Ray Tracing by Means of Resistor Network and Digital Computer", IRE Trans. on Electron Devices, ED-9:1:62-68, (January 1962)

22. Van Duzer, T., C.R. Bucker, and G.R. Brewer, A Trajectory Tracer for Charged Particles which Includes Magnetic Fields and Space-Charge, Electron Tube Laboratory, Hughes Aircraft Company, Culver City, California, Hughes Research Laboratories Research Report #254

23. Barber, M.R., and K.F. Sander, "The Electron Optics of High Current Density Electrostatic Electron Guns", Proc.IEE, part B, supplement #12, vol. 105, pp. 901-905, (1958)

24. Rowe, J.E., and R.J. Martin, "An Electron Trajectory Tracer and its Component Poisson Cell", Proc. IEE, part B, supplement #12, vol. 105, pp. 1024-1032, (1958)

25. Kirstein, P.T., and J.S. Hornsby, "An Investigation into the Use of Iteration Methods for the Analysis of Axially Symmetric and Sheet Beam Electrode Shapes with an Emitting Surface", IEEE Trans. on Electron Devices, ED-11:5:196-204, (May 1964)

26. Deimel, E., "Iterative Computations on High-Perveance Electron Guns Using Digital Computers", Nachrichtentech. Fachber., 22:493-507, (1961)

27. Frost, R.D., O.T. Purl, and H.R. Johnson, "Electron Guns for Forming Solid Beams of High Perveance and High Convergence", Proc. IRE, 50:8:1800-1807, (August 1962)

28. Mathias, L.E.S., and P.G.R. King, "On the Performance of High Perveance Electron Guns", IRE Trans. on Electron Devices, ED-4:3:280-286, (July 1957)

29. Heil, O., and J.J. Ebers, "A New Wide-Range, High-Frequency Oscillator", Proc. IRE, 38:6:645-650, (June 1950)

30. Reed, E.D., "A Tunable, Low-Voltage Reflex Klystron for Operation in the 50 to 60-kmc Band", Bell Sys. Tech. J., 34:3:563-599, (May 1955)

31. Kawamura, M., "High Converging Gun", J. Inst. Elect. Commun. Eng. of Japan, 43:711-718, (1960)

32. Lucken, J.A., "High Perveance, High Compression Electron Guns", Proc. IRE, 51:7:1046-1047, (July 1963)

33. Meltzer, B., "Electron Flow in Curved Paths under Space-Charge Conditions", Proc. Phys. Soc., B, 62:431-437, and 62:813-817, (1949)

34. Sneddon, I.N., Elements of Partial Differential Equations, McGraw-Hill, New York, 1957, ch. 1, sec. 5

35. Gabor, D., "Dynamics of Electron Beams", The Science Forum, pp. 1-23, (September 1944)

36. Kirstein, P.T., Curvilinear Space-Charge Flow with Applications to Electron Guns, Stanford U., California, Microwave Laboratory, M.L. #440, (January 1958)

37. Pease, M.C., "Time-Dependent Electron Flow", J. Appl. Phys., 31:1:70-76, (January 1960)

38. Spangenberg, K., "Use of the Action Function to Obtain the General Differential Equations of Space Charge Flow in More than One Dimension", J. Franklin Inst., 232:365-371, (1941)

39. Walker, G.B., "Congruent Space Charge Flow", Proc. Phys. Soc., B, 63:1017-27, (1950)

40. Meltzer, B., "Single-Component Stationary Electron Flow under Space-Charge Conditions", J. Electron. Contr., 2:2:118-127, (September 1956)

41. Rosenblatt, J., "Three-Dimensional Space Charge Flow", J. Appl. Phys., 31:8:1371-1377, (August 1960), and 32:9:1803, (September 1961)

42. Kirstein, P.T., and G.S. Kino, "Solution to the Equations of Space-Charge Flow by the Method of the Separation of Variables", J. Appl. Phys., 29:12:1758-1767, (December 1958)

43. Kirstein, P.T., R. Kantor, and J. Szëgo, Numerical Solutions to the Space-Charge Limited Flow Obtained by the Separation of Variables Method, Stanford U., California, Microwave Laboratory, M.L. #714, (August 1960)

44. Harker, K.J., and D.S. Colburn, Exact Solutions of the Equations of Space-Charge Limited Flow, Stanford U., California, Microwave Laboratory, M.L. #858, (October 1961)

45. Goursat, M., "Sur une classe de problèmes de Dynamique" Comptes Rendus Académie des Sciences, 116:1050-51, (May 1893)

46. Iwata, G., "Orbits of an Electron in Static Electromagnetic Fields, I", Progr. Theor. Phys., 15:6:513-522, (June 1956)

47. Goldstein, H., Classical Mechanics, Addison-Wesley, Reading, Mass., 1959, ch. 9

48. Morse, P.M., and H. Feshback, Methods of Theoretical Physics, vol. 1, McGraw-Hill, New York, 1953, p. 499

49. Ibid., pp. 443-453

50. Davy, N., "The Field between Equal Semi-Infinite Rectangular Electrodes or Magnetic Pole-Pieces", Phil. Mag., ser. 7, 35:251:819-840, (December 1944)

51. Van Duzer, T., and G.R. Brewer, "Space-Charge Simulation in an Electrolytic Tank", J. Appl. Phys., 30:3:291-301, (March 1959)

52. Kyhl, R.L., and H.F. Webster, "Breakup of Hollow Cylindrical Electron Beams", IRE Trans. on Electron Devices, ED-3:4:172-183, (October 1956)

53. Pierce, J.R., "Instability of Hollow Beams", IRE Trans. on Electron Devices, ED-3:4:183-189, (October 1956)

54. Garebedian, P.R., Partial Differential Equations, Wiley and Sons, New York, 1964, sec. 4.1

55. Ibid., ch. 16, ex. 14

56. Lomax, R.J., "Exact Electrode Systems for the Formation of a Curved Space-Charge Beam", J. Electron. Contr., 3:4:367-374, (October 1957)

57. "Discussion on Electron Optics - I", Proc. IEE, part B, supplement #12, vol. 105, pp. 941-943, (1958)

58. Hadamard, J., Lectures on Cauchy's Problem in Partial Differential Equations, Dover Publications, New York, 1952, pp. 21, 23 and 25

59. Kirstein, P.T., "On the Determination of the Electrodes Required to Produce a Given Electric Field Distribution Along a Prescribed Curve", Proc. IRE, 46:10:1716-1722, (October 1958)

60. Harker, K.J., "Solution of the Cauchy Problem for Laplace's Equation in Axially Symmetric Systems", J. Math. Phys., 4:7:993-997, (July 1963)

61. Sugai, I., "Numerical Solution of Laplace's Equation, Given Cauchy Conditions", IBM J. Res. Dev., 3:2:187-189, (April 1959)

62. Meltzer, B., "The Stability of Computation of the Pierce-Cauchy Problem", J. Electron. Contr., 8:6:449-453, (June 1960)